CADHERIN-11 IN CARDIOVASCULAR MECHANOBIOLOGY: ALTERED IMMUNE RESPONSE AND ENDOTHELIAL CONTRACTILITY

By

Camryn Leigh Johnson

Dissertation

Submitted to the Faculty of the

Graduate School of Vanderbilt University

in partial fulfillment of the requirements

for the degree of

DOCTOR OF PHILOSOPHY

in

Biomedical Engineering

March 31, 2021

Nashville, Tennessee

Approved:

W. David Merryman, PhD

Cynthia Reinhart-King, PhD

Matthew Walker III, PhD

MacRae Linton, MD

David Harrison, MD

ACKNOWLEDGMENTS

"Nothing in life is to be feared, it is only to be understood. Now is the time to understand more, so that we may fear less."

-Marie Curie

TABLE OF CONTENTS

LIST OF TABLES

LIST OF FIGURES

LIST OF ABBREVIATIONS

Term	Description
AF	adventitial fibroblast
Arg-1	arginase-1
αSMA	alpha smooth muscle actin
AVEC	aortic valvular endothelial cell
AVIC	aortic valvular interstitial cell
BMT	bone marrow transplant
CAVD	calcific aortic valve disease
CDH11	cadherin-11 (also ob-cadherin)
CVD	cardiovascular disease
CXCL	c-x-c motif chemokine ligand
EC	endothelial cell
ECM	extracellular matrix
EndMT	endothelial-to-mesenchymal transition
fibAVEC	fibrosa aortic valve endothelial cell
HFD	high fat diet
ICAM-1	intercellular adhesion molecule 1
IFNγ	interferon-γ
IL-	interleukin-
LDL	low-density lipoprotein
LPS	lipopolysaccharide
MCP-1	monocyte chemoattractant protein-1
MHC	major histocompatibility complex
MIP	macrophage inflammatory protein
MMP	matrix metalloproteinase
oxLDL	oxided low-density lipoprotein
PDGF	platelet-derived growth factor
PECAM-1	platelet endothelial cell adhesion molecule-1
ROCK	Rho kinase
SMC	smooth muscle cell
TAM	tumor-associated macrophage
TGFβ	transforming growth factor beta
T_h	helper T cell
TLR	toll-like receptor
TNFα	tumor necrosis factor alpha

VCAM-1	vascular cell adhesion molecule-1
VE-cadherin	vascular endothelial cadherin (also CDH5)
venAVEC	ventricularis aortic valve endothelial cell

CHAPTER 1

Introduction and Motivation

Cardiovascular disease (CVD) is the leading cause of death in the world and represents a substantial global health burden [1]. Because the cardiovascular system is undergoing constant hemodynamics and mechanical forces, mechanotransduction plays a crucial role in the development of many CVD-related illnesses [2]. CVD resulting from atherosclerosis is the cause of nearly a third of the world's deaths [1], and it is the underlying cause of most fatal heart attacks [3]. Atherosclerotic plaques, characterized by the progressive accumulation of lipids in the arterial wall [4], preferentially form at sites of disturbed flow in branchpoints and the curvature of the aortic arch. Calcific aortic valve disease (CAVD), the third leading cause of CVD [5], develops on the fibrosa of the aortic valve, the side facing the aorta which is exposed to low shear stress recirculatory flow patterns. Mechanical strains are constantly imposed on cardiovascular tissue as well, both during the normal cardiac cycle and exacerbated during certain pathologies, such as hypertension [6]. For these reasons, it is important to study mechanically sensitive proteins and their potential impact on disease pathology.

Cadherin-11 (CDH11) is a cell-cell adhesion protein that has been implicated in several diseases associated with fibrosis and inflammation, including pulmonary fibrosis, scleroderma, and rheumatoid arthritis [7]–[10]. CDH11 is a mechanically sensitive protein, with expression that can be altered by shear stress [11]. Furthermore, the connections formed between cells using CDH11 can communicate mechanical signals required for the perpetuation of mechanotransduction. Hutcheson et. al demonstrated that CDH11 was

1

necessary for the communication of tension between myofibroblasts required for the formation of calcific nodules [12]. CDH11 expression is also often characterized by an increased migratory phenotype and has been implicated in varying cellular functions, including invasion, epithelial-to-mesenchymal transition [13]–[15], and wound healing [12]. A study by Schroer et. al also posited the importance of CDH11 engagement, demonstrating that pharmacological targeting of CDH11 improved outcomes post-myocardial infarction, potentially through the disruption of intercellular interactions [16]. The bulk of current CDH11 research focuses on fibroblasts and its upregulation during myofibroblast differentiation [12], [17]; however, it has been shown to be expressed by a wide range of cell types.

Atherosclerosis is not simply due to a passive accumulation of lipids, as was previously believed, but involves an ongoing inflammatory response that contributes to the initiation, progression, and eventual rupture of plaques. Lipoproteins invade the intima where they are oxidized, subsequently activating the endothelial layer and initiating an immune response that ultimately contributes to plaque progression and, later, vulnerability to rupture [18]. A critical step in atherosclerosis progression is the adhesion to and infiltration of the plaque by immune cells, particularly monocytes and CD4+ helper T cells. Once inside the plaque, mature macrophages secrete pro-inflammatory cytokines, recruiting more leukocytes and perpetuating inflammation. Macrophages uptake lipoproteins in the plaque, transforming into foam cells and forming the necrotic core. Macrophages also digest plaque molecules, presenting them as antigens and working in conjunction with helper T cells to secrete pro-inflammatory cytokines, which further contribute to inflammation, and proteolytic enzymes, which degrade the

extracellular matrix (ECM) of the plaque. Although a large plaque has the potential to occlude the vessel, the most common clinical manifestation of atherosclerosis is plaque rupture, resulting from a thinned fibrous cap along with a large necrotic core. The subsequent thrombus formation often leads to myocardial infarction or stroke [19]. More vulnerable plaques have higher macrophage contents [20], reinforcing their important role not only in plaque growth but in a plaque's risk of rupture.

CDH11 has been found to be expressed by macrophages involved in both pulmonary and dermal fibrosis [21], [22]. Although there is not a complete understanding of the role of CDH11 in immune cells, CDH11 often exhibits a relationship with inflammation. CDH11 expression correlates positively with macrophage content in rheumatoid arthritis, and pharmacological treatment of inflammation decreases CDH11 expression [23]. Pharmacologically targeting CDH11 also resulted in decreased interleukin (IL)-6 expression in a mouse model of hypodermal fibrosis [10]. Furthermore, mechanobiology is known to impact macrophage behavior and function [24], [25]. Being involved in the communication of mechanical cues, CDH11 has the potential to impact macrophage mechanotransduction and subsequent signaling changes, as well. Although current research indicates a role for CDH11 in inflammation, it has been difficult thus far to separate that role from the well-established importance of CDH11 in fibrotic processes. Due to a relative lack of fibroblast involvement in plaque progression, atherosclerosis makes an ideal candidate to examine CDH11 in the immune response, isolated from fibrosis. However, the role of CDH11 in the atherosclerotic immune response has been previously unexplored. Furthermore, due to the promising nature of CDH11 as a

therapeutic target in a number of diseases, a more comprehensive understanding of the impact of CDH11 on the immune response is needed.

CAVD is another cardiac disease which has a proven relationship to CDH11. CAVD progresses when the resident aortic valve interstitial cells (AVICs) undergo myofibroblast differentiation, increasing their contraction and ECM deposition. Subsequent cell apoptosis and tissue remodeling leads to thickening of the valve and impaired cardiac function [26]. CDH11 is upregulated during myofibroblast activation, and human calcified valves exhibit increased CDH11 expression [27]. Furthermore, pharmacological targeting of CDH11 improved cardiac function in a mouse model of CAVD [28]. Although primarily driven by AVICs, aortic valve endothelial cells (AVECs) have been shown to have an impact on disease progression as well [29]. Calcification forms preferentially on the fibrosa, the side of the valve which faces the aorta. Each side of the valve experiences drastically different flow patterns, with the aorta-facing side being exposed to low shear stress recirculatory flow and the ventricle-facing side being exposed to high shear stress unidirectional flow [30]. Due to the side-specific calcification observed in CAVD, it is believed that these differing mechanical stresses affect the pathological progression. AVECs, in particular, are posed to be most affected by the differing shear stress patterns, and AVECs isolated from either side of the valve demonstrate distinct gene expression profiles [29].

Although the importance of CDH11 in the AVIC mechanotransduction of CAVD is known, little is known about its role in the endothelium. CDH11 is known to be mechanically altered in endothelial cells (ECs), with unidirectional flow decreasing expression in vascular ECs [11]. Evidence has suggested that RhoA/Rho kinase (ROCK)

activation, a regulator of cell contractility, is downstream of CDH11 [15], [31], and, although CDH11 has been implicated in the contraction of fibroblasts, it has previously not been studied in ECs [27]. A further understanding of the impact of CDH11 in AVECs could contribute to improved therapeutic targeting in the treatment of CAVD.

My doctoral work has been focused on furthering the understanding of the mechanobiology of CDH11 in CVD. As the majority of my time was spent on researching CDH11 in atherosclerosis, that is reflected in this dissertation. Chapter 2 provides background on CDH11 biology, the progression of the diseases addressed in this work, and the relevance of CDH11 to their development. Chapter 3 explores the importance of mechanobiology in macrophage behavior and function. Chapters 4 through 6 address Aim 1 and 2, focusing on CDH11 in the atherosclerotic immune response, specifically with respect to macrophages and their biomechanics. Chapter 7 addresses Aim 3, focusing on the impact of CDH11 in AVECs and potential ramifications for CAVD. Chapter 8 discusses the impact of this work and possible future directions.

This work will address the following specific aims:

Specific Aim 1: Identify the effect of targeting cadherin-11 on the atherosclerotic immune response.

Specific Aim 2: Determine the role of cadherin-11 in macrophage migration.

Specific Aim 3: Investigate the role of cadherin-11 on endothelial cell contractility in aortic valve endothelial cells.

CHAPTER 2

Background: Cadherin-11 in Cardiovascular Disease

2.A—Cardiovascular Disease

CVD represents the leading cause of death in the United States and a substantial economic burden. The cost of CVD in 2010 was estimated to be over $500 billion in the United States and over $850 billion worldwide. Two common CVDs which represent serious health burdens are atherosclerosis and CAVD. Ischemic heart disease, considered an atherosclerotic CVD, is the world's leading cause of death and makes up nearly 85% of cardiovascular deaths and 28% of all deaths [1]. Atherosclerosis, which is the build-up over time of lipid plaques in arteries, develops over decades, often beginning as early as childhood and adolescence [4]. It can lead to myocardial infarction, stroke, ischemic gangrene, coronary artery disease, abdominal aortic aneurysm, and heart failure, and it is considered the underlying cause of most CVD [18]. Atherosclerotic plaque rupture and thrombosis is the primary cause of most myocardial infarction mortality [3]. Additionally, CAVD, characterized by a thickening of the aortic valve, affects 25% of people over 65. Treatment often necessitates valve replacements, due to the lack of pharmacological treatment. Because of the advanced age of most patients, surgical intervention is not an ideal solution, and a better understanding of the molecular mechanisms at play could lead to the development of pharmacological options [26].

2.B—Cadherin-11

CDH11 is a type II (atypical) classical cadherin, a calcium-dependent cell-cell adhesion molecule [14]. CDH11, and cadherins in general, function by forming a homotypic interaction between itself and the extracellular portion of an identical cadherin on a neighboring cell [32]. Strong cell-cell adhesion is possible through connection from the intracellular portion of CDH11 to the actin cytoskeleton via the cytoplasmic cell-adhesion complex. β-catenin and γ-catenin bind to the same site at the carboxyl terminus [33], and p120-catenin binds to the juxtamembrane domain in the cytoplasmic tail [8]. α-catenin then binds to β-catenin or γ-catenin, connecting CDH11 to the cytoskeleton [33]. These signaling interactions are illustrated in **Figure 2.1** below. It has been suggested that CDH11 plays a role in several important functions during embryonic development, including differential cell sorting, migration, invasion, and epithelial-to-mesenchymal transition [14], [21], and increased CDH11 expression is frequently associated with myofibroblast differentiation in wound healing or in pathogenesis [27]. CDH11 has also been implicated in a variety of conditions with inflammatory components, including fibrosis [21], [22], rheumatoid arthritis [34], CAVD [27], and post-myocardial infarction scar formation [35].
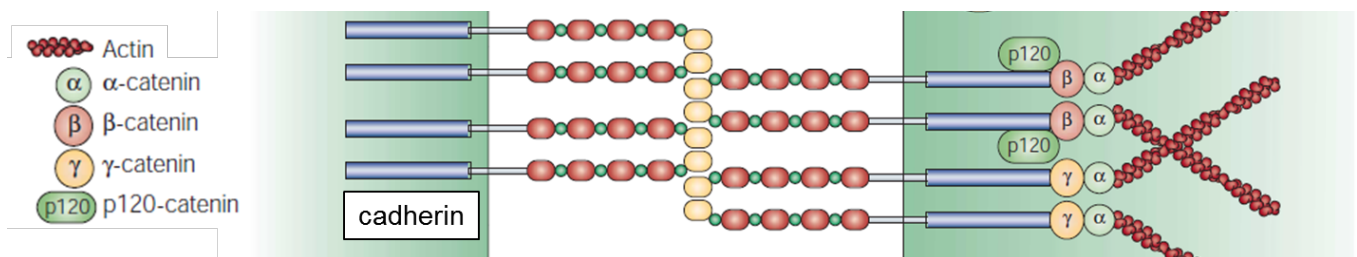
Figure 2.1. An example of cadherin engagement and subsequent anchoring to the actin cytoskeleton. Adapted from [33] with permission.

2.C—Cadherin-11 in Disease

2.C.1—Fibrosis

Schneider et al. demonstrated that patients with pulmonary fibrosis had increased expression of CDH11 in their lung tissue, while healthy patients had no detectable CDH11 protein. A mouse model of pulmonary fibrosis yielded similar results, with CDH11 expressed by fibroblasts, alveolar epithelial cells, and alveolar macrophages. *Cdh11*$^{-/-}$ mice had less fibrosis development, and similarly, animals treated with a CDH11 blocking antibody also had decreased fibrotic tissue [21]. Additionally, Wu et al. showed that patients with scleroderma, a fibrotic disease of the skin and internal organs, also expressed higher levels of CDH11 in the fibroblasts and inflammatory cells in their skin. Both *Cdh11*$^{-/-}$ mice and WT mice treated with a CDH11 blocking antibody resulted in a reduction in fibrosis [22]. Both of these studies posit that the anti-fibrotic effect is mediated by a decrease in macrophage-produced transforming growth factor β (TGF-β), which induces myofibroblast differentiation, and a decrease in the migration and ECM deposition by fibroblasts, via pathways both dependent on and independent of TGF-β [21], [22].

2.C.2—Rheumatoid arthritis

Similar to the fibrosis studies, Lee et. al found that arthritic mice expressed increased levels of CDH11 in the synovial lining, and that both genetically targeting CDH11 and administering a CDH11 blocking antibody reduced inflammation and the severity of arthritis, potentially by reducing the migratory and invasive capabilities of the fibroblast-like synoviocytes [8], [34].

2.C.3—Myocardial infarction

Schroer et. al demonstrated that the CDH11 blocking antibody reduced excessive scar formation and improved cardiac function post-myocardial infarction, as shown in **Figure 2.2**. This study posited that the improved outcomes were due to a disruption in the interaction between cardiac fibroblasts and macrophages, resulting in decreased inflammation and ECM deposition [35].
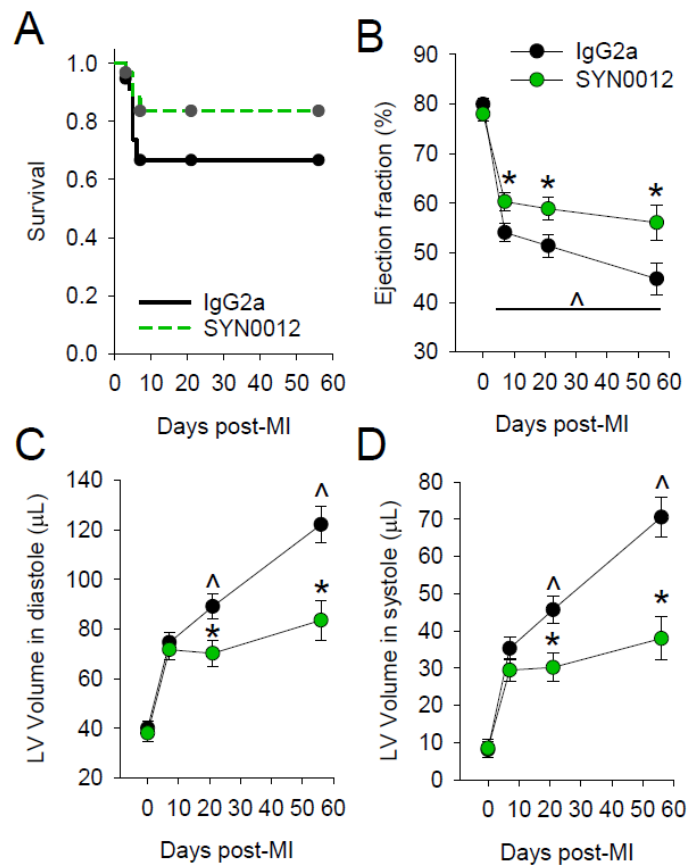
Figure 2.2. Results from mice treated with a CDH11 blocking antibody (SYN0012) and an isotype control (IgG2a) following myocardial infarction (MI). Mice treated with SYN0012 exhibited improved cardiac function up to eight weeks post-MI, demonstrated by increased survival (**A**), ejection fraction (**B**), LV volume in diastole (**C**), and LV volume in systole (**D**).(* indicates $p<0.05$ between treatments; ^ indicates $p<0.05$ between timepoints) Adapted from [35] with permission.

2.D—Atherosclerosis Progression

Atherosclerosis typically initiates when there is a high concentration of cholesterol in the blood. Due to this increased burden, lipoproteins migrate through the EC monolayer

and infiltrate the vessel intima. The development of atherosclerosis is predominantly due to the subsequent inflammatory response. The oxidation theory of atherosclerosis states that, upon infiltration, these lipoproteins are oxidized and otherwise broken down into biologically active phospholipids, which activate the ECs [18]. The early results from this lipid accumulation are known as fatty streaks [20]. Additional factors which could result in EC activation and, as such, are considered risk factors for atherosclerosis include hypertension, smoking, obesity, an unhealthy diet, insulin resistance, and inflammation [3]. Upon activation, ECs increase their expression of several leukocyte adhesion factors, particularly vascular cell adhesion molecule-1 (VCAM-1) [18], which is critical for binding monocytes and lymphocytes [36].

As leukocytes are rolling along the vessel wall, they attach to the upregulated leukocyte adhesion factors and are able to migrate into the intima. Once inside the plaque, leukocytes release additional chemokines, which, in turn, contribute to the recruitment of more immune cells. Inside the plaque, macrophages uptake oxidized low-density lipoprotein (oxLDL), transforming into foam cells and, later, undergoing apoptosis and forming the necrotic core. Activated macrophages secrete pro-inflammatory cytokines, which further compound the inflammation [18]; coagulation factors, which increase the thrombogenicity of the plaque [3]; and proteolytic enzymes, which degrade the ECM of the surrounding plaque [18].

During plaque formation, vascular smooth muscle cells (SMCs) proliferate and increase their production of collagen, resulting in a fibrous cap covering the plaque. The degradation of this fibrous cap due to the activity of proteolytic enzymes produced by the activated macrophages causes the plaque to become less stable and more prone to

rupture. Upon rupture, the inside of the plaque is exposed to the clotting factors in the blood, leading to the formation of a thrombus, which often results in myocardial infarction. **Figure 2.3** shows the initiation, progression, and thrombosis of an atherosclerotic plaque. This thrombus formation is the greatest clinical risk associated with atherosclerosis. Although large plaques can cause stenosis of the vessel, often even very large plaques are asymptomatic. Therefore, the greatest risk comes from unstable plaques with a thin fibrous cap, often containing a large number of activated macrophages [18].
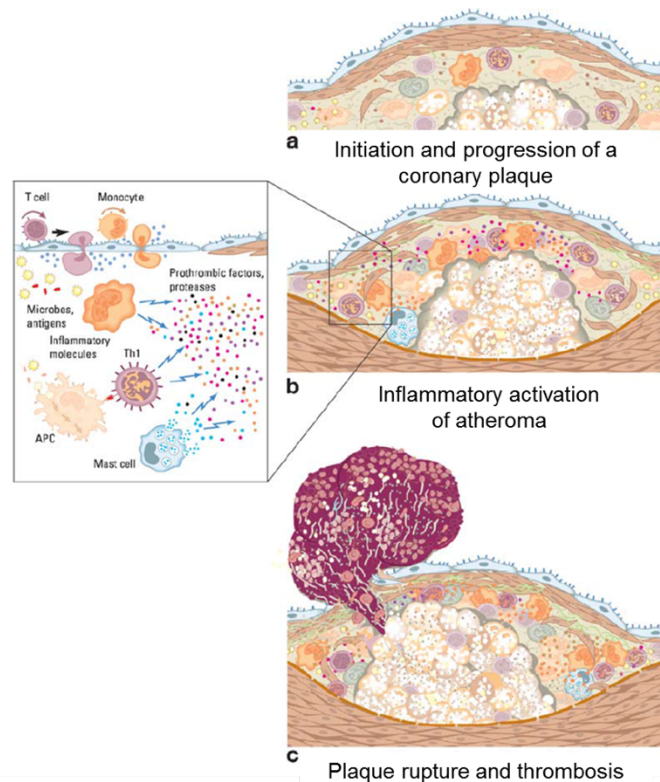
Figure 2.3. An illustration of the initiation, progression, and ultimate rupture of an atherosclerotic plaque. Adapted with permission from [18].

The main cell types involved in the initiation, progression, and thrombosis of atherosclerotic plaques are ECs, SMCs, adventitial fibroblasts (AFs), and immune cells. The specifics of their roles in disease progression are outlined below.

2.D.1—Endothelial Cells

One of the earliest initiating factors of atherosclerosis is endothelial dysfunction, characterized by an imbalance between endothelial-derived relaxing and contracting factors, and the subsequent endothelial activation [37]. A number of factors can induce EC dysfunction and activation, including hypertension, smoking, obesity, an unhealthy diet, and insulin resistance [3]. Treatment for any one of these risk factors has been shown to improve endothelial dysfunction and clinical outcomes [38]. Upon activation, the EC monolayer demonstrates increased permeability. [39] and increased expression of leukocyte adhesion [18] and procoagulant molecules [39]. It is believed that in some way all of these risk factors affect the endothelium by inhibiting endogenous atheroprotective signaling in ECs. A common underlying consequence of each of these factors is oxidative stress, leading to increased production of reactive oxygen species that degrade and inhibit the synthesis of nitric oxide [37], [40]. For example, angiotensin II, a vasoconstrictive molecule associated with hypertension, can increase the production of reactive oxygen species from both ECs and SMCs [36]. Nitric oxide is an anti-inflammatory molecule that inhibits the expression of pro-atherogenic molecules, such as VCAM-1 [36], [41] and tumor necrosis factor (TNF-α) [38], and inhibits SMC proliferation [40], [41]. Because of its protective characteristics, the decrease in bioavailability of nitric oxide can result in increased inflammation and the promotion of atherosclerosis [40].

It is also believed that shear stress and flow play a role in EC activation and inflammation [18]. Under steady, uniform shear stress, ECs produce nitric oxide, while atherosclerotic plaques are found in higher density in regions with disturbed flow, such as branch points and bifurcations [38]. ECs are able to sense mechanical signals via a complex containing platelet endothelial cell adhesion molecule-1 (PECAM-1), vascular

endothelial cadherin (VE-cadherin), and vascular endothelial growth factor receptor 2 (VEGFR2) [42]. The disturbed flow patterns disrupt EC production of nitric oxide and increase the expression of other leukocyte adhesion molecules, such as intercellular cell adhesion molecule-1 (ICAM-1). Both of these factors increase leukocyte infiltration of the plaque, inflammation, plaque development, and risk of rupture [36]. Shear stress is also capable of modulating NFκ-B signaling pathways, further contributing to inflammation [43].

EC activation initiates the subsequent inflammatory response characteristic of atherosclerosis. Leukocytes roll along the vessel via interactions with selectins on the endothelium. Chemokines, such as monocyte chemoattractant protein-1 (MCP-1), IL-8, chemokine ligand 5 (CCL5 or RANTES), and macrophage inflammatory protein-1 (MIP-1) α/β, secreted by ECs, SMCs, or immune cells, signal for activation of integrins on the surface of leukocytes and increased attachment to the endothelium. The more firmly adhered leukocytes now bind to adhesion factors on the surface of ECs, including VCAM-1 and ICAM-1 [39], both upregulated during EC activation [18], [36]. Leukocytes then migrate through the endothelium either paracellularly, through cell-cell contacts, or transcellularly, through the body of the cell. Binding to VCAM-1 promotes Rac1 activation, and binding to ICAM-1 promotes the activation and p38 and Rho [39].

RhoA, activated by the binding of leukocytes to ICAM-1, is a member of the Rho GTPases that has been heavily studied in ECs. RhoA and its downstream target ROCK are involved in the regulation of cell adherence, migration, proliferation, and contraction [37]. Cadherin engagement, including VE-cadherin, N-cadherin, and epithelial cadherin (E-cadherin), has been shown to sometimes be an activator of RhoA [44]. RhoA/ROCK

13

activation has been implicated in several processes relevant to atherosclerotic development. ROCK activation was shown to decrease expression of endothelial nitric oxide synthase, a hallmark of endothelial dysfunction, and it can also prevent the dephosphorylation of myosin light chain, resulting in increased SMC contraction [37]. Furthermore, ROCK activation has been shown to transcriptionally regulate the expression of the chemokines IL-8 and MCP-1, which can recruit immune cells to the site of plaque formation [45]. Interestingly, disturbed flow, a risk factor for plaque formation, is also an activator of RhoA/ROCK signaling [37]. Statins, a common treatment given to patients with high cholesterol, have been shown to inhibit ROCK activation and decrease endothelial dysfunction in humans [46]. Although a certain level of RhoA/ROCK signaling is necessary for typical endothelial function, it is clear that over-activation can promote endothelial dysfunction and increase contraction and permeability, facilitating possible plaque development [37].

The binding of leukocytes to endothelial adhesion molecules and the subsequent signaling activation is believed to increase endothelial permeability by altering endothelial cell-cell junctions, which include a variety of proteins such as PECAM-1, VE-cadherin, junctional adhesion molecules, and CD99 [39]. It has been suggested that endothelial PECAM-1 may bind to leukocyte PECAM-1, facilitating leukocyte infiltration, while VE-cadherin resists their migration. ECs also appear to decrease their substrate adhesion upon monocyte attachment, further enhancing transmigration. Hashimoto et al. proposed that oxLDL stimulation of ECs resulted in increased leukocyte invasion by increasing PECAM-1 and decreasing VE-cadherin [47]. However, the mechanism by which leukocytes migrate through the endothelial layer is still not completely understood [39].

An additional mechanism through which ECs can affect atherosclerosis development is endothelial-to-mesenchymal transition (EndMT). EndMT is a phenotypic switch in ECs that is a key process in development, but can sometimes reappear under pathological conditions [48]. Zeisburg et al. demonstrated that TGF-β-induced EndMT is involved in the process of cardiac fibrosis [49]. Two studies using two different mouse models of atherosclerosis have demonstrated increased levels of EndMT, and another study used lineage-tracing to suggest that ECs having undergone EndMT contributed to the formation of the neointima. EndMT is typically regulated by TGF-β, and inhibition of TGF-β has been shown to reduce EndMT and neointima formation. In addition to contributing to the neointima, the process of EndMT could also result in endothelial dysfunction and increased endothelial permeability, consequently facilitating leukocyte transmigration [48].

2.D.2—Smooth Muscle Cells
During the disease state, SMCs dedifferentiate from a quiescent phenotype into a more proliferative "synthetic" phenotype. In this state, SMCs decrease their contractility and increase their proliferation, migration, and ECM production [50]. Upon switching phenotypes, SMCs migrate from the media into the intima, where they proliferate and increase their synthesis of ECM proteins. This switch is often mediated by platelet-derived growth factor (PDGF)-BB, TGF-β, and bone morphogenic protein (BMP). PDGF-BB promotes the switch to the proliferative state, while TGF-β, an atheroprotective cytokine, and BMP encourage the maintenance of the contractile, quiescent state. An imbalance in this phenotype switching contributes to atherosclerotic plaque development, and better maintenance of SMC phenotype could help reduce plaque burden [51].

SMC phenotype switching and the subsequent proliferation contribute to the progression of atherosclerotic lesions [41] and eventual arterial stenosis [52], but it is also essential to the formation of a stable plaque with a thick fibrous cap [50]. On one hand, SMC proliferation and ECM production can be detrimental to the plaque, even potentially causing occlusion of the vessel [52]. Additionally, disturbed flow patterns and the resulting abnormal wall stresses, common to regions of atherosclerotic plaque development, can induce SMCs to produce proteoglycans, which bind to and increase the retention of lipoproteins [36]. Furthermore, evidence suggests that the interaction between SMCs and macrophages could also contribute to immune cell retention and facilitate inflammation [53]. On the other hand, without the formation of a stable, thick fibrous cap, atherosclerotic plaques are much more prone to rupture [18]. Genetic knockdown of an SMC transmembrane protein, CD98, involved in proliferation resulted in similarly sized but more vulnerable plaques compared to controls. The knockdown plaques had larger necrotic cores and decreased collagen content, likely making them less stable and more prone to rupture [54]. Genetic knockdown of periostin, another ECM protein, resulted in smaller plaques, but disproportionately smaller fibrous caps [50]. There is a cost/benefit tradeoff with SMC proliferation, and the tipping point of this scale is not well understood.

Within the plaque, anti-inflammatory cytokines, predominantly TGF-β, stimulate SMC collagen production [52], while pro-inflammatory cytokines, such as interferon-γ (IFN-γ), inhibit SMC collagen production [41]. EC dysfunction and the associated reduction in nitric oxide, which also functions to keep SMCs in their quiescent phenotype, can also affect SMC collagen production [41].

In addition to more proliferative SMCs, atherosclerotic plaques also contain a large number of dead SMCs, having undergone apoptosis. Apoptosis can be signaled in SMCs by oxLDL accumulation [51] or excess nitric oxide produced by macrophages [20]. The death of SMCs reduces the vessel's repair capabilities, decreasing collagen production and plaque stability [41]. Vulnerable plaques have been shown to contain increased levels of apoptotic SMCs [20], and the most common region of rupture, the plaque shoulder, often has high levels of apoptotic SMCs and few live SMCs [51]. An animal model of vascular SMC apoptosis demonstrated that, while in healthy mice, SMC apoptosis did not result in increased inflammation, in atherosclerotic mice, SMC apoptosis resulted in an increased inflammatory response coupled with a marked thinning of the fibrous cap, indicating that SMC death can contribute to disease development and plaque vulnerability [20].

2.D.3—Adventitial Fibroblasts
Comparatively little focus has been given to the role of the adventitia, the outermost layer of the vessel wall, in vascular inflammation. It is generally thought to function predominantly as support [55]. In atherosclerosis progression, most of the focus is given to what is happening within the intima and the media layers, in what is called the "inside-out" hypothesis. However, some studies have shown a very early inflammatory response in the adventitia, leading to the postulation of an "outside-in" response. A positive relationship has been demonstrated between adventitial inflammation and atherosclerosis development, and some studies have demonstrated increased adventitial inflammation associated with less stable plaques [56]. One study demonstrated early AF activation in a mouse model of atherosclerosis and saw the earliest expression of genes for the chemokine MCP-1 (*JE*) and its receptor (*CCR2*) in the adventitia [55]. Other

studies have observed altered ECM in the adventitia during the development of atherosclerosis, along with an early proliferative change in AFs, although the mechanism is unclear [57]. Furthermore, the adventitia has been shown to contain a high level of lymphocytes, particularly T cells [58]. AFs could also contribute to endothelial dysfunction and inflammation via the production of reactive oxygen species by NADPH (nicotinamide adenine dinucleotide phosphate) oxidase activation [59]. Certain NADPH oxidases correlate with age and atherosclerosis progression in humans [60].

The contribution of AFs has been more widely studied in post-angioplasty neointima formation, where it has been shown that AFs can make up half of the neointima [61], [62]. Post-angioplasty, AFs demonstrate an increase in their expression of alpha smooth muscle actin (α-SMA), indicating a differentiation into the more contractile myofibroblast phenotype. Increased proliferation and myofibroblast differentiation, leading to an increase in pro-inflammatory cytokines and growth factors, has been observed in other CVDs. TGF-β, a cytokine present in atherosclerotic plaques, is a known stimulator of myofibroblast differentiation, and it could also function to attract myofibroblasts and induce migration, along with PDGF and MCP-1 [63]. Notably, two of the same growth factors, PDGF and TGF-β, induce both myofibroblast differentiation in AFs and dedifferentiation in SMCs. Dedifferentiated SMCs do exhibit many similar characteristics to myofibroblasts, and it has been postulated that all of these cell types originate from a common progenitor. Additionally, migration of myofibroblasts has been shown to be facilitated by matrix metalloproteinase (MMP) degradation of ECM, a common symptom of inflamed atheromas [64]. Myofibroblasts also exhibit an increased production of ECM proteins, particularly collagen. TGF-β inhibition in mice post-balloon

angioplasty resulted in decreased restenosis, decreased constrictive remodeling, and increased collagen deposition in the adventitia, indicating that TGF-β inhibition reduced AF myofibroblast differentiation. Although the mechanism has not been fully elucidated yet, mounting evidence indicates that the adventitia plays a role in vascular inflammation, neointima formation, and the progression of atherosclerosis [63].

2.D.4—Immune Cells
The two main immune cells migrating into the plaque are monocytes and T cells. Monocytes make up the largest portion of immune cells in the plaque [3]. They are recruited to the site by chemokines, including MCP-1, which binds their receptor, CCR2 [18]. Genetically ablating either MCP-1 or CCR2 results in decreased plaque development [65]. The activated EC monolayer has increased expression of VCAM-1, promoting monocyte binding and enabling them to infiltrate. As the monocytes move into the plaque, macrophage-colony-stimulating factor stimulates them to differentiate into mature macrophages. Consequently, they upregulate their pattern recognition receptors, including both scavenger receptors and toll-like receptors (TLRs) [18].

Scavenger receptors are responsible for the phagocytic action of macrophages; they bind to molecular markers on pathogens, and the macrophage engulfs the foreign body for digestion. In addition to pathogens, certain scavenger receptors also recognize oxLDL, and internalize it [18]. In particular, the scavenger receptors SR-AI, CD36 [20], and LOX-1 [41] are believed to be important in this oxLDL uptake. A mouse model of LOX-1 overexpression resulted in increased vascular inflammation and atherosclerotic-like plaques in the heart [20]. The expression of ATP-binding cassette transporters ABCAI and ABCGI, which both contribute to removing cholesterol from the cell after ingestion, is inhibited by the pro-inflammatory cytokines being secreted in the plaque. Therefore, the

macrophages retain these lipids, resulting in the formation of what are known as foam cells, due to the lipid "bubbles" in their appearance [66]. Foam cells produce pro-inflammatory cytokines, which further recruit immune cells to the site of the atheroma and stimulate macrophage proliferation [41]. Eventually, these lipid-laden foam cells undergo apoptosis, resulting in the formation of the necrotic core of the plaque [20].

Alternatively, TLRs do not assist in phagocytosis. Instead, they bind to pathogen-like molecular markers and stimulate activation of the macrophage. It is thought that several molecules present in the plaque may be capable of binding to TLRs, including oxLDL and heat shock protein 60. The resultant macrophage activation sets off a chain of signaling that accelerates plaque development, and inhibiting TLRs has been shown to decrease atherosclerosis [18]. In disease, both macrophages and ECs exhibit increased levels of TLRs, and genetically targeting TLR2 and TLR4 signaling resulted in decreased inflammation and plaque development [20]. Additionally, the signaling of TLR3 and TLR4 can downregulate the expression of ABCA1, which contributes to cholesterol transport from the cell. In this way, TLR3 and TLR4 prevent the export of cholesterol from macrophages and, therefore, increase the formation of foam cells [20].

Macrophage activation can lead to the release of reactive oxygen species, which contribute to further oxLDL production [18] and endothelial dysfunction [40]; vasoactive molecules, such as nitric oxide; proteolytic enzymes, which break down the ECM of the plaque; pro-inflammatory cytokines, which exacerbate inflammation [18]; and coagulation factors, which increase the risk of thrombus formation [3]. Proteolytic enzymes, such as MMPs, degrade the collagen of the plaque and cause thinning of the fibrous cap. Vulnerable plaques have been shown to have higher levels of activated macrophages

and to exhibit increased expression of certain MMPs, including MMP1, MMP2, MMP3, MMP8, MMP9, and MMP13 [20], [67]. **Figure 2.4** depicts the process of macrophage activation inside an atherosclerotic plaque.
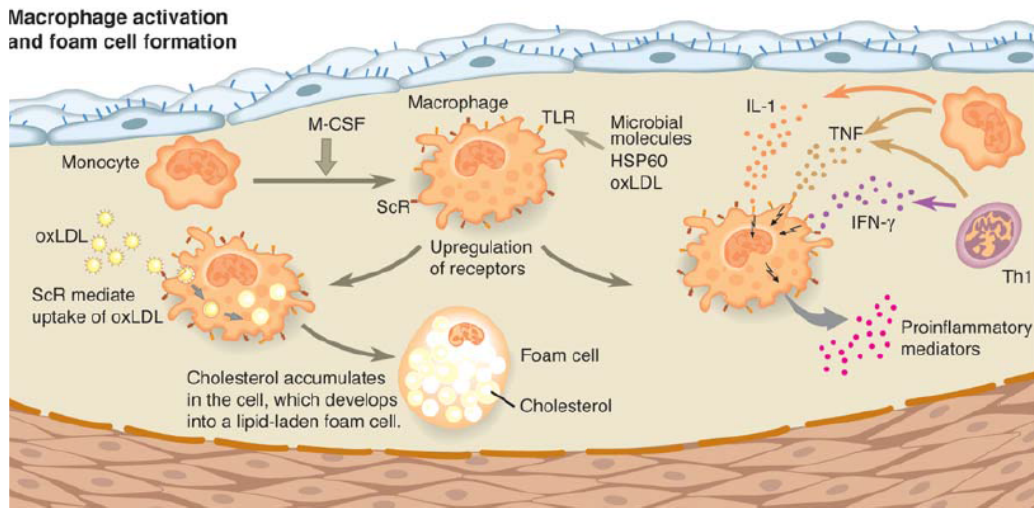
Figure 2.4. A representation of macrophage activity once leukocytes have infiltrated an atherosclerotic plaque. Adapted with permission from [18].

The second most abundant immune cell within atherosclerotic plaques is the T cell. T cells are recruited to the plaque similarly to monocytes. Chemokines which attract T cells include MCP-1, binding CCR2 on T cells; RANTES, binding CCR1 on T cells; and IP-10 (C-X-C motif chemokine ligand- (CXCL)10), monokine induced by IFN-γ (Mig or CXCL9), and IFN-inducible T cell α-chemoattractant (I-TAC or CXCL11), all binding to CXCR3 on T cells. Pharmacological targeting of RANTES has been shown to reduce plaque burden. As with macrophages, T cells also utilize VCAM-1 to adhere to the activated EC layer and migrate into the plaque in response to these chemokines [18].

Most of the T cells found in atherosclerotic lesions are CD4+ T helper (T_h) cells, with a much smaller fraction of CD8+ cytotoxic T (T_c) cells. T_h cells work in concert with

macrophages in order to perpetuate macrophage activation and an ongoing immune response. Macrophages, as antigen-presenting cells, present an antigen using their major histocompatibility complex class II molecules. T cells use costimulatory receptors; first, they bind to the antigen and then to a second surface protein for validation. Upon confirmation, T_h cells release the cytokine IL-2, which increases T_h cell proliferation specific to that antigen [18], and the macrophage is activated, releasing proinflammatory cytokines, procoagulant molecules (such as tissue factor), and proteolytic enzymes (such as MMPs) [41]. The T_h cells then mature into effector, memory, or regulatory T_h cells. 10% of the T cells found in human plaques bind to oxLDL as an antigen. Other T cell antigens identified include HSP65/60, found in certain pathogens, and *Chlamydia pneumonia*. Heat shock protein 60 is a human protein found in atherosclerotic plaques, and T cells specific to pathogenic HSP65/60 cross-react with human heat shock protein 60 [18]. Lipopolysaccharide (LPS), a protein found in *Chlamydia pneumonia*, also increases macrophage uptake of oxLDL, which is thought to be mediated by the TLR2 receptor [20]. Genetically disrupting any of the interactions required for T cell binding to antigen-presenting cells results in a reduction in atherosclerosis [18].

During T cell proliferation, T_h0 cells can differentiate into either T_h1 or T_h2 cells. T_h1 cells are pro-atherogenic and are more commonly found in plaques, while T_h2 cells tend to be atheroprotective [68]. T_h1 cells produce some of the major pro-inflammatory cytokines present in plaques, including IFN-γ and TNF-α [69]. Preventing T_h1 differentiation via loss of a transcription factor results in decreased atherosclerosis. Regulatory T_r1 cells may also be present in plaques, functioning in an atheroprotective manner by controlling inflammation and decreasing atherosclerosis [18]. However,

studies have shown that a high level of cholesterol in mice decreases the number of regulatory T cells in the vessel wall, preventing their anti-inflammatory effect [68].

Plaque rupture and subsequent thrombus formation are the main clinical risks associated with atherosclerosis. Macrophages and T cells are often found close to each other in shoulder regions, where the plaque expands and most commonly ruptures. Activated macrophages and T cells produce pro-inflammatory cytokines, proteases, coagulation factors, reactive oxygen species, and vasoactive molecules, all of which prevent the production or induce the breakdown of a stable fibrous cap and, therefore, increase risk of rupture [18].

2.E—Cadherin-11 in Atherosclerosis

Several of these CDH11-associated diseases share characteristics with atherosclerosis, including inflammation, ECM deposition, and myofibroblast-like cells, indicating the potential for a role for CDH11 in atherosclerosis. TNF-α, a key pro-inflammatory cytokine involved in the disease progression of atherosclerosis, has been shown to drive CDH11 expression in rheumatoid arthritis models [8]. Additionally, *Cdh11*^{−/−} mice exhibit decreased collagen and ECM deposition, a process involved in the progression of complex fibrous atherosclerotic plaques, in both models of pulmonary fibrosis [21] and rheumatoid arthritis [8]. In fact, rheumatoid arthritis and other chronic inflammatory disease are often considered risk factors for the development of atherosclerosis [68].

2.E.1—Immune cells

Studies have demonstrated a correlation between CDH11 expression and immune cell infiltration. In rheumatoid arthritis synovial samples, CDH11 correlated strongly with

the presence of macrophages, and in lung tissue samples of rheumatoid arthritis-associated interstitial pneumonia, CDH11 expression correlated strongly with CD4+ cells. Anti-inflammatory therapeutics also resulted in a decrease in CDH11 expression in synovial tissue [23]. Not much is known about the specific role of CDH11 in immune cells, but it has been found in alveolar macrophages in pulmonary fibrosis [21], macrophages in dermal fibrosis, and in bone marrow-derived macrophages [22]. CDH11 could potentially affect immune cell function in atherosclerotic plaques via altered signaling or interactions between immune cells and ECs or SMCs. Schroer suggested that the improved outcomes post-myocardial infarction in CDH11 blocking antibody-treated mice were due to a disruption in the binding of macrophages to cardiac fibroblasts [35]. CDH11-facilitated binding to ECs could improve leukocytes transmigration. Furthermore, studies have shown that SMCs are also capable of interacting with macrophages, and, in doing so, they increased macrophage retention and prevent apoptosis [53]. CDH11 could also potentially facilitate this interaction. However, the role of CDH11 in immune cell function needs to be investigated more.

2.F—Calcific Aortic Valve Disease Progression

CAVD is characterized by tissue remodeling of the aortic valve and is divided into two categories: aortic sclerosis, a thickening of the valve without obstruction of blood flow, and aortic stenosis, a more severe calcification of the valve which causes obstruction. Aortic sclerosis affects more than 25% of those over the age of 65, and, while the more serious aortic stenosis affects a smaller percentage of patients, it is the second most common cause for cardiac surgery [70]. Although it was previously believed to be the

result of passive tissue degeneration, research now shows that there is an active cellular and molecular pathogenesis involved in valve calcification [71].

The aortic valve consists of three layers: the fibrosa, facing the aorta and composed mainly of collagen; the ventricularis, facing the ventricle and composed of elastin; and the spongiosa in between. The aortic valve undergoes constant mechanical forces, with cyclic strain and shear stress from blood flow. Valve calcification preferentially forms on the side of the fibrosa, which is exposed to recirculatory flow patterns, indicating that hemodynamics can impact disease development. One of the earliest initiating factors in CAVD, similar to atherosclerosis, is believed to be endothelial dysfunction [72]. Alterations in both shear stress and strain can initiate activation to the endothelium and subsequent dysfunction [73]. Furthermore, studies have shown that the aortic valve is very sensitive to this mechanical strain, and it can impact tissue remodeling and signaling. Patients presenting with bicuspid valves, which are exposed to increased mechanical forces, are diagnosed on average 20 years sooner [72], and cyclic stretch has been shown to increase *ex vivo* proliferation and collagen deposition in porcine aortic valves [74]. For these reasons, mechanical forces and mechanotransduction are of substantial interest in the research of CAVD progression.

CAVD involves an active tissue remodeling, mediated by the differentiation of AVICs into activated myofibroblasts. This differentiation results in an increase in their contractility and ECM deposition. Increased contractility leads to increased intercellular tension, resulting in cellular apoptosis and the formation of calcific nodules [26]. Although this process is primarily driven by AVICs, AVECs are capable of impacting both AVIC behavior and disease progression. In fact, AVECs can prevent myofibroblast

differentiation in AVICs, inducing their quiescence [29], [75]. Although AVIC-differentiation into activated myofibroblasts is often associated with wound healing, when left unabated, this excessive activation results in cell death and calcification via apoptosis [27]. End-stage disease pathology is accompanied by severe calcification of the valve (**Figure 2.5**), necessitating surgical intervention when mechanical dysfunction obstructs blood flow and impairs cardiac output [72].
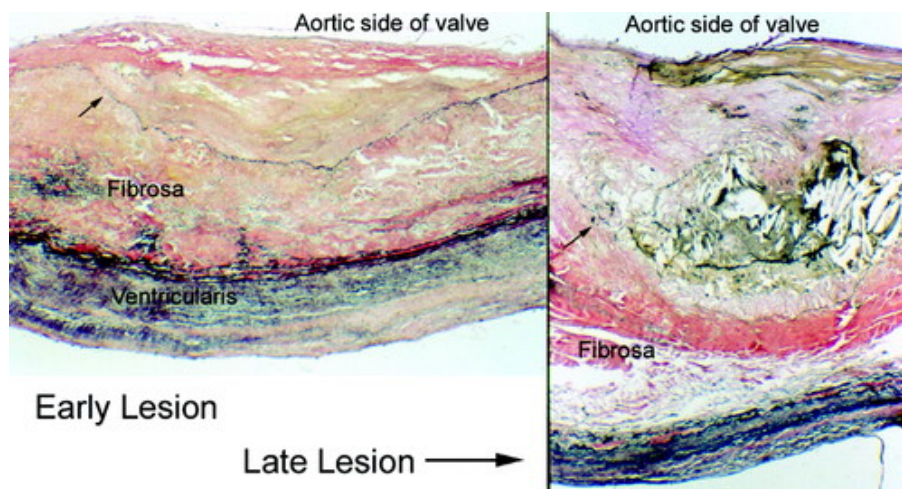
Figure 2.5. An example of early and late-stage CAVD forming on the fibrosa. Adapted from [72] with permission.

2.F.1—Aortic Valve Interstitial Cells

As the primary cell population of the aortic valve, AVICs are believed to be one of the primary drivers of valve calcification. TGF-β, known to be upregulated in calcified valves, promotes AVICs to differentiate into myofibroblasts, resulting in an increase in α-SMA expression [27], accompanied by much higher cell contractility, cytokine secretion, and ECM deposition [76]. Furthermore, the increased contractility of myofibroblasts *in vivo* likely results in activation of latent TGF-β in the surrounding ECM, promoting more differentiation and activation and contributing to disease [26]. This process can also be

26

mechanically regulated. Fisher et. al demonstrated that the highest degree of nodule formation *in vitro* resulted from 24 hours of TGF-β treatment followed by 24 hours of 15% mechanical strain [5]. The increased contractility is also associated with excessive intercellular tension, resulting in membrane disruption and cell apoptosis. Although myofibroblast differentiation is a typical process during wound healing, closely regulated by cytokine secretion and terminated via apoptosis, when left untethered, it can lead to fibrosis and tissue damage. Little to no α-SMA expression can be observed in the AVICs of healthy valves, in contrast to mechanically injured valves with elevated expression [76], and *in vitro* suppression of α-SMA expression prevents the formation of calcific nodules [27]. Increased numbers of myofibroblasts are also associated with matrix disorganization, degeneration, increased proteolytic enzymes, and fibrosis, indicating the crucial nature of myofibroblasts to pathological dysfunction [76]. The research indicates that myofibroblast differentiation of AVICs is a major contributor to the pathogenesis of CAVD and that mechanotransduction can be a significant factor in this process.

2.F.2—Aortic Valve Endothelial Cells
Although AVICs make up the majority of the cells in the aortic valve, AVECs line both the fibrosa, facing the aorta, and the ventricularis, facing the ventricle. Although similar to vascular ECs, AVECs exhibit distinct behavioral differences, such as aligning perpendicular to flow instead of parallel [77]. Because of this, it is important to specifically study AVECs, although this is made challenging by the incredibly difficult isolation due to the size of mouse aortic valves. Endothelial dysfunction is an early initiator in CAVD, indicating the importance of AVECs in disease progression in addition to AVICs [72]. AVECs have been shown to affect AVIC signaling through secretion of chemokines [29],

and *in vitro* co-culture models have proven that AVECs can induce a quiescent phenotype in AVICs [75], suppressing myofibroblast differentiation [29]. Furthermore, elevated TGF-β during disease has an impact on AVECs as well, promoting EndMT [78], which can contribute to CAVD progression [27]. In addition to the mechanical stretch imposed on the valve during the cardiac cycle, each side of the valve is exposed to unique hemodynamic patterns as well. The ventricularis experiences unidirectional high magnitude shear stress, while the fibrosa experiences lower magnitude shear stress with recirculatory flow patterns [30], [79]. **Figure 2.6** illustrates these mechanical forces. Due to the side-specific nature of valve calcification, these disparate flow patterns are suggested to have an impact on disease progression. Reinforcing this hypothesis, AVECs exposed to unidirectional flow, like that typical of the ventricularis, demonstrate anti-calcific gene expression profiles [29], and AVECs of the fibrosa exhibit lower anti-calcific gene expression [30]. Alterations in shear stress can impact EndMT, as well [79]. Despite the primary focus on AVICs and the relative difficulty in isolating AVECs, it is important to consider them in CAVD pathology, as well, as it is clear AVECs can have a significant impact.
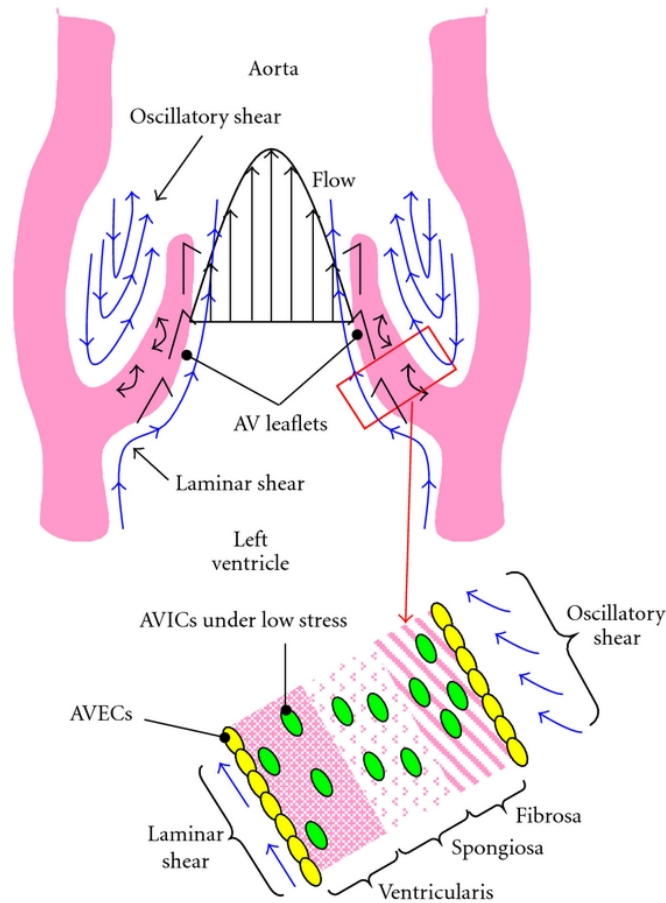
Figure 2.6. An illustration of the mechanical forces exerted on the aortic valve. Adapted with permission from [2].

2.G—Cadherin-11 in Calcific Aortic Valve Disease

CDH11 upregulation is associated with the myofibroblast differentiation occurring during wound healing and, when exacerbated, the pathological progression of valve calcification [80]. Hutcheson et. al investigated the role of CDH11 in CAVD, spurred on by the finding that calcified human aortic valves demonstrated a significant increase in CDH11 expression. They found that increased CDH11 was associated with myofibroblast activation and that CDH11 was an essential component required for the increased cell tension resulting in calcific nodule formation in CAVD [27]. Additionally, a mouse model

of CDH11 overexpression resulted in valve calcification [81], and pharmacological targeting of CDH11 in a mouse model of CAVD improved outcomes [28]. Although it is known that AVECs are capable of influencing AVIC behavior and CAVD progression [29], the role of CDH11 in this process has not been investigated previously. There is a significant body of research investigating the role of CDH11 in AVICs and fibroblasts [16], [27], [80], [82], [83]; therefore, this dissertation is focused on the potential impact of CDH11 expression by AVECs in pathological valve calcification.

2.G.1—Endothelial cells
AVIC contractility is a crucial component of the tissue damage incurred during valve calcification, but there is less understanding of the importance of AVEC contractility. Huynh et. al demonstrated that stiffer substrates can induce increased endothelial cell-cell junction width and vascular EC layer permeability accompanied by an increase in Rho activation, which suggested that increased contractility was the culprit [84]. Although most of the cadherin focus in ECs is given to VE-cadherin, CDH11 is also expressed by ECs [85], although its role has not been thoroughly studied. CDH11 functions uniquely in part because of its strength; CDH11 yields twice the tension as N-cadherin [27]. CDH11 plays a critical role in the contraction of fibroblasts in a range of diseases, and blocking CDH11 with an antibody resulted in decreased contraction in diseased dermal myofibroblasts [17]. CDH11 has also been shown to affect SMC contraction, and *Cdh11*$^{-/-}$ mice exhibited decreased levels of contractility in both bladder and aortic tissue [31]. However, its role in the contraction of ECs has not been previously investigated. Several studies have suggested that RhoA/ROCK pathways are downstream of CDH11 [15], [31], [81]. Alimperti et. al demonstrated that CDH11 immunoprecipitated with ROCK2, indicating that the two are bound directly or indirectly, and knocking down

CDH11 resulted in reduced expression of ROCK1 and ROCK2 [31]. Furthermore, Bowen et. al demonstrated that *Cdh11*-/- mice expressed lower levels of activated RhoA in their aortic valves, and that restoring active RhoA to valve interstitial cells treated with CDH11 siRNA returned their impaired migration to normal [15]. CDH11 overexpression has also been shown to upregulate RhoA in valve interstitial cells [81]. These findings put together indicate that CDH11 is crucial for contractility in several cell types, and therefore, it is reasonable that CDH11 could be involved in endothelial contractility and contribute to calcification.

CHAPTER 3

Background: Macrophage Mechanobiology

3.A—Macrophage Background

First identified by Élie Metchnikoff in the 19th century, macrophages were coined for their expert phagocytic ability [86]–[88]. Macrophages represent a diverse spectrum of cells, both anatomically and functionally [86], [87], and they perform critical tasks both under healthy conditions and in response to injury [86]. Although it was once believed that all resident tissue macrophages developed from circulating monocytes originating in the bone marrow, it is now known that most resident tissue macrophages originated from the yolk sac during development and are a self-sustaining population [87]. These disparate origins of various macrophage populations are one indication of the spectrum of behavior of which they are capable. Although often noted for their role in disease, macrophages are of significant importance to development and homeostasis as well [86]. Macrophages are present in nearly all tissue in adult mammals [88], with responsibilities ranging from digesting apoptotic cells to regulating angiogenesis [86] to the initial response to pathogens [88].

3.B—Macrophage Roles

3.B.1—Development

Often overlooked, macrophages are involved in critical developmental functions. Mouse models deficient in macrophage populations exhibit issues in tissue patterning and branching morphogenesis. Loss of macrophages in the developing bone, for example,

results in osteoporosis. The bone itself forms, but, without the phagocytic activity of macrophages, it lacks the proper cavities required for hematopoiesis. Further structural deficiencies in mice lacking macrophages can be noted in the brain, mammary gland, kidney, and pancreas. Additionally, without macrophage regulation, angiogenesis can result in vascular over-growth during development [86].

3.B.2—Homeostasis

In some ways, acting as the body's "housekeepers" could be considered the macrophage's primary function. Through phagocytosis, macrophages digest apoptotic cells and remove cell debris created during tissue remodeling [88]. Macrophages also regulate the leukocyte population by digesting cells not expressing CD47 and engulfing excessive neutrophils and erythrocytes in the spleen and liver [86]. Furthermore, macrophages play an important role in metabolic homeostasis and in the tissue's response to hypoxia [87]. During an active immune response, leukocytes switch to glycolysis as a fuel source; when macrophages are activated, they induce insulin resistance and increase glucose availability, maintaining homeostasis. Of course, if perpetuated untethered, this process results in chronic low-level inflammation in obesity [86]. In addition to responding to injury, macrophages are critical during healthy conditions as well.

3.B.3—Immune Regulation

The macrophage's primary responsibility is the engulfment of debris and apoptotic cells, and this duty applies to a response to foreign pathogens, as well. However, when this process continues in excess, the subsequent inflammation can cause tissue damage, sometimes severe. MCP-1, secreted by fibroblasts, ECs, vascular SMCs, monocytes, and T cells, is a predominant macrophage recruiter in inflammation. Circulating monocytes

utilize adhesion molecules on the endothelium upregulated during inflammation to infiltrate the tissue. Macrophages use their pattern recognition receptors, scavenger receptors and TLRs, to identify pathogen-associated molecular markers. Scavenger receptors seek to engulf foreign particles for their digestion, while TLRs bind to foreign antigens, resulting in macrophage activation. As antigen-presenting cells, macrophages also connect the innate and adaptive immune systems by presenting foreign peptide fragments to T cells for their activation and antigen-specific proliferation [87]. Although macrophages comprise a component of the body's first line of defense against foreign invasion, when this process continues unrestrained, reactive oxygen species and cytotoxic cytokines, consequents of macrophage activation, can cause tissue damage and contribute to chronic disease [86].

3.B.4—Disease
    Macrophages are involved in a number of chronic diseases. Macrophage infiltration of atherosclerotic plaques plays a crucial role in both their growth and their vulnerability to rupture, often leading to myocardial infarction, and genetically deleting MCP-1, a primary trigger for macrophage chemotaxis, reduces plaque burden [19]. IL-23, a cytokine secreted by macrophages, causes autoimmune joint inflammation in mice. TNF-α, another cytokine secreted by activated macrophages, promotes colonic inflammation, contributing to inflammatory bowel disease [86]. Because of their diverse spectrum of functionality in a number of cellular processes and due to their role in a large number of chronic diseases, understanding macrophage biology for the potential of therapeutic targeting is a significant area of research interest.

3.C—Macrophage Polarization

Macrophages are typically characterized as classically activated (M1) or alternatively activated (M2). This is an imperfect system as macrophages represent a diverse category of cells in every organ on a spectrum of function. In fact, transcriptional profiling of resident macrophages demonstrated high transcriptional diversity, indicating many different subcategories [86]. Nevertheless, the M1/M2 classification system is the predominant method of referring to macrophages with these disparate functions, in place of a better system which has yet to be classified.

3.C.1—Classically activated macrophages (M1)
Classically activated macrophages are also often referred to as pro-inflammatory macrophages. These are often the macrophages which arrive first to the site of injury or infection, initiating the inflammatory response. M1 macrophages are polarized by IFN-γ and LPS and, upon activation, produce TNF-α, IL-1β, IL-6, and nitric oxide. They also secrete IL-12 and IL-23, pro-inflammatory cytokines which promote the differentiation of CD4+ T cells into pro-inflammatory T_H1 and T_H17 cells [86], [87]. M1 macrophages also contribute to the removal of pathogens by activating NADPH oxidase, resulting in the generation of reactive oxygen species [87]. Reactive oxygen species contribute to the perpetuation of inflammation, degrading the anti-inflammatory nitric oxide [37], [89], and can cause tissue damage if left unabated. M1 macrophages also upregulate their expression of T_H1 recruiting chemokines, CXCL9 and CXCL10, in addition to costimulatory receptors CD40, CD80, and CD86, which are necessary for antigen-presentation and binding to T cells [87].

3.C.2—Alternatively activated macrophages (M2)

Alternatively activated macrophages are also often referred to as anti-inflammatory or immunosuppressive macrophages. Conventionally, M2 macrophages arrive to the site of injury after M1 macrophages for the resolution of the inflammation. Likewise, it is also possible that already present inflammatory macrophages undergo a phenotypic shift into a more immunosuppressive behavior [86]. M2 macrophages are typically polarized by IL-4 and IL-13, and they produce anti-inflammatory cytokines IL-10 and TGF-β. These macrophages primarily function by engulfing cellular debris and apoptotic cells, upregulating their scavenger receptors, CD163 and stabilin-1, and promoting angiogenesis and wound healing. They secrete chemokines which promote the differentiation of CD4+ helper T cells to the anti-inflammatory T_H2 phenotype [87]. However, when exacerbated, M2 macrophages continue to secrete factors like TGF-β and Galactin-3, promoting pathological wound healing and subsequent fibrosis [90].

3.C.3—M1/M2 macrophages in disease

The balance between M1 and M2 macrophages in the inflammatory process is often a large determinant of the tissue's fate. Likewise, the switch between phenotypes is often critical to both the execution and resolution of the immune response. In fact, some bacteria, such as *Myobacterium tuberculosis*, are able to evade the immune system by forcing a phenotypic shift from M1 to M2 [87]. M1 macrophages play a large part in the inflammation of diabetes, contributing to pathological insulin resistance, beta cell dysfunction, and impaired wound healing, and weight loss is associated with a shift of macrophages to M2 [87]. M2 macrophages are capable of protecting the central nervous system from demyelination in mice through the secretion of anti-inflammatory cytokines TGF-β and IL-10 [86]. However, an M2 phenotype is not always beneficial. Allergic

diseases are typically associated with M2 macrophages. Pulmonary macrophages secrete factors which increase smooth muscle contraction and ECM degradation, contributing to allergic asthma. Tumor associated macrophages (TAMs), distinct enough to warrant their own classification, exhibit a phenotype similar to M2 macrophages [91], promoting angiogenesis, ECM degradation, and inhibiting anti-tumor T_H1 differentiation. In fact, potential therapeutics could treat tumors via M2 to M1 phenotypic shifting. Outside of disease, the balance of M1/M2 is crucial in pregnancy as well, regulating fetal tolerance and angiogenesis [87]. Although conventional understanding of macrophage polarization is based on secreted factors and receptor binding, the cell's mechanical environment has been shown to play a critical role in determining macrophage phenotype. Understanding the way macrophage phenotype is determined and adjusted could be of critical importance for the treatment of a number of diseases.

3.D—Biomechanical Regulation

Mechanotransduction is the translation of mechanical forces to intracellular biochemical signaling [92]. Mechanical signals are imposed on cells even under healthy conditions, particularly in the cardiovascular system. Valves are exposed to cyclic stretch [5], and vessels are exposed to constant hemodynamic patterns [6]. Furthermore, disease can induce significant mechanical changes, contributing to altered cell behavior. Fibrosis can cause tissue stiffening [93]; other conditions involve the degradation of ECM and tissue softening [94]. Tissue engineered implants expose cells to new mechanical environments, and understanding the impact on cell signaling is of significant importance for improved design [95], [96]. Likewise, cells possess their own mechanical properties which influence their behavior, via cellular tension and morphogenesis [24], [97].

Particularly with macrophages, mechanical cues impact polarization [24], [98], of which an appropriate balance is crucial for the resolution of inflammation across a wide spectrum of diseases. A more complete grasp on the impact of mechanobiology on macrophage function, particularly in macrophage polarization, could have significant implications in therapeutics for a range of diseases.

3.E—Macrophage Biomechanical Properties

3.E.1—Cortical tension

The cortex of a cell is made up of a network of actin filaments and actin-binding proteins on the underside of a cell's plasma membrane. Contractions generated through myosin proteins in this network determine a cell's cortical tension and many of the cell's mechanical properties [99]. Cortical tension is in part regulated by myosin, and the knockdown of certain myosin proteins decreases cell elasticity [100]. The generation of cortical tension is necessary for a number of a cell's functions, including migration, division, and adhesion [99]. Cortical tension in some ways maintains the structural integrity of the cell; however, it is also known that changes in membrane tension can affect intracellular signaling through mechanotransduction [101].

Cytokine treatment and subsequent polarization can have an impact on macrophage cortical tension. Patel et. al demonstrated that treatment with LPS or IFN-γ, polarizing RAW 264.7 macrophages towards M1, resulted in an increase in the cell's membrane elasticity [102]. Atomic force microscopy measurements also demonstrated a decrease in the Young's modulus for LPS-stimulated macrophages compared to resting macrophages [103]. Other studies report an increase in membrane tension of THP-1 macrophage-like cells with LPS stimulation [104], confirming the impact of cytokine

polarization on macrophage mechanical properties. Along with an increase in membrane tension, LPS treatment also induced actin polymerization in the macrophages and promoted cell spreading [102], a necessary step during phagocytosis [105]. It is known that Fc-receptor-mediated phagocytosis also results in the accumulation of actin polymerization factors [101], further confirming a relationship between phagocytosis and cortical tension. Likewise, a stiffer substrate induced both phagocytosis and an increase in cell membrane elasticity in human alveolar macrophages as well. Furthermore, biaxial stretch reduces cell elasticity along with decreasing phagocytosis, too. Other studies have shown that an increase in cortical tension is associated with important phases of contraction during frustrated phagocytosis in RAW 264.7 macrophages, and altering the cell's membrane cortical tension increased cell spreading and delayed the onset of the contraction [101].These results indicate that an increase in cortical tension, which can be induced via LPS-stimulation, is correlated with an increase in phagocytosis and vice versa. These results also demonstrate how macrophage mechanotransduction can affect mechanical properties of the cell and subsequent cell function. Because macrophages cultured on stiffer substrates demonstrated increased actin polymerization, these results also suggest that the effect of substrate stiffness on phagocytosis could be mediated through changes in the cell's cortical tension.

For a cell to extend pseudopodia, the membrane's cortical tension must be overcome. One obvious way to achieve this is to decrease the cell's cortical tension [106]. Neutrophils have been shown to increase their membrane tension during protrusion, thus preventing additional protrusion formation via inhibition of Rac1. Macrophages experiencing an increase of membrane tension during phagocytosis (previous studies

have observed a two-fold increase [107]) also exhibit the inhibition of Rac1 [108] and actin assembly [101]. Increasing macrophage membrane tension results in delayed pseudopod extension concurrent with inhibition of Rac1 [107]. This feedback loop prevents multiple pseudopodia protrusions and impaired chemotaxis [108]. Likewise, the generation of cortical tension at the leading edge of migration has been shown to be critical in neutrophil motility. The increase in tension results in a spatial distribution of Rac1 signaling, preventing additional protrusions and maintaining the leading front and polarization [109]. Reducing overall membrane tension through hypo-osmotic shock generates an excess of leading fronts [97]. Through these pathways, it is likely that cortical tension plays a role in macrophage migration and chemotaxis as well. It is also of note that macrophages and other cells often contain membrane reservoirs, folds of membrane that allow for a sudden change in membrane area and respond to changes in membrane tension [97]. When certain stresses are applied to the cell, membrane tension increases, resulting in the unfolding of these reservoirs and an increase in membrane area. In this way, the cell has a dynamic way of adjusting membrane area and tension [110].

Additionally, inhibiting human U937 macrophage actin polymerization, and decreasing the cell's membrane elasticity, resulted in decreased responsiveness to LPS, a trait characteristic of macrophages which have already been exposed to LPS. This result proposes that a macrophage's tolerance to LPS post-treatment is also mediated through altered cortical tension and actin polymerization [102]. This evidence suggests a role for macrophage cortical tension not only in phagocytosis, but in the cell's ability to be polarized and activated. The cumulative weight of this data indicates the importance of

cortical tension for a variety of macrophage functions and the way that tension can be mediated through both molecular and mechanical signaling.

3.E.2—Morphology

It is well-characterized that M1 macrophages exhibit a round, pancake-like morphology, while M2 macrophages are more elongated [24], [111]. Data has shown that forcibly altering macrophage morphology can impact phenotype substantially. Spatial confinement can occur *in vivo*, both naturally, in inflammation and dense tissue, and in tissue-engineered porous implants [112], restricting macrophage spread and affecting their shape. An examination of TAMs in human colorectal liver metastasis indicated a strong correlation between 5-year disease free survival and a higher percentage of small area TAMs [113], indicating a relationship between macrophage morphology and phenotype.

It has been shown that forcing unpolarized macrophages to develop an elongated phenotype via micropatterning results in increased Arginase-1 (Arg-1) expression, typical of M2 macrophages, and decreased secretion of pro-inflammatory cytokines CD54, IFN-γ, and MIP-1α. Forced elongation also enhanced cytokine-induced M2 polarization and reduced cytokine-induced M1 polarization. Spatial confinement, preventing elongation, also reduced the expression of Arg-1 in macrophages treated cytokines to induce M2 polarization. These results indicate that macrophage spreading and elongation is necessary for the development of an M2 phenotype. Furthermore, inhibiting actin polymerization or actin-associated contractility eliminated the M2 polarizing effect from patterning, despite the cells still exhibiting an elongated shape. Although polarization from patterning was abrogated, inhibition of actin polymerization or actin-associated contractility did not prevent the macrophages from cytokine-induced M2 polarization [24].

41

These results demonstrate that cell morphology-induced polarization is mediated by actin signaling, while cytokine-induced polarization is not. Relevant to tissue-engineered biomaterials, macrophages respond to grooved substrates [114], [115], with one study showing the highest degree of elongation occurring in 400-500 nm grooves and to a lesser extent on both wider and narrower grooves [116]. Additionally, substrate micropatterning can be further manipulated in an attempt to alter morphology and tune a more favorable M2/M1 ratio [117].

Jain et. al found that spatially confining bone marrow-derived macrophages, preventing characteristic M1 spreading, decreased the expression of certain late-response LPS-stimulated genes, including *IL-6*, *CXCL9*, and *IL-1β*, suggesting an impairment of M1 activation with altered cell morphology. However, they found that while the cell spreading was necessary for activation, the change to a more circular shape was not. This study also demonstrated that the changes in late-responsive LPS-stimulated genes were due to decreased translocation of myocardin-related transcription factor-A, mediated by a decrease in actin polymerization induced by confinement [112]. Inhibition of histone deacetylase activity also induces an elongated morphology and increased Arg-1 expression, characteristic of M2 macrophages, further indicating the importance of epigenetic modifications to macrophage morphology and polarization [118]. Additionally, spatial confinement reduced macrophage phagocytosis and secretion of pro-inflammatory cytokines [112], and decreasing macrophage spreading via reduced substrate biocompatibility also results in decreased TNF-α secretion [119]. Taken together, these results demonstrate the importance of cell morphology on macrophage

polarization, and the potential for manipulating cell shape in the treatment of macrophage-associated pathologies.

3.F—Macrophage Mechanotransduction

3.F.1—Substrate

Substrate stiffness is an important mediator of mechanotransduction, particularly in the pathology of certain diseases. Changes in tissue stiffness are associated with a range of diseases, including multiple sclerosis, atherosclerosis, and liver disease [120]. During osteoarthritis progression, pro-inflammatory cytokines and MMPs degrade the ECM within the joint, resulting in a substantial decrease in cartilage stiffness [94]. Higher stiffness in patient breast cancer samples positively correlates with macrophage infiltration [91]. Understanding the effect of substrate on macrophage behavior is also critical to the design and choice of biological implants [95], [96]. Furthermore, because higher TAM-infiltration correlates with higher mortality, implantable scaffolds have been proposed to be used to alter the immune response in tumors via altered stiffness [121], [122]. In addition to affecting tissue stiffness, disease can also impact ECM morphology. Samples of diseased lungs show more disorganized collagen I structure compared to healthy lungs [123]. A more complete knowledge of the impact of substrate stiffness and composition on macrophages could lead to the development of therapeutics for control of their phenotype, which would be applicable to a wide range of diseases.

Stiffer substrates are known to have a number of effects on macrophages. First, stiffer substrates induce increased LPS-stimulated phagocytosis in macrophages. Additionally, bone-marrow derived macrophages grown on stiff glass also demonstrated

a larger surface area and decreased circularity [111], [124]. Blakney et. al demonstrated that a higher stiffness increased cell spreading in bone marrow-derived macrophages, along with a more organized F-actin network [125]. This is consistent with other studies showing an increase in F-actin organization on stiffer substrates [124]. Substrate stiffness can also have an effect on macrophage migration, with primary human macrophages exerting higher forces while migrating on substrates with higher stiffnesses (ranging from 2.5 kPa to 15.6 kPa). Inhibition of ROCK signaling decreased the force generated [126]. Macrophages also migrated quicker in short time intervals on stiffer substrates [124].

Substrate stiffness can also impact macrophage polarization. One study found that RAW 264.7 macrophages cultured in fabricated scaffolds with a lower elastic modulus (1.6 MPa) exhibited an increase in production of cytokines associated with fibrosis, IL-1β and IL-10 [94]. Blakney et. al observed an increase in cytokines associated with an M1 phenotype (IL-1β, IL-6) with stiffer substrate (840 kPa), along with a decrease in markers associated with an M2 phenotype (Arg-1) [125]. Another study using bone marrow-derived macrophages aligns with this result, observing an increase in markers for M1 macrophages (IL-1β, TNF-α) and a corresponding decrease in markers for M2 macrophages (IL-10, Arg-1) with an increase in substrate stiffness [127]. Chen et. al tested RAW 264.7 macrophages on polyacrylamide hydrogels with stiffnesses of approximately 2.5 kPa (collagen fibers), 35 kPa (osteoid), and 65 kPa (pre-calcified bone). Macrophages grown on 35 kPa hydrogels demonstrated a more elongated phenotype typical of an M2 macrophage, compared to both the softer and stiffer gels, along with increased CD206 expression, a typical M2 marker. These changes were accompanied by decreases in IL-1β secretion and increases in IL-4 secretion, also

characteristic of M2 phenotype. Likewise, similar results were observed when the hydrogels were implanted *in vivo* [128]. Similarly, in another study it was also the intermediate stiffness which induced the transition toward an M2 phenotype. Implantable scaffolds with a substrate modulus of 24 MPa increased angiogenesis and collagen in rats, consistent with a more regenerative M2 phenotype [96]. In addition to substrate stiffness, the make-up of the substrate can impact macrophage behavior as well. Globular collagen structures induced higher CD206 expression, a marker of the M2 phenotype, in addition to decreased migration compared to fibrous collagen structures [123]. Although the impact of changing substrate stiffness on macrophage polarization is well-known, it is clear that the exact mechanics are neither linear nor completely understood. A confluence of data yields a consensus that lower substrate stiffnesses tend to induce a more M1-like phenotype [120], [129], although this effect is not necessarily linear and varies among cell type. It is likely that there is a moderate level of biologically-typical stiffness, and any perturbation from that homeostasis affects macrophage phenotype.

Although the effect of substrate stiffness on macrophage phenotype is clear, the exact mechanism remains elusive. Classic mechanotransduction involves integrin attachment to the ECM and subsequent downstream signaling involving ROCK1/2, cdc42, and Rac [111]. ROCK signaling is also known to be a regulator of macrophage polarization [91], and inhibition of ROCK enhances TLR activation and signaling [111]. Evidence suggests that mechanotransduction can occur in macrophages both through integrin engagement and via actin cytoskeletal signaling [130]. Another mechanistic suggestion is via NF-κB (nuclear factor-κB) signaling. Culturing bone marrow-derived macrophages on lower stiffnesses induces activation of NF-κB signaling, promoting the

secretion pro-inflammatory cytokines [128]. Other studies have suggested that downstream NF-κB activation is mediated by enhanced TLR4 activation in response to increased stiffness [120]. Another study hypothesized that stiffness-induced alterations to macrophage phenotype were potentially occurring through a mechanism involving the nuclear transport of YAP [127]. ECM stiffening also induces PI-3K (phosphoinositide 3-kinase) activation [131], which is also associated with pressure-induced macrophage phagocytosis [132] and is involved in oncogenesis [91].

3.F.2—Pressure

It has been known for years that pressure can have an impact on macrophage signaling and behavior [133]. Pressure exerted on macrophages is known to increase their migration [133] as well as their expression of scavenger receptors, crucial to their phagocytic activity, and very high cyclic pressure results in increased secretion of pro-inflammatory cytokines [134]. Alterations in interstitial pressure occur physiologically during edema or inflammation in a confined space, resulting in increased pressure, or, during unconfined inflammation, often resulting in decreased pressure [135], making the resultant effect on macrophage behavior of therapeutic relevance. The tumor microenvironment often experiences increased interstitial fluid pressure, as well [136].

Studies have shown that exposure of LPS-activated M1 macrophages to low intensity shock waves reduced expression of M1 markers, as well as M1 secreted pro-inflammatory cytokines, CCL5, CXCL9, CXCL10, and IL-1β. Additionally, shock waves also enhanced M2 phenotype on IL-4-polarized macrophages, increasing gene expression of M2 markers and secretion of anti-inflammatory cytokines. This result is promising because of the potential for extracorporeal shock wave therapy for clinical applications in tissue repair [137]. Likewise, pressures that simulate biological

inflammatory conditions (typically resulting in a pressure decrease of 1-150 mm Hg) resulted in an increase in IL-1β secretion when macrophages were stimulated with LPS, compared to higher pressure, which inhibited production of the cytokine [138]. Higher pressures that simulate biological edema (~20 mm Hg) increased phagocytosis in THP-1 macrophage-like cells [134] and primary human peripheral monocytes [139], likely through pressure-induced inhibition of FAK-Y397 (focal adhesion kinase) phosphorylation and downstream decreased ERK (extracellular signal-related kinase) activation [134]. Pressure also induced an increase in p38 MAPK (mitogen-activated protein kinase) phosphorylation, and an inhibition of that phosphorylation resulted in decreased phagocytosis [139]. Similarly, it has been shown that pressure applied to THP-1 macrophage-like cells results in activation and subsequent translocation of PI-3K to the membrane, resulting in downstream Akt2 phosphorylation. Inhibition of Akt2 phosphorylation prevented the pressure-induced increase in phagocytosis previously observed [140]. Higher phagocytic activity is associated with an M2-like phenotype [132], indicating that increased pressure could drive M2 polarization. Furthermore, tumor tissue exhibits higher interstitial pressure [141], and tumor-associated macrophages possess an M2-like phenotype [87]. These results suggest a role for pressure-related mechanotransduction involved in synergistic macrophage polarization and in the phagocytic ability of macrophages, specifically that higher pressure induces an M2-like phenotype, while lower pressure typical of inflammation induces an M1-like phenotype. A more complete understanding of the pathways involved could lead to the ability to better control macrophage phenotype in pathological pressure alterations.

Positive-pressure mechanical ventilation is a life-saving technique used in cases of respiratory failure, but it can often result in secondary lung damage. One of the reasons for this consequence is the increase in inflammatory cell recruitment believed to be affected by the increased thoracic pressure and stretching of airways. Models of this ventilation in rodents have been shown to increase the production of pro-inflammatory cytokines TNF-α, IL-1β, IL-6, and IL-8 [142]. For these reasons, it is critical to examine the ways in which macrophages can be affected by the mechanical forces exerted during ventilation and the impact on their function in order to effectively counteract the negative consequences observed clinically. An *in vitro* model of mechanical ventilation, using cyclic pressure-stretch, in human primary alveolar macrophages demonstrated an increase in IL-8 production over 24 hours, along with increased TNF-α, IL-6, and IL-10 when combined with LPS treatment. With both TNF-α and IL-6, the increase in secretion was substantially larger with mechanical ventilation and LPS combined, compared to LPS alone [142]. Likewise, an in vitro model of mechanical ventilation using only stretch in combination with LPS demonstrated a greater increase in MIP-2 production, a rodent analog of IL-8, than LPS alone [143]. These results indicate that cyclic pressure-stretch can induce M1 polarization and pro-inflammatory cytokine secretion. A mouse model of ventilation-induced lung injury showed higher expression by macrophages of adhesion molecules, crucial components involved in macrophage infiltration [144]. Mechanical ventilation induced quick adhesion of macrophages, and depletion of alveolar macrophages decreased the severity of lung damage in a mouse model of ventilator-induced lung injury [145]. Studies of alveolar macrophages indicated a role for TRPV4 channels (ion channels) for mechanical transduction during mechanical ventilation.

TRPV4^{-/-} alveolar macrophages demonstrated reduced spreading, and WT mice receiving *TRPV4^{-/-}* macrophages in an *in vivo* model of mechanical ventilation exhibited decreased lung injury [146]. Other studies demonstrated a decrease in LPS response in *TRPV4^{-/-}* macrophages [111]. These results together indicate that mechanotransduction in macrophages resulting from pressure and stretch is involved in the pathology of ventilator-induced lung injury, and further understanding of these pathways could improve clinical outcomes.

3.F.3—Stretch

Many tissues of the body are subjected to mechanical strain both during a healthy state and during certain disease pathologies. Valves of the heart experience up to 15% stretch during the cardiac cycle and during the progression of CAVD [5]. Hypertension induces strain on vessel walls [6]. Furthermore, surgical procedures can induce abnormal strain on tissue, exacerbating inflammation [147]. Even orthodontic appliances can apply mechanical strain to periodontal tissues [148].

Cyclic strain is known to induce changes in macrophages, resulting in increased protein production and altered morphology [149]. Low magnitude cyclic strain (3%) induced *in vitro* upregulation of class A scavenger receptors in both human monocytes/macrophages and THP-1 monocytes, and hypertension increased macrophage expression of class A scavenger receptors in atherosclerotic plaques [6]. In a mouse model for hair regeneration, skin undergoing higher magnitudes of cyclic strain (33%) demonstrated both increased macrophage infiltration and increased M2 polarization, associated with an increase in Arg-1 expression and IL-4 secretion [150]. However, Bonito et. al found that human peripheral blood mononuclear cell-derived macrophages in electrospun 3D scaffolds tended to exhibit an increase in the ratio of

M1/M2 polarization with increased cyclic strain (14%), as quantified by a panel of pro- and anti-inflammatory cytokines [151]. Consistent with this finding, another study showed static mechanical strain of 20% increased gene expression of M1 markers, including IL-6, IL-1β, and MIP-1α, in rat peritoneal macrophages. This study also showed that static strain of peritoneal macrophages enhanced LPS-stimulated M1 polarization [147]. Likewise, a study in U937 macrophage-like cells demonstrated higher IL-6 expression with 10% uniaxial cyclic strain [152]. RAW 264.7 macrophages also exhibited an increase in pro-inflammatory cytokines with exposure to both tensile and compressive strain [148]. A positive correlation between mechanical stretch and pro-inflammatory cytokine production would also be consistent with *in vitro* studies mimicking mechanical ventilation with pressure-stretch cycles [142], [143]. One study showed that 7% cyclic strain induced the expression of typical M1 markers after 1 day, with a subsequent shift towards an M2 phenotype over time [153]. This is particularly relevant because a typical inflammatory response initiates with an influx of M1 macrophages, to target the injury, followed by M2 macrophages, to resolve the inflammation. In this same study, 12% strain did not induce the same expression of M1 markers; however, 12% strain resulted in cell loss and no subsequent M2 phenotypic shift. The ratio of M2/M1 increased over time with 7%, but decreased with 12% strain [153]. When comparing effects between biaxial and uniaxial strain, macrophages have been shown to align more in uniaxial strain, with an elongated morphology, while biaxial strain induced a more spread and irregular shape [154]. Additionally, mechanical strain has also been demonstrated to decrease phagocytosis in macrophages *in vitro* [155]. The combination of these results indicates a role for increased

cyclic stretch in the polarization of M1 macrophages; however, this relationship does not seem to be linear and incompletely understood.

Bones are a significantly mechanically sensitive tissue. Bone-resorption is an important role of osteoclasts, the macrophages of bone, both in development [86] and in the pathology of skeletal diseases like osteoporosis [156]. Interestingly, bone-resorbing enzymes were shown to be increased in osteoclasts with application of cyclic strain [156]. Similarly, Xu et. al showed that higher mechanical strain increased expression of MMP9 and RANK, both promoting bone-resorption [157]. Although necessary for proper bone formation in development [86], improper bone-resorption is associated with a number of skeletal diseases in adults [157]. Further understanding of the effect of mechanical strain on osteoclasts could elucidate the mechanism between mechanical loading of bone and skeletal diseases.

3.F.4—Shear Stress
Shear stress is a common mechanical force in the body, and fluid dynamics often play a role in disease pathology. Hemodynamics impact the progression of both CAVD and atherosclerosis. Low magnitude shear stress in recirculatory flow patterns experienced in branchpoints of the aorta and bends of the aortic arch are preferential sites of plaque formation [155]. Likewise, the high magnitude shear stress that the ventricle-facing side of the aortic valve is exposed to is believed to be protective against the calcification experienced on the aortic-facing side of the valve [30]. Furthermore, tumors are known to experience elevated interstitial fluid flow [136], [141].

An *in vitro* model simulating tumor interstitial flow polarized bone marrow-derived macrophages towards an M2 phenotype, upregulating Arg-1, TGF-β, and CD206 in similar quantities as traditional IL-4 treatment [141]. This study showed that flow-

dependent M2 polarization was the result of phosphorylation of STAT3 and STAT6 (signal transducer and activator of transcription), transcription factors which have both been indicated in M2 polarization, mediated by β1 integrin engagement and downstream Src signaling. On the other hand, STAT1, indicated in M1 polarization, was unaffected by flow. Exposure to interstitial flow also increased macrophage migration via Akt and FAK activation, also mediated by β1 integrin engagement. Specifically, exposure increased macrophage migration against the direction of flow, possibly stimulated by actin accumulation at the site of flow. Interestingly, macrophages treated with interstitial flow were also capable of affecting the morphology of co-cultured cancer cells, and conditioned media from these macrophages increased the migration of cancer cells through higher levels of TGF-β in the media [141]. Other studies have shown the promotion of M1 polarization under low shear stress conditions in the formation of vulnerable atherosclerotic plaques [159]. Although the role of shear stress in macrophage function is incompletely understood, it could prove important in the pathology of certain diseases.

3.G—Conclusions

The mechanical properties of macrophages as well as the mechanical signals they are exposed to can have a substantial impact on macrophage behavior. Particularly with respect to polarization, the tuning of the mechanotransduction in macrophages could have significant impact on the regulation of inflammation in a number of diseases.

CHAPTER 4

Altered macrophage migration and T cell activation with loss of cadherin-11 in atherosclerosis immune response

Text for Chapter 4 was adapted from: **Camryn L. Johnson**, Matthew Bersi, Lance Riley, MacRae F. Linton, and W. David Merryman. "Altered macrophage migration and T cell activation with loss of cadherin-11 in atherosclerosis immune response." *ATVB*. Submitted February 2021.

4.A—Abstract

OBJECTIVE: Inflammation caused by infiltrating macrophages and T cells promotes plaque growth in atherosclerosis. CDH11 is a cell-cell adhesion protein implicated in several fibrotic and inflammatory diseases. Much of the research on CDH11 concerns its role in fibroblasts, although its expression in immune cells has been noted as well. The objective of this study was to assess the effect of CDH11 on atherosclerosis and its impact on the inflammatory cells involved.

APPROACH AND RESULTS: *In vivo* studies of atherosclerosis indicated an increase in CDH11 in plaque tissue. However, global loss of CDH11 resulted in increased atherosclerosis and inflammation. It also altered the immune response in circulating leukocytes, decreasing myeloid cell populations and increasing T cell populations, suggesting possible impaired myeloid migration. Bone marrow transplants (BMTs) from *Cdh11*-deficient mice resulted in similar immune cell profiles. *In vitro* examination of *Cdh11*$^{-/-}$ macrophages revealed reduced migration, despite upregulation of a number of genes related to locomotion. Flow cytometry revealed an increase in CD3+ and CD4+ helper T cell populations in the blood of both the global *Cdh11* loss and the BMT animals,

possibly resulting from increased expression by *Cdh11$^{-/-}$* macrophages of major histocompatibility complex class II molecule genes, which bind to CD4+ T cells for coordinated activation.

CONCLUSIONS: CDH11 fundamentally alters the immune response in atherosclerosis, resulting in part from impaired macrophage migration and altered macrophage-induced T cell activation.

4.B—Introduction

CVD is the world's leading cause of death [1], with an estimated economic burden of $500 billion in the US [160] and resulting in nearly one million deaths in 2016 [161]. Atherosclerosis, the build-up of lipid plaques in vessel walls, is considered to be the underlying cause of most CVD, often leading to severe clinical outcomes, including myocardial infarction, stroke, and heart failure [19]. Atherosclerotic plaque rupture is considered to be the primary cause in most myocardial infarction fatalities [36].

Atherosclerosis is caused by an abundance of circulating low-density lipoprotein (LDL) and subsequent infiltration into the vascular endothelium, initiating an immune response [19], [39]. Although once believed to be simply due to the passive accumulation of lipids in the arterial wall, it is now known that an active inflammatory response is involved in progression and ultimate rupture of atherosclerotic plaques. Leukocytes invade the plaque, secreting pro-inflammatory cytokines and proteolytic enzymes, breaking down the fibrous cap which protects the plaque from rupture [162], [163]. Although large plaques may cause vascular occlusion [52], size is not the most common clinical concern with severe atherosclerosis. The combination of a large necrotic core with a thinned fibrous cap increases the likelihood of plaque rupture, whereby thrombogenic

components of the plaque are exposed to the blood leading to clot formation and subsequent myocardial infarction [162].

The inflammatory response present in the plaque is the predominant contributor to both the growth of the plaque and the risk for rupture. The two main immune cell types responsible for this are macrophages and helper T cells. Mature macrophages in the plaque upregulate their pattern recognition receptors: scavenger receptors for phagocytosis and TLRs for antigen-binding and activation [162]. Certain scavenger receptors mediate uptake of oxidized LDL in the plaque [41], [162]. Cholesterol efflux from the macrophage is inhibited by pro-inflammatory cytokines, preventing the macrophage from processing the lipids and resulting in the formation of the characteristic foam cells [66]. Foam cells perpetuate inflammation in a positive-feedback manner by secreting pro-inflammatory cytokines, recruiting and inducing proliferation of macrophages [41], and ultimately undergoing apoptosis to form the necrotic core [162]. TLRs are believed to recognize molecules in the plaque resulting in macrophage activation and leading to a number of consequences, including the secretion of more inflammatory cytokines, coagulation factors [36], and proteolytic enzymes [162]. Indeed, deletion of MCP-1, a main recruiter of macrophages, results in decreased plaque area [65]. Consequently, macrophages are a fundamental contributor to the atherosclerosis inflammatory response, which not only facilitates the growth of the plaque, but its vulnerability to rupture as well [164].

CD4+ helper T cells are a lesser, but still present, contributor to plaque inflammation. Similar to macrophages, T cells are recruited to and infiltrate the plaque, and pharmacological targeting of RANTES, a potent T cell chemokine, results in

decreased plaque area [19]. Macrophages present antigens using their major histocompatibility complex (MHC) class II molecules. T cells bind to the antigen and a secondary costimulatory receptor, inducing proliferation specific to that antigen. In this way, T cells work in concert with macrophages to induce activation, resulting in an increase in proinflammatory cytokines, which perpetuate inflammation and recruit more immune cells; procoagulant molecules, which increase the risk of thrombus formation; and proteolytic enzymes, which degrade the fibrous plaque and increase risk of rupture [19].

CDH11 is a cell-cell adhesion protein which functions by forming homotypic bonds with identical neighboring cadherins [14], [165]. CDH11 provides strong adhesion by anchoring the intracellular portion to the actin cytoskeleton via catenins [166], [167]. CDH11 has been implicated in a wide range of cellular processes, including migration, invasion, epithelial-to-mesenchymal transition [13]–[15], and wound healing [12]. CDH11 has also been associated with a number of diseases, especially those involving fibrosis [10], [12], [13], [16], [22], [28] and inflammation [34]. A study by Schroer et. al showed that targeting CDH11 improved scar formation post-myocardial infarction, reducing inflammation and ECM deposition [16]. CDH11 has also been implicated in pulmonary fibrosis [13], scleroderma [10], [22], and shown to be upregulated in a mouse model of hypodermal fibrosis [10]. Much of this CDH11 research concerns its role in fibroblasts and their differentiation into myofibroblasts [12], [17], increasing their contraction and ECM deposition, promoting wound healing and, when untethered, pathological fibrosis [12]. However, CDH11 expression was observed in alveolar macrophages during pulmonary fibrosis [13] and is known to be expressed by certain immune cells [22].

Rheumatoid arthritis synovial samples exhibit a correlation between CDH11 expression and macrophage content, and anti-inflammatory therapies decrease CDH11 in synovial tissue [23]. Similarly, treatment with a CDH11 blocking antibody resulted in decreased IL-6 expression in a mouse model of hypodermal fibrosis [10]. Despite these findings, not much is known about the contribution of CDH11 to immune cells and pathological inflammation.

Atherosclerosis shares a number of similarities with CDH11-associated diseases, including endothelial activation, inflammatory cell activation [164], and collagen degradation [167], positing that CDH11 could play a role in plaque progression. Despite these comparisons, CDH11 has not been previously studied in atherosclerosis development. Although it has been suggested that CDH11 is involved in immune cell function and inflammation, when studying fibrotic diseases, it is difficult to isolate the inflammatory impacts of CDH11 from the fibrotic processes it is known to affect. Studying CDH11 in the context of atherosclerosis better enables the understanding of its specific role in inflammation and immune cell function. Our objective in this study was to determine the effect of CDH11 on atherosclerotic plaque progression and to characterize behavioral changes in macrophages as a result of a loss of CDH11 expression.

4.C—Materials and Methods

4.C.1—Animal studies

$Apoe^{-/-}$ mice on the C57BL/6 background were acquired from Jackson Laboratory and bred with a *Cdh11* mutant line [26]. For the plaque isolation study, female $Apoe^{-/-}$ were placed on a high fat Western-type diet (HFD) containing 19.6% fat and 1% cholesterol (TestDiet, 5TJT) at five weeks old for ten weeks. For the plaque quantification

and flow cytometry study, male *Apoe$^{-/-}$*, *Apoe$^{-/-}$;Cdh11$^{+/-}$*, and *Apoe$^{-/-}$;Cdh11$^{-/-}$* were placed on the same HFD at five weeks old for ten weeks, as well. Mice were sacrificed using CO_2 exposure.

4.C.2—Quantitative PCR
Quantitative PCR was performed on plaque tissue and aortic arches dissected from experimental mice. The sequences for the primers used are listed in **Appendix A**.

4.C.3—Bone marrow transplants
Recipient mice were given a dose of lethal irradiation (9 Gy) from a Cesium source at six weeks of age, and bone marrow transplantation was performed as described [168]. Bone marrow was isolated from the femur and tibia of adult donor mice. Injections of $2x10^6$ cells in 100 μL were given retro-orbitally to recipient mice. Male *Apoe$^{-/-}$* recipients were given BMTs from male *Apoe$^{-/-}$*, *Apoe$^{-/-}$;Cdh11$^{+/-}$*, and *Apoe$^{-/-}$;Cdh11$^{-/-}$* donors. Mice were allowed six weeks for reconstitution of the bone marrow niche, placed on a HFD for ten weeks, and sacrificed for subsequent analysis.

4.C.4—En face staining
Following sacrifice, mice were perfused with PBS followed by formalin. Aortas were dissected and placed in formalin for fixation. Perivascular adipose and connective tissue were carefully removed, and the aortas were opened and pinned (Fine Science Tools, 26002-20) onto a black dissection tray. Aortas were stained with Sudan IV (Sigma-Aldrich, S4261-25G) (5 grams, 500 mL 70% ethanol, 500 mL acetone, filtered) for 15 minutes at room temperature, followed by a 20 minute rinse in 80% ethanol. Images were taken using a Leica microscope and quantified via custom image processing analysis based on color segmentation [169]. The percentage of plaque coverage was quantified

as the ratio of red pixels to background pixels for each pinned aorta; all analysis was performed in MATLAB.

4.C.5—Flow cytometry

Mice were sacrificed for tissue collection and all samples were kept on ice for the duration of the protocol. Bone marrow was isolated from the femur and tibia, and peripheral blood was isolated retro-orbitally using micro blood collecting tubes (Fisher Scientific, 02-668-10). Aortas were dissected and digested in a collagenase solution adapted from Wu et. al [170] (1 mg/mL collagenase A, 1 mg/mL collagenase B, and 100 μg/mL DNAse in phenol-free RPMI 1640 with 5% FBS) for 30 minutes at 37°C. All samples were strained using a 100 μm strainer, spun down at 350 g, and resuspended in room temperature 1x red blood cell lysis buffer (BioLegend, 420301). Samples were again spun down and resuspended in flow buffer (PBS with 3% FBS). Cells were then counted, blocked at a concentration of 0.5 μL/million cells (Purified Rat Anti-Mouse CD16/CD32 Fc Block, BD Pharmingen, 553141), and stained with conjugated antibodies (**Appendix B**). Cells were resuspended in flow buffer and stained with DAPI prior to quantification by flow cytometry.

4.C.6—Macrophage isolation

Adapted from a previously described protocol [171], bone marrow was isolated from the femur and tibia. Cells were spun down and resuspended in RPMI 1640 + L-glutamine (Corning, 10-040-CMR) with 10% FBS, 20% L929 conditioned media, and 1% penicillin-streptomycin. Cells were plated at 2×10^6 cells/plate in 10 mL of media in non-adherent p100 dishes. On day 3 of differentiation, 5 mL of media were added to each plate. Cells were ready for experimentation on day 7.

4.C.7—RNAseq

Adherent cells were homogenized in TRIzol reagent and RNA was isolated using the Zymo Direct-zol RNA Microprep kit (Zymo, R2060). RNA integrity was measured with an Agilent Bioanalyzer prior to library preparations (**Appendix C**). Sequencing and read alignment were performed by the Vanderbilt Technologies for Advanced Genomics (VANTAGE) center as described in Snider *et al.* (2021) to an average depth of 38.5 ± 1.8 M reads per sample [172]. Differential expression analysis was performed using DEseq2 with Cook's outliers to filter low gene counts (mean count < 6) and p_{adj} = 0.01[173]. GO over-representation analysis was performed on differentially expressed, protein-coding genes with an absolute $\log_2$ fold-change greater than 1 using the R package clusterProfiler's *enrich* function [174]. Gene sets were considered over-represented if p_{adj} < 0.05. Redundant enriched GO terms were removed using clusterProfiler's *simplify* function with a cutoff = 0.5. Visualizations were generated using ggplot2 in R. RNA sequencing data have been deposited in GEO (Gene Expression Ominbus) of NCBI under accession code GSE165942.

4.C.8—Migration assay

After *in vitro* differentiation, macrophages were lifted using Cellstripper (Corning, 25-056-CI) and resuspended in RPMI 1640 + L-glutamine + 10% FBS + 1% penicillin-streptomycin. Millicell Cell Culture Inserts (Millipore Sigma, PI8P001250) with a pore size of 8 μm were placed a 24-well plate. 100,000 cells were seeded onto the membrane and allowed to settle in the incubator for 10 minutes. Subsequently, 600 μL of the chemoattractant media (25 ng/mL MCP-1 or without, for control) was added to each well. Plates were replaced in the incubator, and cells were allowed to migrate for 24 hours. For wells receiving treatment with a CDH11 blocking antibody SYN0012 or IgG2a isotype

control, both the cell solution and the chemoattractant solution contained 10 μg/mL SYN0012 or IgG2a (i.e. there was no pre-treatment). For cytochalasin D (Sigma-Aldrich, C2618200UL) treatment, cells were pre-treated in 10 μM for two hours. After 24 hours of migration, the inserts were removed and a cotton swab was used to remove any cells remaining on top of the membrane. Following fixation in 70% ethanol, a scalpel was used to remove the membrane, and it was mounted on a coverslip in ProLong™ Gold Antifade Mountant with DAPI (Thermo Fisher, P36931). Images were taken using an Olympus microscope, and the cell number was quantified via MATLAB.

4.C.9—Micropipette aspiration
Micropipette aspiration was used to determine the cortical tension of bone marrow-derived macrophages using methods reported previously [175], [176]. Briefly, 1 mm diameter capillary tubes were pulled to a taper, fractured to an internal diameter of approximately 5 μm, and bent to ensure the micropipette was parallel to the microscope stage. Using an inverted microscope, cells were visualized using Hoffman Modulation Contrast and micropipettes were manually positioned to be in contact with cells prior to aspiration. Negative pressures were applied using an MCFS-EZ microfluidics controller (Fluigent, Le Kremlin-Bicêtre, France).

Aspiration testing was performed by linearly increasing the suction pressure by 4 Pa/s over 150 seconds to a final aspiration pressure of 0.6 kPa. For the continuous change in pressure ΔP the aspirated length L of each cell was tracked and the cortical tension T was calculated as:

$$T = \frac{\pi E}{3\phi \left(\frac{1}{r_p} - \frac{1}{r_c} \right)}$$

where ϕ is a constant equal to 2.1, r_p is the radius of the pipette, r_c is the radius of the

cell, and E is the cell stiffness calculated as $E = (3\phi r_p/2\pi)(\Delta P/L)$. Note, the term $\Delta P/L$

is the slope of the linear applied pressure vs. aspirated cell length curve.

4.D—Results

4.D.1—Atherosclerotic plaques contained higher expression of Cdh11 and correlated with markers of plaque inflammation

In order to assess the potential role of CDH11 in atherosclerosis plaque

development and inflammation, we first sought to quantify *Cdh11* levels in disease.

Female Apoe^{-/-} mice were placed on a HFD for ten weeks to induce atherosclerosis

(**Figure 4.1A**). Upon sacrifice, portions of the aortic arch containing plaque were

dissected, along with a nearby portion of vessel lacking plaque. Plaque tissue samples

exhibited higher expression of genes associated with plaque development and

inflammation, including *Adgre1*, the gene for the macrophage marker F4/80, and *Mmp12*

and *Mmp13*, matrix metalloproteinases secreted by macrophages (**Figure 4.1B**). Plaque

tissue samples also demonstrated approximately three-fold higher gene expression of

Cdh11 (**Figure 4.1C**). Furthermore, expression of *Adgre1* and *Mmp12*, both markers of

plaques and macrophage infiltration, was positively correlated with *Cdh11* gene

expression in plaque samples (**Figures 4.1D and 4.1E**).

4.D.2—Genetic deletion of Cdh11 resulted in increased plaque burden

Motivated by our observation of increased *Cdh11* expression in plaques, we

crossed *Cdh11*^{-/-} mice onto the *Apoe*^{-/-} background to determine the effect of *Cdh11*

deletion on plaque development. *Apoe*^{-/-}, *Apoe*^{-/-};*Cdh11*^{+/-}, and *Apoe*^{-/-};*Cdh11*^{-/-} male mice

were placed on a HFD for ten weeks to induce atherosclerosis (**Figure 4.2A**).
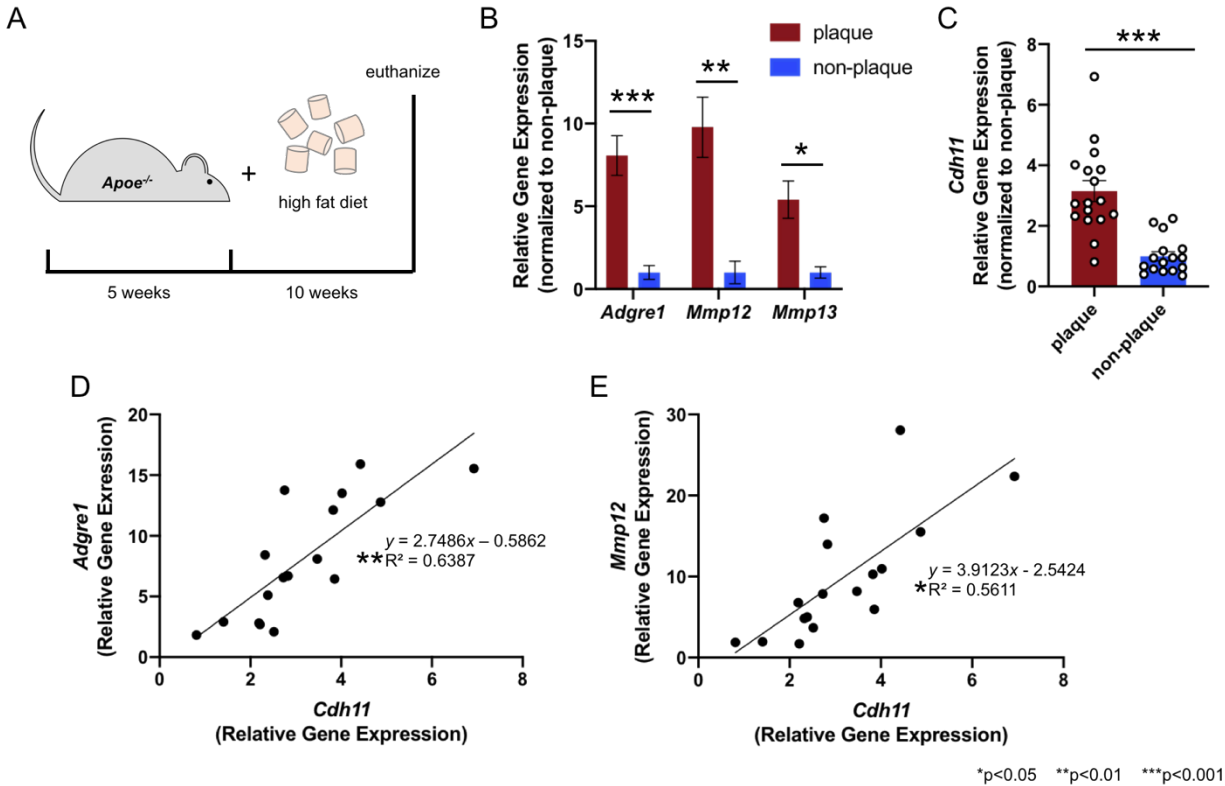
Figure 4.1. (**A**) *Apoe$^{-/-}$* mice were placed on a HFD for 10 weeks. (**B**) qPCR analysis of plaque tissue showed higher expression of genes associated with plaque progression, *Adgre1*, *Mmp12*, and *Mmp13*. (**C**) Plaque tissue also demonstrated higher expression of *Cdh11*. Gene expression of *Cdh11* positively correlated with *Adgre1* (**D**) and *Mmp12* (**E**) expression.

Apoe$^{-/-}$;Cdh11$^{-/-}$ aortas exhibited a trend for higher plaque area as measured in *en face* staining (p=0.053) (**Figure 4.2B**). Aortic arches dissected from *Apoe$^{-/-}$; Cdh11$^{-/-}$* mice showed significantly higher gene expression of markers typically associated with plaques and inflammation: *Adgre1*, the gene for the macrophage marker F4/80; *IL-1b*, a pro-inflammatory cytokine; *Vcam-1*, a leukocyte adhesion molecule; *Mmp12*, a proteolytic enzyme secreted by macrophages; and *Tgfb1*, a cytokine found in plaques (**Figure 4.2C**).

4.D.3—Atherosclerotic mice deficient in Cdh11 showed altered immune cell profiles
    Because of this unexpected finding of increased pro-inflammatory gene expression in mice lacking *Cdh11*, we next performed flow cytometry to examine the immune cell populations in the blood of atherosclerotic mice, including adult *Apoe$^{-/-}$* mice

as a normal chow control. In response to the development of atherosclerosis, the *Apoe*$^{-/-}$ mice exhibited a decrease in the CD3+ T cell population and a corresponding increase in the CD11b+ myeloid cell population. With loss of *Cdh11*, the increase in myeloid cells was not as substantial, with a larger percentage of CD3+ T cells and smaller percentage of CD11b+ myeloid cells in *Apoe*$^{-/-}$;*Cdh11*$^{-/-}$ mice compared to *Apoe*$^{-/-}$ mice (**Figure 4.2D**).

A multi-color flow cytometry panel (**Appendix D**) staining for CD45 (leukocytes), CD11b (myeloid cells), CD3 (T cells), CD19 (B cells), CD4 (helper T cells), CD8 (cytotoxic T cells), CD11c (pro-inflammatory macrophages), and CD206 (anti-inflammatory macrophages) was used to determine immune cell distributions in the bone marrow, blood, and aorta isolated from atherosclerotic *Apoe*$^{-/-}$, *Apoe*$^{-/-}$;*Cdh11*$^{+/-}$, and *Apoe*$^{-/-}$;*Cdh11*$^{-/-}$ mice in addition to normal chow *Apoe*$^{-/-}$ controls (**Appendix E**). With a loss of *Cdh11*, the percentage of CD45+ leukocytes in the blood was increased back to the level of normal chow controls suggesting a possible decrease of leukocyte tissue infiltration in the *Cdh11*-deficient mice (**Figure 4.2E**). Additionally, the myeloid cell population in the blood was decreased in the *Apoe*$^{-/-}$;*Cdh11*$^{-/-}$ mice relative to *Apoe*$^{-/-}$, despite the myeloid population in the bone marrow being significantly larger than in the atherosclerotic *Apoe*$^{-/-}$ mice (**Figure 4.2F**). As with the leukocyte population in the blood, both of these myeloid cell populations in the *Apoe*$^{-/-}$;*Cdh11*$^{-/-}$ mice more closely resemble the normal chow *Apoe*$^{-/-}$ control than either of the other atherosclerotic groups. However, the population of CD206+ CD11c- F4/80+ macrophages, often thought to have an anti-inflammatory phenotype [177], was decreased in the *Apoe*$^{-/-}$;*Cdh11*$^{-/-}$ aortas relative to the atherosclerotic *Apoe*$^{-/-}$ (**Figure 4.2G**).

A

Apoe^{-/-}

Apoe^{-/-};Cdh11^{+/-}   +

Apoe^{-/-};Cdh11^{-/-}   high fat diet

euthanize

5 weeks   10 weeks

B

Plaque Area (Fraction of Total Aorta)

Apoe^{-/-}   Apoe^{-/-};Cdh11^{+/-}   Apoe^{-/-};Cdh11^{-/-}

C

Adgre1   IL-1b   Vcam-1   Mmp12   Tgfb1

Relative Gene Expression (normalized to Apoe^{-/-})

** *** for Adgre1; * for IL-1b; * *** for Vcam-1; * *** for Mmp12; *** for Tgfb1

Apoe^{-/-}   Apoe^{-/-};Cdh11^{+/-}   Apoe^{-/-};Cdh11^{-/-} (repeated for each)

D   Peripheral Blood:

CD11b+ (black)
CD3+ (pink)
CD19+ (teal)

Apoe^{-/-}: CD11b+ 34.41%, CD3+ 49.03%, CD19+ 16.66%

Apoe^{-/-}: CD11b+ 71.07%, CD3+ 17.26%, CD19+ 11.67%

Apoe^{-/-};Cdh11^{+/-}: CD11b+ 66.41%, CD3+ 18.81%, CD19+ 14.78%

Apoe^{-/-};Cdh11^{-/-}: CD11b+ 52.94%, CD3+ 31.51%, CD19+ 15.55%

HFD

E

Leukocytes:

blood

CD45+ (% of Viable Non-RBCs)

*** ***

Apoe^{-/-}   Apoe^{-/-}   Apoe^{-/-};Cdh11^{+/-}   Apoe^{-/-};Cdh11^{-/-}

HFD

F

Myeloid Cells:

blood   bone marrow

CD11b+ (% of CD45+)   CD11b+ (% of CD45+)

** *   *** *

Apoe^{-/-}   Apoe^{-/-}   Apoe^{-/-};Cdh11^{+/-}   Apoe^{-/-};Cdh11^{-/-}

HFD

G

Anti-Inflammatory Macrophages:

aorta

CD206+ CD11c- (% of CD11b+ F480+)

*

Apoe^{-/-}   Apoe^{-/-}   Apoe^{-/-};Cdh11^{+/-}   Apoe^{-/-};Cdh11^{-/-}

HFD

*p<0.05   **p<0.01   ***p<0.001

65

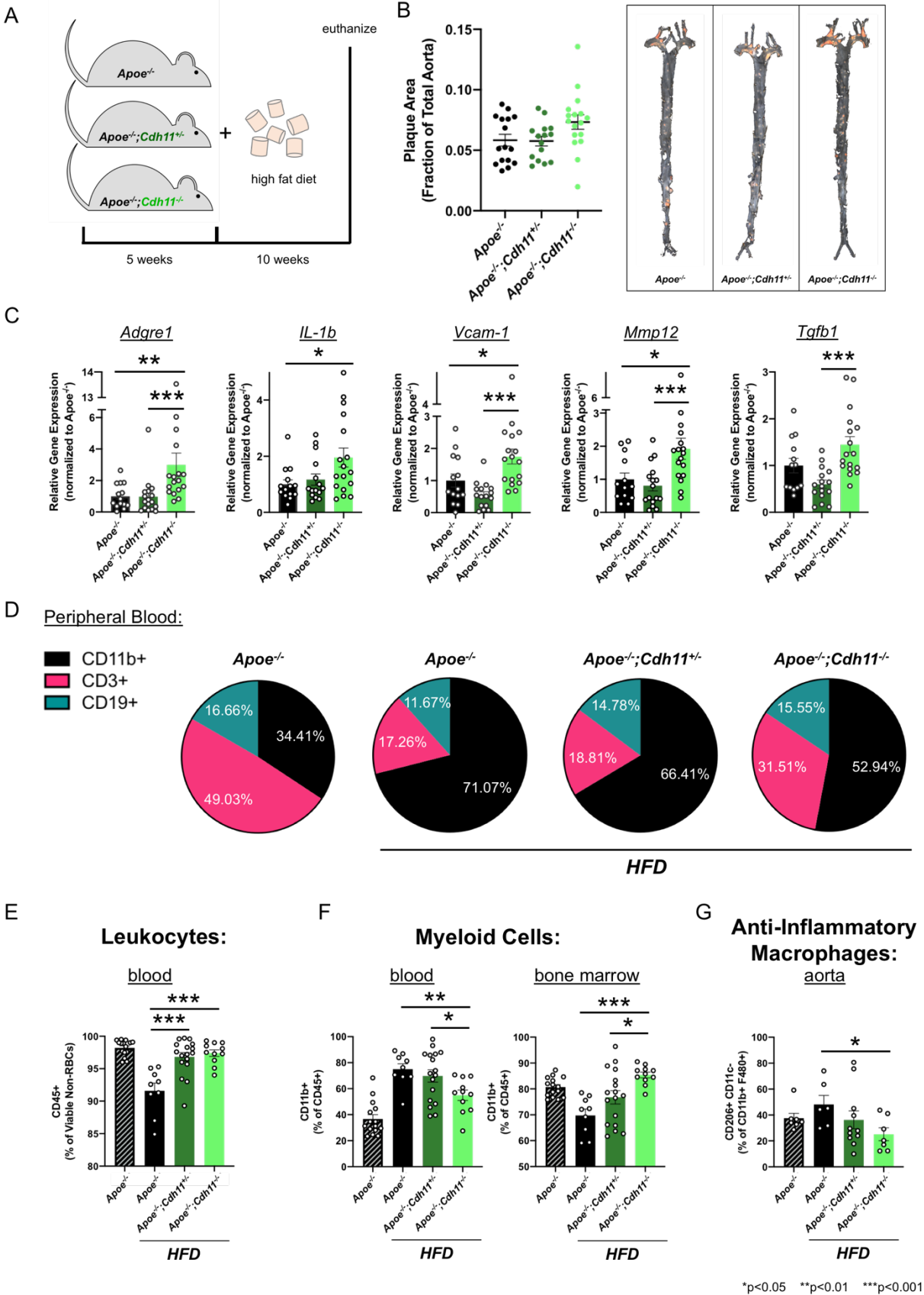**Figure 4.2**. (**A**) *Apoe*$^{-/-}$, *Apoe*$^{-/-}$*;Cdh11*$^{+/-}$, and *Apoe*$^{-/-}$*;Cdh11*$^{-/-}$ mice were placed on a HFD for 10 weeks. (**B**) *Apoe*$^{-/-}$*;Cdh11*$^{-/-}$ mice exhibited a trend for higher plaque area (p=0.053). (**C**) *Apoe*$^{-/-}$*;Cdh11*$^{-/-}$ mice showed increased expression of inflammatory markers *Adgre1*, *IL-1b*, *Vcam-1*, *Mmp12*, and *Tgfb1*. (**D**) *Apoe*$^{-/-}$ mice on a HFD demonstrate an increase in the circulating myeloid cell population and a corresponding decrease in the T cell population, when compared to normal chow *Apoe*$^{-/-}$ mice. With loss of *Cdh11*, this influx in circulating myeloid cells is decreased. *Apoe*$^{-/-}$*;Cdh11*$^{+/-}$ and *Apoe*$^{-/-}$*;Cdh11*$^{-/-}$ mice show fewer circulating leukocytes (**E**) along with fewer circulating myeloid cells, despite more myeloid cells in the bone marrow (**F**). (**G**) *Apoe*$^{-/-}$*;Cdh11*$^{-/-}$ aortas contain fewer anti-inflammatory macrophages.

4.D.4—Bone marrow transplants from Cdh11-deficient mice resulted in no change to plaque burden

Due to this observed difference in immune cell populations with loss of *Cdh11*, we performed BMTs to determine the specific effect of *Cdh11* deletion in immune cells. Male *Apoe*$^{-/-}$ mice received BMTs from male *Apoe*$^{-/-}$, *Apoe*$^{-/-}$*;Cdh11*$^{+/-}$, or *Apoe*$^{-/-}$*;Cdh11*$^{-/-}$ mice and were placed on a HFD to induce atherosclerosis (**Figure 4.3A**). Surprisingly, we found no difference in plaque area between any of the groups (**Figure 4.3B**).

4.D.5—Bone marrow transplants from Cdh11-deficient mice resulted in altered immune cell profiles

We again performed flow cytometry to examine the distributions of circulating immune cell populations in the blood of these BMT mice, including adult *Apoe*$^{-/-}$ mice as a normal chow control. Similar to the atherosclerotic *Apoe*$^{-/-}$ mice, in response to the HFD, the *Apoe*$^{-/-}$*;Apoe*$^{-/-}$ BM mice demonstrated a decrease in the CD3+ T cell population and an increase in the CD11b+ myeloid cell population. In mice receiving bone marrow from *Apoe*$^{-/-}$*;Cdh11*$^{-/-}$ mice, the myeloid cell population increase was smaller, with these mice containing more CD3+ T cells and fewer CD11b+ myeloid cells compared to the *Apoe*$^{-/-}$*;Apoe*$^{-/-}$ BM mice (**Figure 4.3C**). The same flow cytometry panel (**Appendix D**) was used to identify immune cell distributions in the bone marrow, blood, and aortas from atherosclerotic *Apoe*$^{-/-}$*;Apoe*$^{-/-}$ BM, *Apoe*$^{-/-}$*;Apoe*$^{-/-}$*;Cdh11*$^{+/-}$ BM, and *Apoe*$^{-/-}$*;Apoe*$^{-/-}$*;Cdh11*$^{-/-}$ BM mice in addition to adult *Apoe*$^{-/-}$ mice as a normal chow control (**Appendix F**). The CD45+ leukocyte population in the aortas of mice receiving BMTs

from $Apoe^{-/-};Cdh11^{-/-}$ mice was significantly less than control. Additionally, the CD45+ leukocyte population in the blood was increased with a loss of $Cdh11$ in the bone marrow at a level similar to the normal chow $Apoe^{-/-}$ control (**Figure 4.3D**). Both of these results indicate a potential decrease in leukocyte infiltration with $Cdh11$-deficient BMT. Furthermore, the myeloid cell population in the blood was decreased in the $Apoe^{-/-};Cdh11^{-/-}$ BM mice, although the myeloid population in the bone marrow was increased relative to the $Apoe^{-/-};Apoe^{-/-}$ BM control (**Figure 4.3E**), matching the same trend observed in the global deletion. As with the leukocyte population in the blood, the myeloid population in the blood of $Apoe^{-/-};Apoe^{-/-};Cdh11^{-/-}$ BM is similar to the normal chow control. Despite the lack of plaque area phenotype, the population of CD11c+ CD206- F4/80+ macrophages, associated with a more pro-inflammatory phenotype and most relevant to atherosclerotic disease severity, is decreased with $Cdh11$-deficient BMT (**Figure 4.3F**).

4.D.6—Bone marrow-derived leukocytes deficient in Cdh11 showed lower intensity CD45 staining
        In addition to the observed differences in leukocyte populations, the median fluorescent intensity of CD45 was decreased in the aorta (**Figure 4.3F**) and bone marrow (**Figure 4.3G**) with loss of $Cdh11$, indicating a decrease in overall CD45 expression. Although CD45 is frequently used as a marker for leukocytes, it also has its own distinct roles, one of which is involvement in macrophage migration and adhesion [178]. Rather than just a difference in immune cell populations, this result indicates a fundamental difference in the function of the leukocytes themselves.
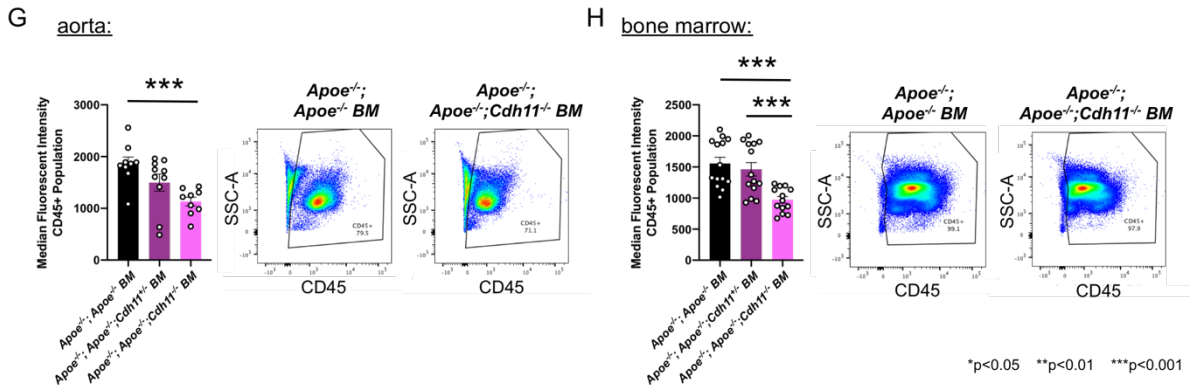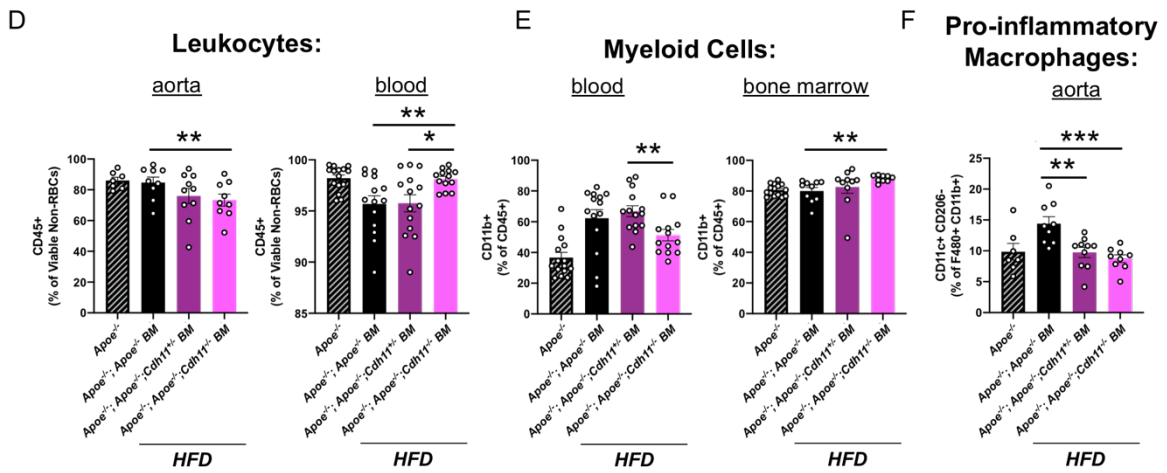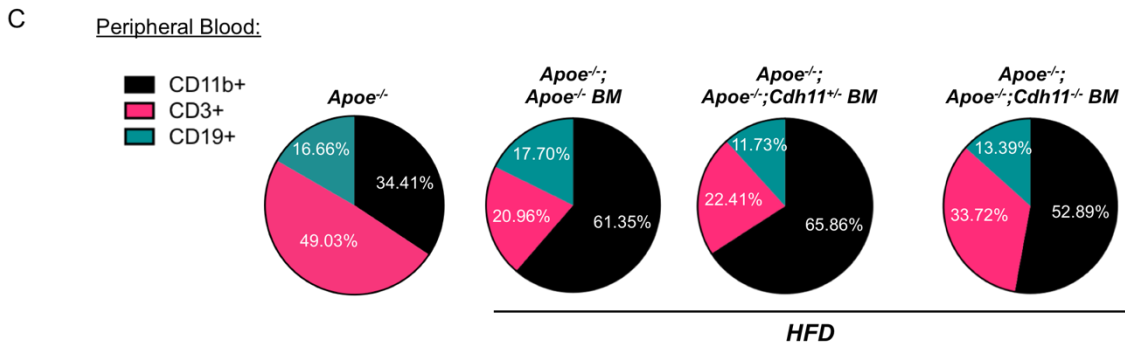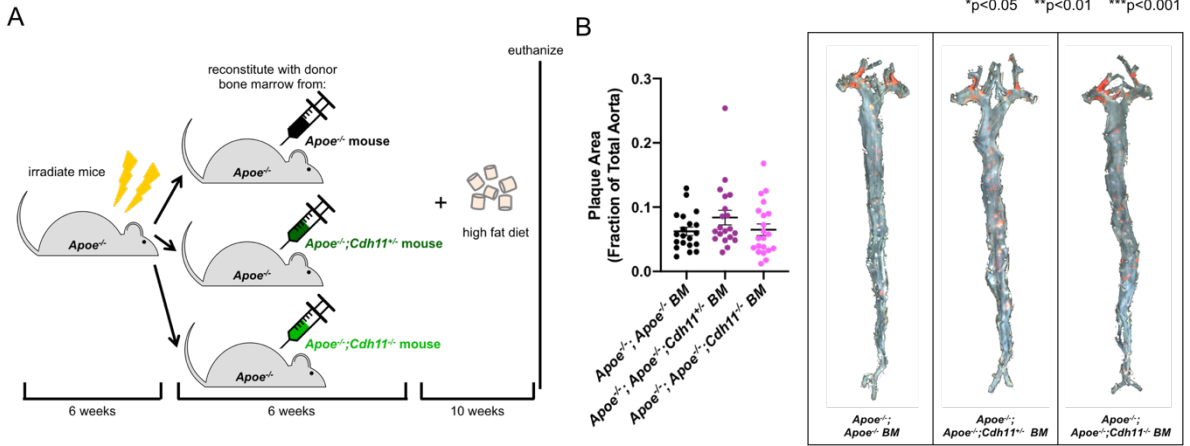
Figure 4.3. (**A**) *Apoe*$^{-/-}$ mice were given BMTs from *Apoe*$^{-/-}$, *Apoe*$^{-/-}$;*Cdh11*$^{+/-}$, or *Apoe*$^{-/-}$;*Cdh11*$^{-/-}$ mice. (**B**) BMT from *Cdh11*-deficient mice had no effect on plaque area. (**C**) *Apoe*$^{-/-}$;*Apoe*$^{-/-}$ BM mice on a HFD demonstrate an increase in the circulating myeloid cell population and a corresponding decrease in the T cell population, when compared to normal chow *Apoe*$^{-/-}$ mice. With loss of *Cdh11* in the bone marrow, this influx in circulating myeloid cells is decreased. *Apoe*$^{-/-}$;*Apoe*$^{-/-}$;*Cdh11*$^{+/-}$ BM and *Apoe*$^{-/-}$;*Apoe*$^{-/-}$;*Cdh11*$^{-/-}$ BM mice show fewer leukocytes both in the aorta and the blood (**D**) along with fewer circulating myeloid cells, despite more myeloid cells in the bone marrow (**E**). (**F**) *Apoe*$^{-/-}$;*Apoe*$^{-/-}$;*Cdh11*$^{-/-}$ BM aortas contain fewer pro-inflammatory macrophages. With loss of *Cdh11* in the bone marrow, leukocytes in the aorta (**G**) and bone marrow (**H**) show decreased expression of CD45.

4.D.7—Cdh11$^{-/-}$ macrophages exhibited increased expression of genes associated with cell cycle regulation and migration.

Motivated by these findings, we isolated bone marrow-derived macrophages from WT and *Cdh11*$^{-/-}$ mice for RNAseq (**Figure 4.4A**). Upon harvesting these cells for experiments, we also observed a difference in the number of cells present post-macrophage differentiation. In both *Cdh11*$^{+/-}$ and *Cdh11*$^{-/-}$ genotypes, fewer macrophages were present at harvest after the seven-day differentiation (**Figure 4.4B**). RNAseq results yielded 553 differentially expressed genes between WT and *Cdh11*$^{-/-}$ ($p_{adj} < 0.01$ and absolute $\log_2$ fold change > 1). The top ten enriched genes that met these thresholds are annotated on the volcano plot (**Figure 4.4C**). GO over-representation analysis on differentially expressed genes show upregulation of genes related to the cell cycle and leukocyte migration (**Figure 4.4D**). Further, the genes associated with leukocyte migration are linked to other categories related to inflammation and biomechanical processes (**Figure 4.4E**).

4.D.8—Cdh11$^{-/-}$ macrophages exhibit lower migration and decreased cortical tension

Due to these results indicating a change in expression of genes associated with migration, we performed migration assays using WT, *Cdh11*$^{+/-}$, and *Cdh11*$^{-/-}$ macrophages and MCP-1 as a chemoattractant. *Cdh11*-deficient macrophages exhibited decreased migratory capabilities, and in fact yielded migration indexes of approximately one, indicating little to no response to MCP-1 at all (**Figure 4.4F**). Macrophages treated

69

A 7 day differentiation WT *Cdh11⁻/⁻* RNAseq NovaSeq600 DESeq2 |log2fold change| > 1 padj < 0.01 clusterProfiler GO ORA padj < 0.05 *simplify* = 0.5

B # of Cells Harvested Post-Differentiation (in millions) WT *Cdh11⁺/⁻* *Cdh11⁻/⁻* ** **

C adjusted p<0.01 -log₁₀ p_adj log₂ fold change *Cpe Rab27b Ache Spta1 Hecw2 Vsig8 Zfp365 Jchain Pde10a Prss34*

D wound healing · nuclear division · hemostasis · coagulation · blood coagulation · DNA replication · regulation of mitotic cell cycle phase transition · leukocyte migration · regulation of cytokine secretion · positive regulation of locomotion -log₁₀ adjusted p-value

E logFC 1 3 inflammatory response; positive regulation of cellular component movement; regulation of cell activation; response to wounding; negative regulation of cell adhesion; homotypic cell-cell adhesion; regulation of cell morphogenesis; regulation of mitotic cell cycle

F Migration Index for MCP-1 WT *Cdh11⁺/⁻* *Cdh11⁻/⁻* * ; WT NT, WT + MCP-1, Cdh11⁺/⁻ NT, Cdh11⁺/⁻ + MCP-1, Cdh11⁻/⁻ NT, Cdh11⁻/⁻ + MCP-1

G Migration Index for MCP-1 MCP-1 only, IgG2a+MCP-1, SYN0012+MCP-1 * ; WT + MCP-1, WT + MCP-1 + IgG2a, WT + MCP-1 + SYN0012

H apply vacuum

I Cortical Tension WT *Cdh11⁻/⁻* *

J 149 s WT *Cdh11⁻/⁻*
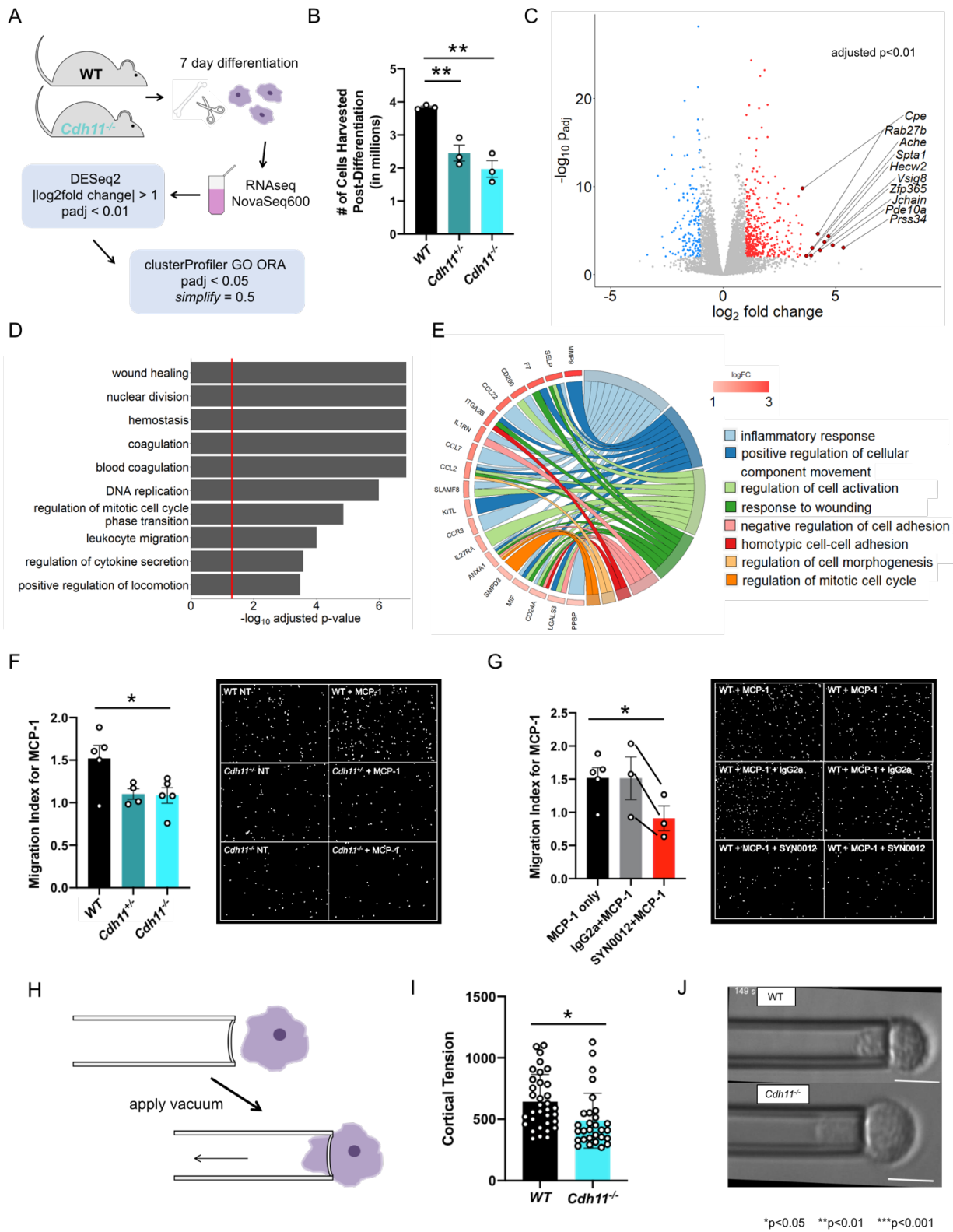
*p<0.05 **p<0.01 ***p<0.001

70

Figure 4.4. (**A**) Bone marrow-derived macrophages were isolated from *Cdh11*-deficient mice, and RNAseq was performed. (**B**) Fewer macrophages were present post-differentiation with loss of *Cdh11*. (**C**) Volcano plot from RNAseq analysis illustrating the top 10 most upregulated genes in the *Cdh11*$^{-/-}$ macrophages. (**D**) The top 10 most significant upregulated gene categories in *Cdh11*$^{-/-}$ macrophages revealed in RNAseq. (**E**) A chord plot of RNAseq data demonstrating upregulated genes associated with leukocyte migration (left) and other gene categories they are associated with. (**F**) *Cdh11*$^{-/-}$ macrophages migrate less in response to MCP-1 compared to WT. (**G**) WT macrophages treated with a CDH11 blocking antibody (SYN0012) migrate less in response to MCP-1. (**H**) A cartoon illustrating micropipette aspiration. (**I**) *Cdh11*$^{-/-}$ macrophages exhibit decreased cortical tension as measured by micropipette aspiration. (**J**) Still images taken from the end of the 150 second aspiration.

with a CDH11 blocking antibody, SYN0012, also demonstrated decreased migratory capabilities (**Figure 4.4G**). Because of the relevance of CDH11 to cell biomechanics and RNAseq results showing differences in genes related to cell morphogenesis, we sought to quantify changes in the mechanical properties of *Cdh11*$^{-/-}$ macrophages using micropipette aspiration (**Figure 4.4H**). *Cdh11*$^{-/-}$ macrophages exhibited decreased cortical tension compared to WT. **Figure 4.4J** shows the distance representative cells have aspirated into the microcapillary tube after 150 seconds of aspiration. Because of these results, we treated macrophages with cytochalasin D, a reagent known to decrease a cell's cortical tension [179], and measured resulting migration. Macrophages from all genotypes showed little to no migration after treatment with cytochalasin D (**Figure 4.5**).

4.D.9—Cdh11-deficiency resulted in increased T cell and helper T cell populations
In addition to the macrophage phenotype observed in this study, we also observed changes in T cell populations. In both the global deletion and the BMT, loss of *Cdh11* resulted in increased CD3+ T cell populations in the aorta, though only trending, and in the blood (**Figure 4.6A**). Additionally, the population of CD4+ T cells (represented as a percentage of T cells) is significantly increased as well, in both the aorta and blood (**Figure 4.6B**). RNAseq data showed that *Cdh11*$^{-/-}$ macrophages demonstrated increased expression of MHC class II genes *H2-Aa*, *H2-Ab1*, and *H2-Eb1* (**Figure 4.6C**). MHC class

71

II molecules are expressed by macrophages and used to interact with CD4+ T cells to perpetuate inflammation.

Figure 4.5. WT, *Cdh11*^{+/-}, and *Cdh11*^{-/-} macrophages were treated with cytochalasin D and stimulated for chemotaxis with MCP-1. None of the macrophages were capable of significant migration.

4.E—Discussion

CDH11 is primarily associated with diseases involving fibrosis and inflammation [10], [13], [16], [22], [34]. There is a large swath of research on its role in fibrosis [12], [13], [17], but its impact on inflammation is less well understood. It has been observed in immune cells, particularly macrophages [13], [22], but the understanding of its role in these cells is incomplete. Because of the limited role of fibroblasts in the progression of atherosclerosis [55], examining CDH11 in the current study allowed for the ability to assess its impact in inflammation separate from its role in fibrosis. The results from this study illustrate the effect of *Cdh11*-deficiency on the immune response in atherosclerosis,
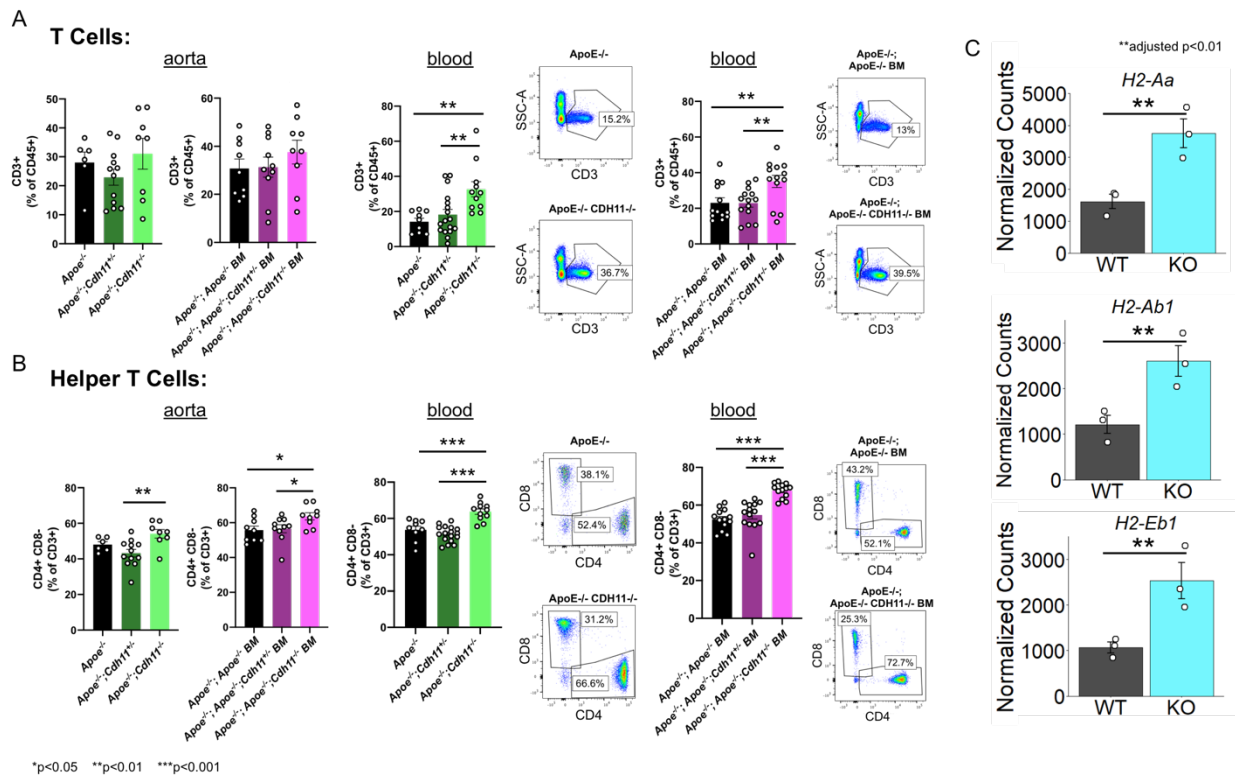
Figure 4.6. Both the global deletion and BMTs exhibit increased T cell populations in the aorta (not significantly) and in the blood (significantly) (**A**) as well as increased CD4+ helper T cell populations in the aorta and blood (**B**). (**C**) RNAseq revealed increased expression of MHC class II molecule genes in *Cdh11^-/-* macrophages.

including altered myeloid and T cell phenotypes, in addition to decreased macrophage migration and cortical tension.

In order to examine the impact of CDH11 on atherosclerosis development, we first determined that plaque samples contained higher expression of *Cdh11* compared to non-plaque vessel samples. Furthermore, *Cdh11* expression in the plaques correlated with typical markers of plaques and inflammation, including *Adgre1*, *Mmp12*, and *Mmp13*. This suggests that higher *Cdh11* expression correlates with higher inflammation and, thus, increased disease severity [164]. Other studies have noted a correlation with CDH11 and inflammatory markers as well, such as a correlation between CDH11 and infiltrating

macrophages in rheumatoid arthritis synovium [23]. This could indicate that expression of CDH11 encourages the perpetuation of an inflammatory response.

An atherosclerotic mouse model with a deficiency in *Cdh11*, however, did not give the expected outcome of decreased plaque development. *Apoe$^{-/-}$;Cdh11$^{-/-}$* mice on a HFD, in fact, demonstrated increased inflammatory markers and a trend for increased plaque area. Because this is a global deletion and CDH11 is expressed by nearly all of the cells involved in atherosclerosis progression (ECs [180], vascular SMCs [181], and fibroblasts [12]), there are a number of factors that could have affected plaque development. One reasonable explanation is that, by removing CDH11 from the endothelium, barrier function was impeded and leukocyte transmigration was made easier, as is the case when pharmacologically targeting VE-cadherin [182]. However, it is difficult to determine the exact reasons for the trend in increased plaque burden observed in the *Apoe$^{-/-}$;Cdh11$^{-/-}$* mice.

Flow cytometry demonstrated altered immune cell populations in circulation with a loss of *Cdh11*. While *Apoe$^{-/-}$* mice on a HFD demonstrated an influx of CD11b+ myeloid cells corresponding with a decrease in CD3+ T cells, *Apoe$^{-/-}$;Cdh11$^{-/-}$* mice on a HFD looked much closer to the normal chow control, with a smaller population of CD11b+ myeloid cells and more CD3+ T cells compared to the atherosclerotic *Apoe$^{-/-}$* mice. This contradicts the qPCR and plaque area results, which showed higher disease severity, very dissimilar from a normal chow mouse. Further quantification of leukocyte populations in the bone marrow, blood, and aortas suggested impaired migration of myeloid cells with loss of *Cdh11*. There were more leukocytes in the blood of *Apoe$^{-/-}$;Cdh11$^{-/-}$* mice, indicating a potential decrease in infiltration, and, once again, more closely resembling

the normal chow mice. A decrease in the myeloid cells in the blood, despite an increase in the myeloid cell population of the bone marrow, also suggests that the myeloid cells are struggling to migrate. A decrease in the anti-inflammatory macrophages [177] in the aorta is likely a contributor to the increased inflammation observed in the $Apoe^{-/-};Cdh11^{-/-}$ mice.

BMTs from *Cdh11*-deficient mice provided an opportunity to more specifically look at the result of losing *Cdh11* in the immune system, reducing the complications arising from deleting *Cdh11* in a range of cell types all involved in atherosclerosis. Surprisingly, there was no difference in the plaque area between any of the groups, in contrast to the trends in the global deletion. This result does, however, indicate that the trend for increased plaque area observed in the global deletion was a consequence of a loss of *Cdh11* in cells other than leukocytes. Flow cytometry analysis of the circulating immune cells in the BMTs demonstrated almost identical trends to the global deletion. Despite having disparate levels of plaque severity, *the* $Apoe^{-/-};Cdh11^{-/-}$ mice and the $Apoe^{-/-};Apoe^{-/-};Cdh11^{-/-}$ *BM* mice have very similar immune cell profiles. Mice receiving BMTs from *Cdh11*-deficient mice exhibited decreased leukocytes in the aorta along with an increase in the blood, again indicating an infiltration impairment. A similar myeloid cell phenotype persisted from the global deletion to the BMTs as well, with fewer being present in the blood despite a comparatively larger population in the bone marrow. The most marked difference between the global mutants and the BMTs was a decrease in pro-inflammatory macrophages [177] in the aortas of the mice receiving BMTs from *Cdh11*-deficient mice. This would typically suggest an improved disease phenotype [164]; however, that was not seen in the *en face* staining for plaque area. Decreased CD45

expression in the aorta and bone marrow of *Apoe-/-;Apoe-/-;Cdh11-/- BM* mice illustrated an instance of differential protein expression with loss of *Cdh11*, suggesting the potential for additional gene expression disparities between the two genotypes. Furthermore, it also points to a migration phenotype, as CD45 is involved in the migration and adhesion of macrophages and other leukocytes [178], [183]. These results together motivated *in vitro* studies of myeloid cells, of which the most important in atherosclerosis inflammation is the macrophage [19], [164].

In vitro culture of bone marrow-derived macrophages yielded a disparity in the number of cells harvested post-differentiation, indicating decreased proliferation or decreased differentiation into macrophages. Given the previous descriptions for the role of CDH11 in proliferation [184] and differentiation [17], [31], both are reasonable possibilities. RNAseq analysis on WT and *Cdh11-/-* macrophages yielded two broad groups of enriched gene categories: 1) genes associated with the cell cycle and 2) genes associated with migration and other cellular biomechanical processes. Both of these conclusions were contradictory to previous observations. Fewer cells were harvested post-differentiation, suggesting that the upregulation in cell cycle-related genes is due to compensation. Likewise, an increase in migratory genes is counter to what the flow cytometry results indicated. Of the top 10 upregulated genes in *Cdh11-/-* macrophages, three were related to the cell cycle, *Hecw2*, *Jchain*, and *Zfp365*, and two were related to cell morphogenesis, *Ache* and *Spta1*. Given that CDH11 functions by anchoring to the actin cytoskeleton [166], it is possible that certain genes, such as *Spta1*, which encodes for a scaffold protein, would be upregulated as compensation. Additionally, the top 10 most significantly upregulated gene categories included those related to the cell cycle

76

(nuclear division, DNA replication, and regulation of the mitotic cell cycle phase transition) and several related to migration (leukocyte migration and positive regulation of locomotion). Due to CDH11's previously described role in migration [185] and other mechanotransduction [12], it is reasonable that these genes related to migration and cell morphogenesis could be upregulated as a compensation to the biophysical impairment of $Cdh11^{-/-}$ macrophages. If leukocyte migration genes are being upregulated in a compensatory mechanism for the lack of $Cdh11$, then these upregulated genes would have secondary consequences which could have a negative impact on disease progression and inflammation. Upregulated leukocyte migration genes were also involved in other processes relevant to atherosclerosis, including inflammatory response and regulation of cell activation, as well as other biomechanical processes, including cell adhesion and morphogenesis.

The contradictory nature of the RNAseq results and our previous observations about leukocyte migration motivated *in vitro* functional migration assays. In contrast with the RNAseq results, the migration assay showed that $Cdh11$-deficient macrophages migrated less in response to the chemoattractant MCP-1. In fact, $Cdh11^{+/-}$ and $Cdh11^{-/-}$ macrophages barely increased their migration in response to the stimulus. WT macrophages treated with a CDH11 monoclonal blocking antibody, SYN0012, also exhibited decreased migration. This result is of particular significance in part because the cells were not pre-treated with SYN0012. They were exposed to SYN0012 during the entire 24-hour migration, but, without pre-treatment, this would not seem to be a long enough duration for large downstream signaling changes. This result could suggest that $Cdh11$-deficiency results in a biophysical impairment to the macrophage, rather than a

signaling effect. Together, these results would also indicate that the cells are, in fact, overcompensating by upregulating migration genes, causing secondary effects potentially detrimental to disease severity. The differential expression of genes relating to cell morphogenesis also point to biomechanical changes with *Cdh11*-deficiency. Micropipette aspiration demonstrated decreased cortical tension in the *Cdh11*$^{-/-}$ macrophages. Membrane tension [102], cell shape, and the cell's ability to transduce mechanical signals is critical to macrophage behavior and particularly to a macrophage's ability to polarize into a pro- or anti-inflammatory phenotype [24]. Therefore, decreased cortical tension could have a significant impact on macrophage behavior and cytokine secretion, which could have consequences on plaque development in atherosclerosis [164]. Furthermore, the ability to control cortical tension is an important component of cell migration [99], and this decrease in tension could play a role in the migratory capability of *Cdh11*$^{-/-}$ macrophages. This concept was also seen in migration assays performed on WT, *Cdh11*$^{+/-}$, and *Cdh11*$^{-/-}$ macrophages after being treated with cytochalasin D to disrupt actin structure and decrease cell membrane tension [179]. None of these cells after treatment with cytochalasin D were able to migrate, reinforcing the relevance of cortical tension in the migratory ability of macrophages.

Despite these changes in macrophage phenotype indicating decreased infiltration, this was not consequently translated into a decrease in plaque area in *Cdh11*-deficient mice. One explanation for this is the changes in T cell populations exhibited with *Cdh11*-deficiency. There are larger populations of CD4+ helper T cells in both the aorta and blood of both the global *Cdh11* deletion and the *Cdh11*$^{-/-}$ BMTs. Helper T cells are the second most predominant immune cell responsible for perpetuating inflammation in

atherosclerotic plaques [19]. Particularly notable is that this disparity is present in equal measure in both the global deletion and the BMT. The bone marrow is not a significant source of T cells, and, therefore, the majority of T cells remain unchanged in the BMT. Despite this, the T cell population sizes in the BMT are changed in nearly identical amounts as in the global deletion. This result demonstrates that the change in T cell population sizes is not due to differences in the T cells themselves, but rather another leukocyte affecting them. RNAseq results showed that macrophages without *Cdh11* have higher expression of several MHC class II complex genes, specifically *H2-Aa*, *H2-Ab1*, and *H2-Eb1*, which bind to CD4+ T cells for activation [19]. This provides a possible explanation both for why the CD4+ helper T cell population increases with loss of *Cdh11* and why there is no decrease in plaque area in the *Cdh11*-deficient BMTs. Despite the decrease in pro-inflammatory macrophages, the increase in helper T cells could be counteracting the positive benefits of reduced macrophage content. Additionally, MHC class II complex genes are in part regulated by the cell cycle [186], and the upregulated cell cycle genes could as a consequence be causing an upregulation in these MHC class II genes and subsequent T cell phenotype.

Although the most complete understanding of CDH11 in disease is limited to fibrosis, it clearly plays an important role in immune cells and inflammation. This study demonstrates that both a global deletion of *Cdh11* and a BMT from *Cdh11*-deficient mice result in substantially altered immune profiles, despite no decrease in plaque severity. This research also shows that *Cdh11*-deficient macrophages suffer impaired migration, despite the upregulation of many genes related to migration and locomotion. In addition to impaired migration, these cells exhibited decreased cortical tension, contributing to the

decrease in migration and likely resulting in other functional consequences. As a result of these changes due to loss of *Cdh11*, these macrophages also likely contribute to increased activation and recruitment of helper T cells due to increased expression of MHC class II complex genes. Although it is clear that CDH11 can have a profound effect on inflammation in disease, it is currently incompletely understood and warrants further study. Although CDH11 does not appear to be a viable therapeutic target for atherosclerosis, it certainly is for a range of other diseases, and a more thorough comprehension of its role in leukocytes would be beneficial.

4.F—Acknowledgments

4.G—Sources of Funding

CHAPTER 5

The effect of cadherin-11 deletion on non-atherosclerotic mice

5.A—Introduction

In order to determine the effect of loss of *Cdh11*, we sought to examine the differences in the immune cell populations during an inflammatory response (described in Chapter 4) and under healthy conditions. Although *Apoe*$^{-/-}$ mice are characterized by generally elevated levels of systemic inflammation, young adult mice (ages 8-12 weeks) on a regular diet should not have developed large, complex plaques yet.

5.B—Materials and Methods

5.B.1—Animal studies

Apoe$^{-/-}$ mice were acquired from Jackson Laboratory and bred with a *Cdh11* mutant line [26]. Mice were sacrificed between 8 and 12 weeks old (no HFD) using CO_2 exposure.

5.B.2—Flow cytometry

Mice were sacrificed for tissue collection and all samples were kept on ice for the duration of the protocol. Bone marrow was isolated from the femur and tibia, and peripheral blood was isolated retro-orbitally using micro blood collecting tubes (Fisher Scientific, 02-668-10). Aortas were dissected and placed in PBS-/- on ice prior to digestion in a collagenase solution adapted from Wu et. al [170] (1 mg/mL collagenase A, 1 mg/mL collagenase B, and 100 μg/mL DNAse in phenol-free RPMI 1640 with 5% FBS) for 30 minutes at 37° C. All samples were strained using a 100 μm strainer, spun down at 350 g, and resuspended in room temperature 1x red blood cell lysis buffer

(BioLegend, 420301). Samples were again spun down at 350 g and resuspended in flow buffer (PBS-/- with 3% FBS). Cells were then counted, blocked at a concentration of 0.5 μL/million cells (Purified Rat Anti-Mouse CD16/CD32 Fc Block, BD Pharmingen, 553141), and stained with conjugated antibodies (**Appendix B**). Cells were resuspended in flow buffer and stained with DAPI prior to quantification by flow cytometry. Analysis was performed using FlowJo.

5.C—Results

A multi-color flow cytometry panel (gating strategy displayed in **Appendix D**) was performed on the bone marrow, blood, and aortas of healthy $Apoe^{-/-}$, $Apoe^{-/-};Cdh11^{+/-}$, and $Apoe^{-/-};Cdh11^{-/-}$ mice, staining for CD45 (leukocytes), CD11b (myeloid cells), CD19 (B cells), CD3 (T cells), CD4 (helper T cells), CD8 (cytotoxic T cells), F4/80 (macrophages), CD11c (pro-inflammatory macrophages), and CD206 (anti-inflammatory macrophages). The only significant differences observed were a higher number of leukocytes in the blood of $Apoe^{-/-};Cdh11^{-/-}$ mice compared to $Apoe^{-/-};Cdh11^{+/-}$ mice and a decrease in the cytotoxic T cell population in the aorta of the $Apoe^{-/-};Cdh11^{-/-}$ mice compared to both the $Apoe^{-/-}$ and $Apoe^{-/-};Cdh11^{+/-}$ mice (**Figure 5.1**).

5.D—Discussion

In order to more completely understand the effect of the loss of $Cdh11$ on the immune response, we needed to determine if there were any baseline changes in immune cell populations in healthy mice deficient in $Cdh11$. The results indicate that the $Cdh11$-deficient mice remain relatively unchanged from the $Apoe^{-/-}$ mice. This is interesting because it is known that $Cdh11$-deficient mice exhibit certain impairments compared to

*p<0.05   **p<0.01   ***p<0.001

Leukocytes:

aorta   blood   bone marrow

B Cells:

aorta   blood   bone marrow

Myeloid Cells:

aorta   blood   bone marrow

T Cells:

aorta   blood   bone marrow

Macrophages:

aorta   blood   bone marrow

Helper T Cells:

aorta   blood   bone marrow

Pro-Inflammatory Macrophages

aorta

Anti-Inflammatory Macrophages

aorta
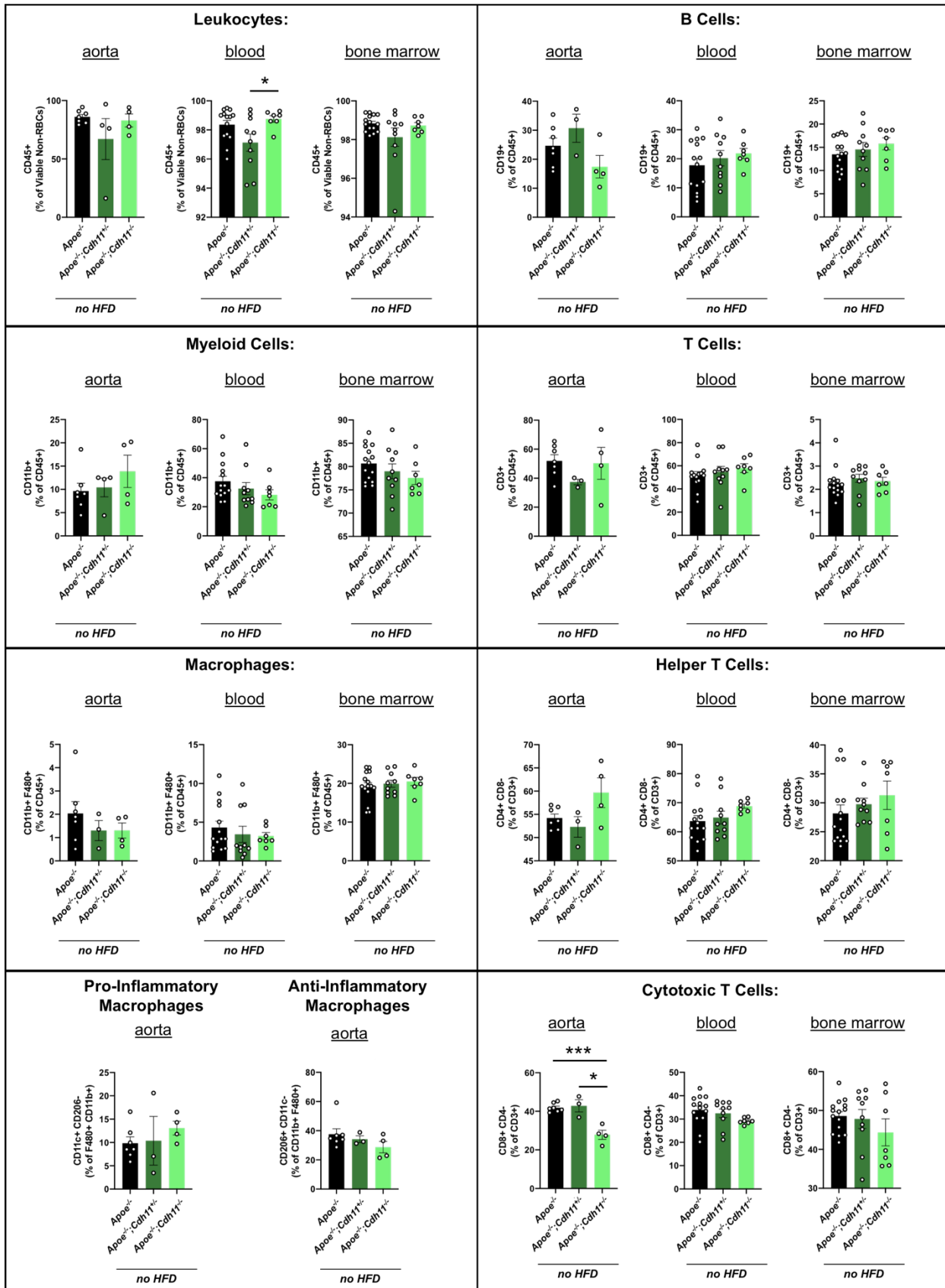
Cytotoxic T Cells:

aorta   blood   bone marrow

83

Figure 5.1. A flow cytometry panel was performed on the aorta, blood, and bone marrow of adult, healthy *Apoe*^{-/-}, *Apoe*^{-/-};*Cdh11*^{+/-}, and *Apoe*^{-/-};*Cdh11*^{-/-} mice. Antibodies stained for populations of leukocytes (CD45+), myeloid cells (CD45+ CD11b+), B cells (CD45+ CD19+), T cells (CD45+ CD3+), helper T cells (CD45+ CD3+ CD4+ CD8-), cytotoxic T cells (CD45+ CD3+ CD8+ CD4-), macrophages (CD45+ CD11b+ F4/80+), pro-inflammatory macrophages (CD45+ CD11b+ F4/80+ CD11c+ CD206-), and anti-inflammatory macrophages (CD45+ CD11b+ F4/80+ CD206+ CD11c-). There were almost no changes in populations between genotypes under these baseline healthy conditions.

WT mice [15], [187]; therefore, it is useful to know that the baseline immune response remains relatively unchanged, and that the effects described in Chapter 4 result from a response to inflammation. Although there are almost no significant differences across the panel, it is of interest to note that some trends align with what is observed during the atherosclerotic immune response. The population of myeloid cells in the blood decreases with loss of *Cdh11*, as the T cell population increases, although this difference is so small that it does not reach significance. Likewise, the CD4+ T cell population increases in the aorta and blood with loss of *Cdh11*; however, once again, the change is too subtle to be significant. These trends align with the changes observed in the *Cdh11*-deficient atherosclerotic mice. These results suggest that, although the baseline response remains statistically unchanged, there are likely some innate differences in *Cdh11*-deficient immune cells causing very subtle differences under healthy conditions which are difficult to detect.

5.E—Acknowledgments

5.F—Sources of Funding

CHAPTER 6

Therapeutic targeting of cadherin-11 in atherosclerosis

6.A—Introduction

CDH11 has been associated with a number of different fibrotic and inflammatory diseases, including pulmonary fibrosis, dermal fibrosis, CAVD, and rheumatoid arthritis [7], [8], [28], [34], [188]. Furthermore, treatment with a CDH11 blocking antibody has been shown to improve outcomes in CAVD [28], rheumatoid arthritis [34], and scar-formation post-myocardial infarction [16]. Due to the similarities between atherosclerosis and several of these CDH11-associated diseases, including immune cell infiltration, endothelial activation, and ECM degradation, we sought to determine if a CDH11 blocking antibody had therapeutic potential in atherosclerosis.

6.B—Materials and Methods

6.B.1—Animal studies

Apoe$^{-/-}$ male mice were acquired from Jackson Laboratory. Mice were placed on a HFD at five weeks old for a duration of ten weeks. Mice were weighed and given intraperitoneal injections of IgG2a or SYN0012 (10 mg/kg) every ten days. At the end of the study, mice were sacrificed using CO_2.

6.B.2—Quantitative PCR

Quantitative PCR was performed aortic arches dissected from experimental mice. The sequences for the primers used are listed in **Appendix A**.

6.B.3—En face staining

     Following sacrifice, mice were perfused with PBS-/- followed by formalin. Aortas were dissected and placed in formalin for fixation. Perivascular adipose tissue and connective tissue was carefully removed, and the aortas were opened and pinned (Fine Science Tools, 26002-20) onto a black dissection tray. Aortas were stained with Sudan IV (Sigma-Aldrich, S4261-25G) (5 grams, 500 mL 70% ethanol, 500 mL acetone, filtered) for 15 minutes at room temperature, followed by a twenty minute rinse in 80% ethanol. Images were taken using a Leica microscope and quantified via custom image processing analysis based on color segmentation [169]. The percentage of plaque coverage was quantified as the ratio of red pixels to background pixels for each pinned aorta; all analysis was performed in MATLAB.

6.B.4—Immunohistochemistry

     The aortic arch was removed during dissection and frozen in OCT (Optimal Cutting Temperature) at -80° C. Tissue blocks were sectioned in 10 μm sections on a cryostat and placed on SuperFrost Plus Slides (Fisher Scientific, 12-550-15). After dissolving the OCT in PBS-/-, slides were blocked in 1% BSA (bovine serum albumin) for one hour followed by staining in antibodies diluted in 1% BSA at 4° C overnight. Slides were washed in PBS-/- and mounted in DAPI. Slides were allowed to set overnight before being imaged on an Olympus microscope. Immunostaining was performed using the following antibodies: CD68 Monoclonal Antibody (FA-11) PE-conjugated, Thermo Fisher Scientific, #12-0681-80, 1:50 dilution; and Prolong™ Gold Antifade Mountant with DAPI, P36931.

6.C—Results

Aortas dissected from mice treated with a CDH11 blocking antibody (SYN0012) did not show a statistically significant change in plaque area as measured via *en face* staining (**Figure 6.1**). However, the aortas containing the highest percentage of plaque area were from mice treated with the isotype control (IgG2a).
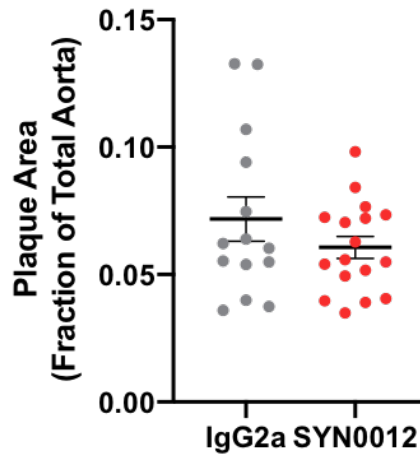
Figure 6.1. There was no difference in plaque area between IgG2a- and SYN0012-treated mice.

In addition to measuring plaque area, we also quantified markers of inflammation via qPCR. Likewise, aortic arches dissected from mice treated with SYN0012 did not exhibit any statistically significant changes in the plaque and inflammatory markers: *Adgre1*, the gene for F4/80, a macrophage marker; *IL-1b*, a pro-inflammatory cytokine; *Vcam-1*, a leukocyte adhesion molecule upregulated in plaques; *Mmp12*, a proteolytic enzyme secreted by macrophages in plaques; and *Tgfb1*, a cytokine present in plaque tissue (**Figure 6.2.A**). Histological samples of the aortic arch stained for the macrophage marker CD68 did not show any differences, either (**Figure 6.2.B**).

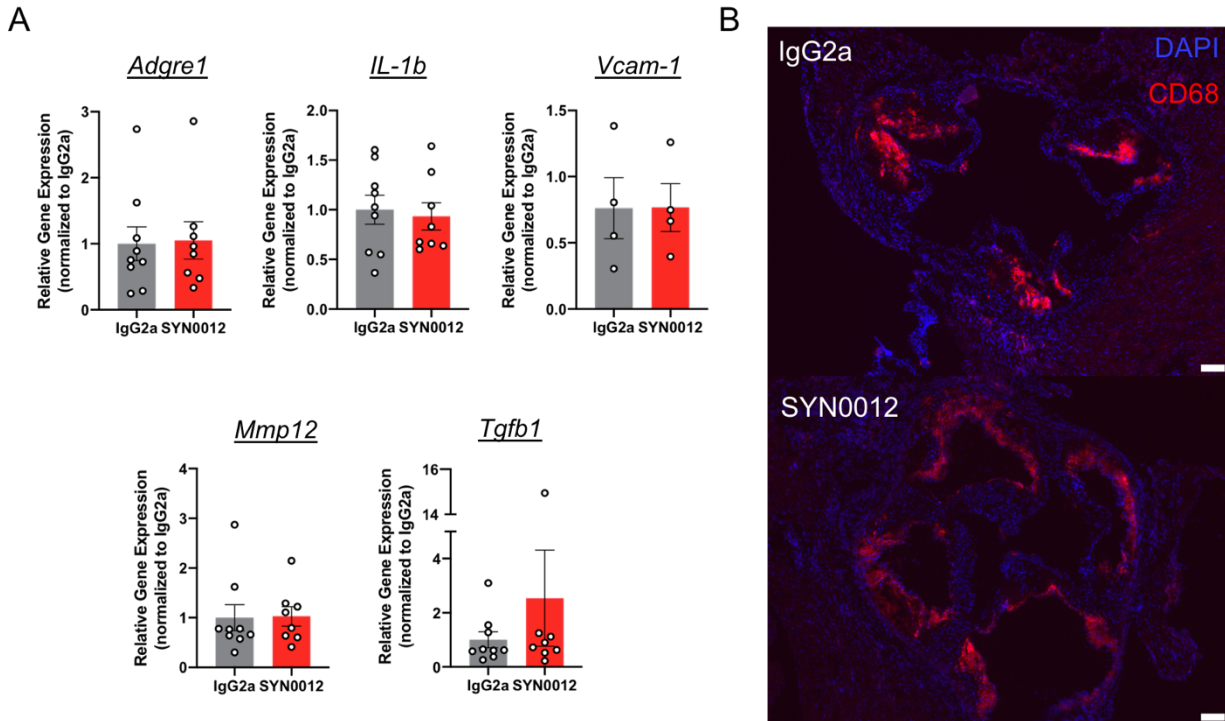**Figure 6.2**. Markers of inflammation (**A**) and macrophage content (**B**) are unchanged between IgG2a- and SYN0012-treated mice.

6.D—Discussion

In order for a complete exploration of the potential of CDH11 as an atherosclerotic therapeutic target, we sought to determine the effect of a CDH11 blocking antibody (SYN0012) on plaque burden. Despite the proven efficacy of treatment with a CDH11 blocking antibody in other mouse models of disease, including CAVD [28], there did not seem to be an effect on atherosclerosis plaque area or inflammation with SYN0012 treatment. Although the aortas with the largest plaque areas were from IgG2a-treated mice, the disparity was too subtle to reach statistical significance. Although SYN0012 treatment affected macrophage migration *in vitro* (described in Chapter 4), the impact was not sufficient enough to reduce plaque burden *in vivo*. It is also possible that different timepoints could yield different results, and a longer duration of HFD and subsequent

higher disease severity could make the difference between treatments more pronounced. Future studies should also determine if the same changes in immune cell populations were present in the SYN0012-treated mice as were observed in the global deletion and BMT described in Chapter 4.

6.E—Acknowledgments

6.F—Sources of Funding

CHAPTER 7

Side-specific valvular endothelial-interstitial cell mechano-communication via cadherin-11

7.A—Abstract

CAVD is a condition causing stiffening of the aortic valve, impeding cardiac function and resulting in significant morbidity worldwide. CAVD is thought to be driven by the persistent activation of the predominant cell type in the valve, AVICs, into myofibroblasts, resulting in subsequent calcification and stenosis of the valve. Although much of the research into CAVD focuses on AVICs, AVECs have been shown to regulate AVICs and maintain tissue homeostasis. Exposed to distinct flow patterns during the cardiac cycle, the AVECs lining either side of the valve demonstrate crucial differences which could contribute to the preferential formation of calcific nodules on the aorta-facing (fibrosa) side of the valve. CDH11 is a cell-cell adhesion protein which has been previously associated with AVIC myofibroblast activation, nodule formation, and CAVD in mice. In this study, we investigated the role of CDH11 in AVECs and examined side-specific differences. The aorta-facing or fibrosa endothelial cells (fibAVECs) express higher levels of CDH11 than the ventricle-facing or ventricularis endothelial cells (venAVECs). This increase in expression corresponds with increased contraction of a free-floating collagen gel compared to venAVECs. Additionally, co-culture of fibAVECs with AVICs demonstrated decreased contraction compared to an AVIC+AVIC control, but

increased contraction compared to the venAVECs co-culture. This aligns with the known preferential formation of calcific nodules on the fibrosa. These results together indicate a potential role for CDH11 expression by AVECs in regulating AVIC contraction and subsequent calcification.

7.B—Introduction

CAVD is a condition characterized by the formation of calcific deposits on the aortic valve, resulting in impaired cardiac function and presenting in up to 25% of Americans over 65 [26]. This calcification predominantly occurs on the side of the leaflets facing the aorta, known as the fibrosa (the ventricle-facing side of the leaflet is known as the ventricularis) [30]. CAVD is primarily considered to be a fibroblast-driven disease orchestrated by the majority cell type populating the leaflets, AVICs. However, the AVECs lining either side of the leaflets, exposed to blood flow through the valve, are able to transduce mechanical signaling [189] and alter AVIC signaling via chemokine secretion [29]. A hallmark of disease progression is the activation and differentiation of fibroblasts into myofibroblasts, increasing their proliferation, ECM deposition, and contraction [12]. Co-culture models have demonstrated that AVECs can inhibit this AVIC myofibroblast differentiation [29] and induce AVICs to maintain quiescence [75]. Under unidirectional flow conditions, AVECs exhibit anti-calcific gene expression profiles [29]. Furthermore, endothelial dysfunction is often an early sign of valve disease [29], [79], [190]. For these reasons, it is important to further incorporate AVECs into CAVD research in order to more fully understand their impact on AVIC signaling and disease progression.

The aorta-facing or fibAVECs and the ventricle-facing or venAVECs exist in very different hemodynamic environments and exhibit distinct gene expression profiles [30].

During the opening of the valve, venAVECs experience high shear stress unidirectional flow, whereas upon closure of the valve, fibAVECs are exposed to low recirculatory shear stress flow patterns [30], [79]. These distinct flow environments alter the ability of AVECs to inhibit myofibroblast differentiation and thus impact valve calcification. Anti-calcific gene expression profiles are found in AVECs exposed to unidirectional flow [29]. Likewise, the fibrosa endothelium presents lower expression of anti-calcific genes [30]. Due to CAVD predominantly developing on the fibrosa where the endothelium is exposed to these recirculatory flow patterns, the differences in AVEC populations could be critical in further understanding contributions to disease initiation and progression.

CDH11 is a cell-cell adhesion protein which functions via homophilic extracellular bonds and anchoring to the actin cytoskeleton via catenins [166]. CDH11 is involved in migration and differentiation [185], often associated with a more invasive phenotype [166], and implicated in a range of fibrotic and inflammatory diseases, including pulmonary fibrosis [13], scleroderma [22], rheumatoid arthritis [34], [167], and CAVD [12], [28]. Diseased human valves with CAVD show enrichment of CDH11 [191]. Additionally, AVICs treated with TGF-β, a known inducer of myofibroblast differentiation and a key initiator in valve calcification [5], demonstrate significant CDH11 upregulation [12], [17], [192]. Previous studies have described the necessity of CDH11 expression by AVICs for nodule formation *in vitro* [12], [191]. Interestingly, *Cdh11$^{-/-}$* murine AVICs demonstrate lower contraction *in vitro*, despite increased α-SMA, a common indicator of contractile ability that is significantly upregulated during myofibroblast differentiation [26]. Furthermore, targeting CDH11 reduced aortic valve stenosis in a mouse model of CAVD [28]. Despite this body of research on CDH11 in myofibroblasts and fibrotic tissue, little is

92

known about the role of CDH11 in AVECs. CDH11 is known to be mechanically regulated, showing decreased expression in AVECs under unidirectional flow conditions [180], such as those found in the environment of the venAVECs. However, it is unknown whether there is a side-specific difference in AVEC CDH11 expression or whether that has an impact on AVEC signaling and subsequent AVIC behavior. Our objective in this study was to determine if side-specific AVECs demonstrated differences in CDH11 expression and if that difference resulted in altered contraction profiles either in single culture or in co-culture with AVICs.

7.C—Materials and Methods

7.C.1—AVEC isolation

Aortic valves were isolated from pig hearts obtained at a local abattoir (Hampton Meats, Hopkinsville, KY). Valves were transported in PBS on ice, and cells were isolated within 8 hours of dissection. Side-specific EC isolation was done as described previously by Gould, et al [193]. Briefly, aortic valves were digested in collagenase II, placed in a dish with the fibrosa side face up, and a cotton swab was used to gently release the ECs from the surface. Cells were plated in endothelial media (Endothelial Growth Media Bullet Kit, Lonza, #CC-3162) on tissue culture-treated plastic coated with 1% gelatin. The leaflets were flipped, and this process was repeated for the ventricularis side. Colonies were purified via clonal expansion according to Cheung et al [194]. Briefly, cells were lifted and plated in a 96-well plate at a final concentration of 0.3 cells/well, resulting in approximately one-third of the wells containing a cell and giving a high probability of colonies originating from a single cell. After two weeks, thriving colonies of endothelial morphology were passaged and grown until confirmation of phenotype. After phenotype

confirmation, lines arising from several different wells were combined in order to prevent the final cell line from being completely homogenous.

7.C.2—Immunostaining and western blots
Immunostaining was performed using the following antibodies: CDH11, Thermo Fisher Scientific, #71-7600, 1:50 dilution; α-SMA, Cy3-conjugated, Millipore Sigma, C6198, 1:300 dilution; Prolong™ Gold Antifade Mountant with DAPI, P36931. Western blotting was performed using the following antibodies: CDH11, Cell Signaling Technologies, #4442BF, 1:4000 dilution; α-SMA, Abcam, ab5694, 1:1000 dilution; α-Tubulin, Vanderbilt MCBR Core, 1:1000 dilution.

7.C.3—Gel contraction assays
Gel contraction assays were performed using a free-floating collagen gel. For single-cell assays, 100,000 cells were seeded onto the top of the gel. For co-culture assays, 50,000 AVICs were embedded within the gel during polymerization, and 50,000 AVICs, fibAVECs, or venAVICs were seeded on top of the gel post-polymerization. Media was changed every 48 hours. Gels were allowed to contract for up to 96 hours, and images were taken periodically for quantification. ImageJ was used to quantify the fraction of contraction.

7.D—Results

7.D.1—Clonal expansion ensured purity of isolated AVEC populations
The side-specific ECs were first clonally expanded prior to experimentation to ensure both that the populations were free from contaminating AVICs isolated along with the AVECs and that the ECs did not undergo EndMT. Clonal expansion resulted in purified AVEC populations. Immunostaining was performed using CD31 as an endothelial marker and α-SMA as a marker of AVIC contamination. Another sample from the line of

venAVECs was allowed to grow without clonal expansion and used as a control for comparison. **Figure 7.1** illustrates the confirmation of endothelial phenotype with minimal presence of other cell types. Both the clonally expanded venAVEC and fibAVEC lines show strong CD31 expression with minimal to no α-SMA expression. Without clonal expansion, the venAVEC line was overtaken with fibroblasts, demonstrating minimal CD31 expression and an abundance of α-SMA fibers.
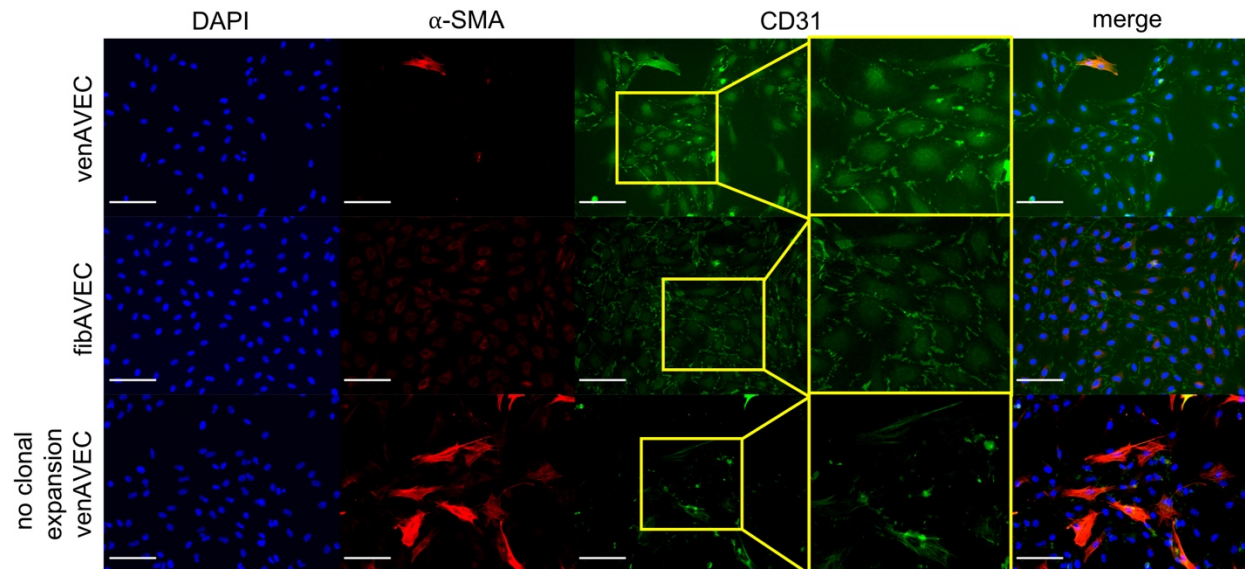
Figure 7.1. Both clonally expanded AVEC lines (venAVEC and fibAVEC) were stained using CD31 as an endothelial marker and α-SMA as a fibroblast marker, confirming endothelial phenotype. A line of non-clonally expanded venAVECs was used as a control. Scale bar is 100 μm.

7.D.2—Fibrosa AVECs demonstrated higher expression of CDH11 compared to ventricularis AVECs

Previous studies have established distinct gene expression profiles between venAVECs and fibAVECs [30]. Due to prior work implicating CDH11 expression by AVICs in nodule formation and in valve calcification[12], [191], we sought to examine possible differences in CDH11 expression by AVECs. Both AVEC lines were grown on 1% gelatin-coated tissue culture plastic, and cell lysates were analyzed via Western blot. We found

that fibAVECs expressed approximately three times as much CDH11 compared to the venAVECs (**Figure 7.2A**). Interestingly, the fibAVECs also had slightly higher expression of CDH11 compared to AVICs. Neither AVEC line expressed α-SMA, and we observed no differences in eNOS expression (**Figure 7.2A**). Immunostaining of both venAVECs and fibAVECs confirmed the Western blot results, illustrating higher levels of CDH11 in the fibrosa-side ECs compared to the ventricularis-side (**Figure 7.2B**).
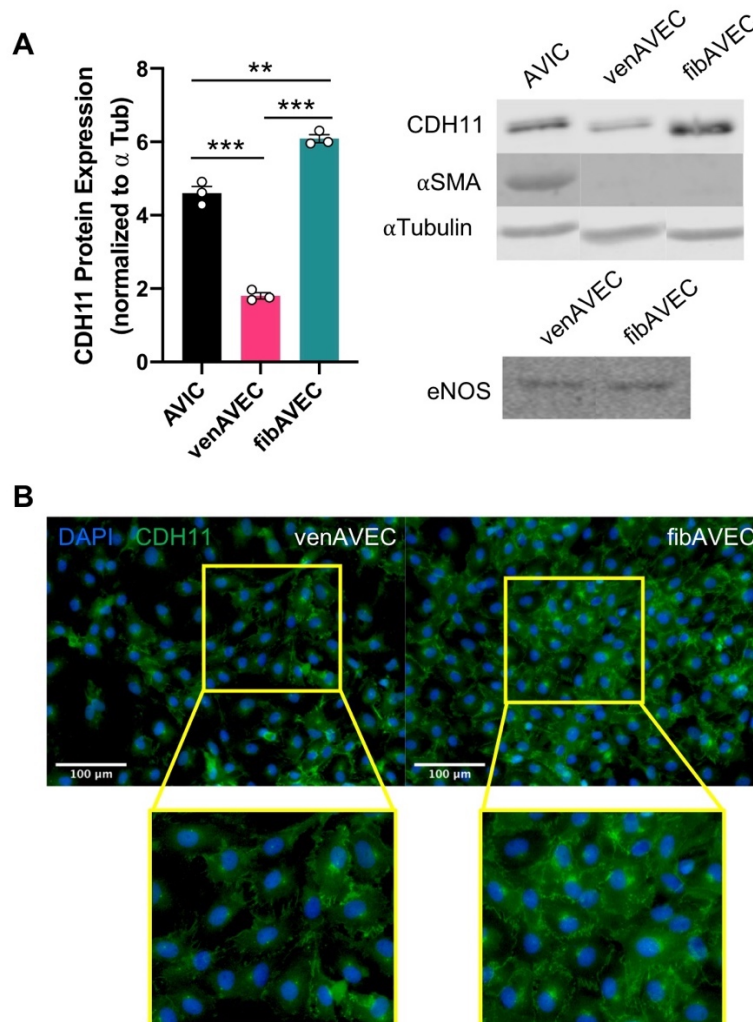
Figure 7.2. (**A**) FibAVECs express higher levels of CDH11 as measured by Western blot compared to both venAVECs and AVICs, while venAVECs express substantially less CDH11 than both. Neither of the AVEC lines demonstrated any α-SMA. There were no changes in eNOS expression between the two AVEC lines. (**B**) Immunostaining also illustrated higher expression of CDH11 by fibAVECs compared to venAVECs. ** indicates $p<0.01$; *** indicates $p<0.001$

7.D.3—Fibrosa AVECs exhibit higher contraction of a free-floating collagen gel both in single culture and in co-culture with AVICs when compared to ventricularis AVECs
In order to determine any differences in contraction between the side-specific ECs, we performed a gel contraction assay. Cells were seeded onto a free-floating collagen gel and allowed to contract for up to 96 hours in order to measure the degree of contraction. **Figure 7.3A** illustrates the culture conditions for the single and co-culture models. For single cultures (**Figure 7.3B**), gels were seeded with either venAVECs, fibAVECs, or AVICs. Predictably, the AVICs contracted sooner and to a greater degree than either of the endothelial lines. However, although neither of the AVEC cell lines express detectable α-SMA, a typical marker of contractile ability, the fibAVECs began to contract earlier at 36 hours and sustained that contraction until the experiment ended at 96 hours.

Additionally, the collagen gels were also used to perform co-culture contraction experiments (**Figure 7.3C**), with one cell type embedded within the gel (AVICs) and one seeded on top (AVECs), representative of the aortic valve structure. One group contained AVICs both embedded and seeded on top of the gel to be used as a control. After 12 hours, both the AVIC+AVEC co-culture collagen gels had contracted less than the AVIC+AVIC control. The AVIC+fibAVEC gels contracted significantly more than the AVIC+venAVEC gels, aligning with the difference in contraction seen in the single culture model.
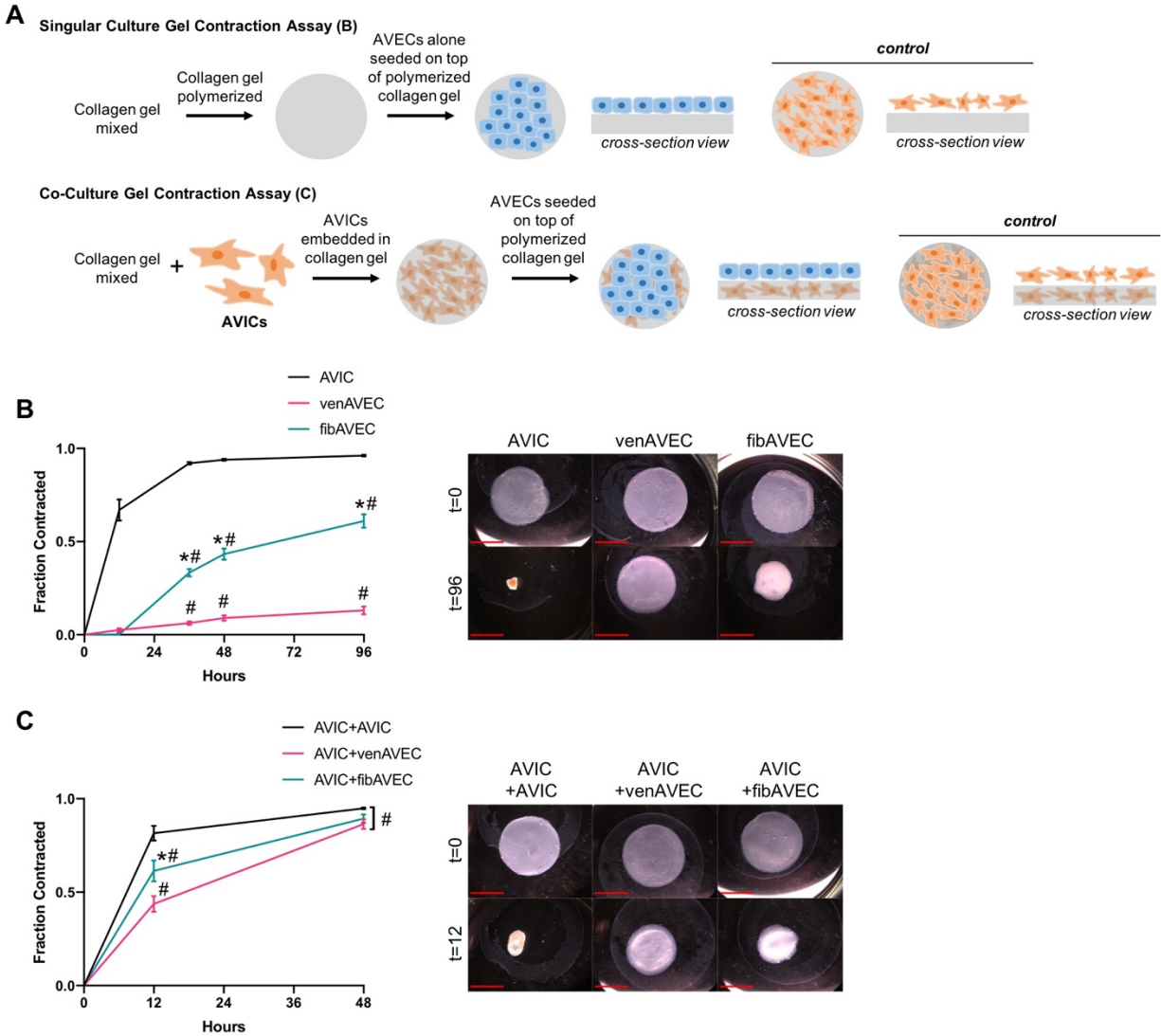
Figure 7.3. (**A**) An illustration of the set-up for both the single and co-culture gel contraction assays. (**B**) FibAVECs contracted a free-floating collagen gel significantly more than venAVECs over a 96 hour period. Each point represents n=3. (**C**) In a co-culture with AVICs, fibAVECs contracted a free-floating collagen gel less than an AVIC-AVIC co-culture at 12 hours, but significantly more than an AVIC-venAVEC co-culture. Each point for AVIC+venAVEC and AVIC+fibAVEC represents n=6, and for AVIC+AVIC, each point represents n=5. Scale bar is 1 mm.
* indicates difference of $p<0.05$ between fibAVEC and venAVEC at the same timepoint; # indicates difference of $p<0.05$ from AVIC at the same timepoint

7.E—Discussion

Previous research has examined the role of CDH11 in the activation, proliferation, and contraction of myofibroblasts, as well as its role in the formation of AVIC calcific nodules characteristic of CAVD [12], [17]. However, despite the known ability of AVECs

to inhibit myofibroblast activation and otherwise affect calcification [29], little is known about the role of CDH11 in AVECs and that impact on AVIC disease pathology. The results from this study both show significant CDH11 expression by AVECs and demonstrate a previously unreported difference in CDH11 expression between the AVECs of the fibrosa and ventricularis sides of the aortic valve. This is of importance due to the side-specific nature of the clinical disease progression, with preferential calcification on the fibrosa [30]. Additionally, this lines up with what is known about CDH11 mechanotransduction. Previous studies have shown that CDH11 expression is decreased in AVECs under unidirectional flow [180]. The venAVECs, exposed to high shear stress unidirectional flow in the valve, correspondingly exhibited lower expression of CDH11. Of clinical relevance, healthy human aortic valves show higher expression of CDH11 along the endothelium, while diseased samples show CDH11 distributed more evenly through the interstitium [12], indicating that CDH11 expression by the endothelium could play a role earlier in disease initiation. Given the established link between CDH11 expression and CAVD, this finding could have implications in further understanding the disease pathology.

The gel contraction results demonstrate an innate difference between the fibrosa and ventricularis AVECs *in vitro*. Although the single cultures of AVECs lacked any α-SMA expression, there was still observable gel contraction and a disparity between the venAVECs and fibAVECs. This difference in gel contraction may likely be a result of the difference in CDH11 expression between the fibAVECs and venAVECs. Murine *Cdh11$^{-/-}$* AVICs contract less in culture despite an upregulation of α-SMA [26], opposing conventional understanding of contractile ability and underlining the importance of CDH11

in contraction. However, it is also possible that this difference in gel contraction observed is not due to the cells contracting, but due to the cells exerting traction forces on the collagen gel. It is important to note that these expression differences in CDH11 observed here were measured in two-dimensional culture, and the three-dimensional nature of the gels could have affected protein expression. Additional studies could gather pertinent information by quantifying protein expression in the contracted gels. Likewise, although these VEC populations remained endothelial in phenotype during static culture, the possibility that they underwent EndMT in the softer environment of the collagen gel cannot be ruled out. Higher rates of EndMT could be an explanation for the higher gel contraction observed in the fibAVECs. Although these results cannot conclusively link the CDH11 disparity between venAVECs and fibAVECs to their contractile differences, it is reasonable to consider CDH11 a likely perpetrator due to the previously established relationship between CDH11 expression and contraction both in other cell types, most notably AVICs [26], and in CAVD [12]. These results illustrate another side-specific difference between AVECs and reveal another possible pathway through which AVEC signaling could impact AVIC function during disease progression. Future studies can draw stronger conclusions by utilizing a method of genetic knockdown of CDH11 in both cell types in the same assay.

The co-culture of both AVEC lines with AVICs demonstrated decreased contraction compared to AVICs alone, exhibiting another beneficial effect of AVEC co-culture. However, the co-culture of fibAVECs+AVICs exhibited higher contraction at 12 hours compared to venAVECs+AVICs. Although studies have reported preferential nodule formation on the fibrosa of porcine valves cultured *ex vivo* [29] in addition to lower

expression of anti-calcific genes by the fibrosa [30], a difference in contraction had not been previously observed. This is similar with what is observed in *vivo*, with the fibrosa side of the valve demonstrating the majority of the calcification. Given previous findings illustrating the importance of CDH11 expression by AVICs in nodule formation [12] and the predisposition for calcification on the fibrosa side of the leaflet [30], these results are relevant in further understanding of the disease pathology of CAVD. Further study will be crucial in understanding to what extent CDH11 is directly involved in the contractile differences observed between the two different types of AVECs.

7.F—Acknowledgments

7.G—Sources of Funding

CHAPTER 8

Impact and Future Directions

8.A—Societal Impact

CVD represents a substantial global health burden, and atherosclerosis and CAVD make up two significant components of that problem [1], [72]. A more comprehensive understanding of the molecular mechanisms involved in the pathology of these diseases could contribute to the development of improved pharmacological therapies, particularly in CAVD for which surgical intervention is the only current option [26]. Furthermore, CDH11 is a viable therapeutic target for a range of diseases, from pulmonary fibrosis to CAVD to rheumatoid arthritis [7], [28], [34], [188], and a broader knowledge of the impact of CDH11 is critically important. This study first sought to further our understanding of the role of CDH11 in cell types beyond fibroblasts, of which there is substantial current research [17], [26], [195], and to specifically investigate the role of CDH11 in macrophages in the immune response to atherosclerosis and in AVECs in the contraction characteristic of CAVD.

First, we explored the role of CDH11 in atherosclerosis. This research indicates that, despite increased *Cdh11* expression in plaques which also positively correlated with the expression of inflammation markers, a genetic loss of *Cdh11* negatively impacts atherosclerosis, with both increased markers of plaque inflammation and increased plaque area. However, a loss of *Cdh11* proved to have a profound impact on the immune response in atherosclerosis. *In vivo* studies of both a genetic deletion of *Cdh11* and BMT

from *Cdh11*-deficient mice suggested an impaired myeloid cell migration phenotype with loss of *Cdh11*, and *in vitro* experiments confirmed decreased migration in *Cdh11$^{-/-}$* macrophages. This research also indicates that the impairment of *Cdh11$^{-/-}$* macrophages resulted from impaired biomechanical properties, including decreased cortical tension. Although it is well-known that CDH11 is a mechanically sensitive protein involved in mechanotransduction [195], very little is known about the impact of CDH11 in macrophage mechanobiology. These results for the first time point to a change in macrophage behavior with loss of *Cdh11* which results from impaired mechanical properties. Furthermore, RNAseq results demonstrate that macrophages could be altering T cell recruitment and proliferation via increased expression of MHC class II molecules, promoting CD4+ helper T cell activation. This corresponds to an observed increase in CD4+ T cells in both the blood and aorta of atherosclerotic *Apoe$^{-/-}$;Cdh11$^{-/-}$* and mice given BMTs from *Cdh11*-deficient mice. This trend is also maintained in healthy *Cdh11*-deficient *Apoe$^{-/-}$* mice, although not significantly, due to very small differences. This difference in T cell population could be of substantial importance when considering targeting CDH11 in disease. Although a CDH11 monoclonal blocking antibody (SYN0012) was ineffective at altering plaque phenotype, CDH11 remains a hopeful therapeutic target for a number of other diseases, many of which involve an active inflammatory process. This research provides one explanation for how CDH11 impacts the immune response and a pathway through which targeting CDH11 could affect macrophage and T cell phenotype.

Second, we investigated the role of CDH11 in AVECs. Although significant work has been devoted to the function of CDH11 in AVICs and their pathology during CAVD

progression [17], [26], [195], relatively little has been known about CDH11 in AVECs. Due to the differences in hemodynamic environments, it is important isolate AVECs from either side of the aortic valve. However, this is impossible to do in mice, due to the size of the aortic valve leaflets, and therefore makes side-specific studies more challenging and rarer in literature. Here, we isolated porcine side-specific AVECs in order to investigate the role of CDH11 in their function. *In vitro* studies demonstrated that fibAVECs exhibited higher CDH11 expression compared to venAVECs. Furthermore, this study showed that fibAVECs contracted a free-floating collagen gel more than venAVECs, both when cultured alone or when co-cultured with AVICs. Although it cannot be conclusively determined based on these results alone, it is a reasonable hypothesis that this difference in contraction is related to the disparate expression of CDH11, as CDH11 has been thoroughly characterized to play a role in the contraction of other cell types [26]. These findings are of particular importance due to the side-specific calcification on the fibrosa side of the aortic valve, and these results indicate one potential explanation for the side-specific nature of the disease. With no good current pharmacological treatments, a more complete understanding of the mechanism of CAVD is of significant importance.

CDH11 is a promising therapeutic target, particularly in fibrosis, and a more complete understanding of its role in other cell types is imperative. The work described here both details changes in the immune response with loss of *Cdh11*, as well as providing an explanation for the differences in macrophage and T cell phenotype. Additionally, this work confirmed a difference in the contractile phenotype between fibAVECs and venAVECs, possibly due to CDH11 expression, and posing another potential pathway through which AVECs impact CAVD progression.

8.B—Future Directions

8.B.1—Cadherin-11 in the Atherosclerotic Immune Response

The increased plaque burden observed in the genetic deletion of *Cdh11* cannot be conclusively explained with the data described here alone. Many of the cell types in atherosclerosis express CDH11, including ECs, vascular SMCs, and AFs, and *Cdh11* loss in any of those cells could have caused the worsened disease phenotype observed. Future studies could investigate the role of CDH11 in these cell types utilizing Cre-specific genetic knockouts.

The specific timeframe utilized in this study, ten weeks, could have also limited the findings. A loss of *Cdh11* could impact fibrotic processes, which could be more pronounced at later timepoints [196], [197]. Additional studies quantifying disease progression for a longer duration of HFD, potentially 14 weeks, could demonstrate differing results.

Additional *in vivo* studies could also reveal more details about the impact of *Cdh11* deletion in inflammation. The work in this dissertation suggests that a loss of *Cdh11* leads to impaired myeloid trafficking during atherosclerotic inflammation. Future studies could utilize fluorescent labeling to quantify myeloid trafficking *in vivo* [198]. This could more definitively reveal the relationship between loss of *Cdh11* and a decrease in the myeloid population of the blood. Furthermore, although CD4+ helper T cells are typically disease-aggravating in atherosclerosis, this is not always the case. Other disease models could be improved with this observed change in T cell phenotype, and exploration of *Cdh11* deletion in this model could prove to elucidate the role of CDH11 in this mechanism more completely. Likewise, an adoptive transfer of *Cdh11*-deficient monocytes could more conclusively explore the relationship between *Cdh11* expression by macrophages in

atherosclerosis development [198], isolated from the impact of *Cdh11* loss in other leukocytes. Although the present study clearly presents a relationship between CDH11 and the atherosclerotic immune response, these future studies could provide more details about the mechanism involved.

There is substantial potential for future studies concerning CDH11 in immune cells. Due to the observed altered mechanical properties of *Cdh11*$^{-/-}$ macrophages, specifically decreased cortical tension, it would certainly be of interest to investigate mechanotransduction in macrophages. Future experiments could exert mechanical forces (strain, flow) on *Cdh11*$^{-/-}$ macrophages and determine if a loss of *Cdh11* prevents the translation of those cues into changes in intracellular signaling. Research has shown that macrophages plated on a micropatterned surface, forcing the cells into an elongated phenotype characteristic of M2 macrophages, resulted in changes into behavior typical of M2 macrophages, in the absence of cytokine polarization. However, with inhibition of actin polymerization, macrophages were capable of elongating, but not capable of translating that morphological cue into intracellular signals [24]. Future studies could determine, first, if *Cdh11*$^{-/-}$ macrophages have altered morphology or are capable of elongation and, second, if *Cdh11*$^{-/-}$ macrophages are able to translate those cues into biochemical signals. Because of the proven importance of mechanical regulation to macrophage polarization, CDH11 could play a substantial role in those processes.

Furthermore, the work in this study suggests that *Cdh11*$^{-/-}$ macrophages alter T cell phenotype, as well. Future *in vivo* studies should determine exactly which CD4+ T cell subtype is increased with loss of *Cdh11*, each of which could have a different implication for atherosclerosis and other inflammatory diseases. *In vitro* studies could also

be utilized to explore this further. Migration assays using conditioned media of $Cdh11^{-/-}$ macrophages could be performed to assess if T cell recruitment is affected. Activation assays could be performed as well, to determine if $Cdh11^{-/-}$ macrophages impact T cell activation and cytokine secretion, either through conditioned media or binding and antigen presentation. Co-culture experiments could demonstrate whether a loss of *Cdh11* affects macrophage binding to T cells, either directly or indirectly, through altered expression of co-stimulatory receptors.

8.B.2—Cadherin-11 in Calcific Aortic Valve Disease
Although the work presented here posits that differences in CDH11 expression could explain the differences in contractility between fibAVECs and venAVECs, that cannot be definitively concluded without further experiments. Future studies should utilize siRNA knockdowns of CDH11 in fibAVECs to determine if the contractile phenotype, both in single- and co-culture, is abrogated with loss of CDH11 expression. This would be significant because it would indicate that increased CDH11 expression and subsequent increased contraction could play a role in the side-specific calcification of the fibrosa.

STATISTICAL ANALYSIS

When data was normally distributed, statistics were performed using one-way ANOVA with post-hoc Holm-Sidak test for multiple comparisons and a student's t-test for two-group comparisons. When data was not normally distributed, non-parametric statistics were performed with post-hoc Tukey's and Dunn's tests for multiple comparisons. For all statistical comparisons, a value of at least $p < 0.05$ was considered significant; statistically significant differences are indicated in figures as appropriate.

PROTECTION OF RESEARCH SUBJECTS

All mice used in experiments are treated in accordance with the Institutional Animal Care

and Use Committee (IACUC). This study did not use any human subjects or samples.

APPENDIX A: Primers for Quantitative PCR

Gene	Forward	Reverse
Adgre1	ACCACAATACCTACATGCACC	AAGCAGGCGAGGAAAAGATAG
Mmp12	CCCATCTGGTATTCAAGCTGC	TTCACAGATGCAGAGAAGCC
Mmp13	GATTATCCCCGCCTCATAGAAG	TCTCACAATGCGATTACTCCAG
Cdh11	ACACCATGAGAAGGGCAAG	ACCGGAGTCAATGTCAGAATG
Il-1β	CGGACCCATATGAGCTGAAAG	AGATTCTTTCCTTTGAGGCCC
Vcam-1	GCAAAGGACACTGGAAAAGAG	TCAAAGGGATACACATTAGGGAC
Tgf-β1	CCTGGGTTGGAAGTGGATC	TTGGTTGTAGAGGGCAAGG

APPENDIX B: Antibodies for Flow Cytometry

Marker	Fluorophore	Company	Catalog #	Dilution: Bone Marrow	Dilution: Blood	Dilution: Aorta
DAPI	Pacific Blue	Thermo Fisher	D1306	1:200,000	1:1,000,000	1:500,000
Ter119	VF450	Tonbo Bioscience	75-5921	1:400	1:800	1:400
CD4	PE	BioLegend	100408	1:1600	1:3200	1:1600
F4/80	APC-eFluor780	Thermo Fisher	47-4801-80	1:400	1:400	1:800
CD19	FITC	Tonbo Bioscience	35-0193	1:800	1:800	1:800
CD45	PE-eFluor710	Thermo Fisher	61-0454-80	1:1600	1:1600	1:1600
CD3	BV510	BD Biosciences	563024	1:100	1:200	1:100
CD8	PE-Cy7	Tonbo Bioscience	60-0081	1:1600	1:3200	1:3200
CD11b	BV711	BioLegend	101241	1:800	1:800	1:800
CD11c	PerCP-Cy5.5	Tonbo Bioscience	65-0114	1:800	1:800	1:400
CD206	APC	Thermo Fisher	17-2069-41	1:400	1:200	1:800

Descriptions of RNA integrity (RIN) and number of sequencing reads for each sample used in RNA sequencing.

Sample	RIN	Total Yield (Reads)
WT macrophage 1	7.9	47526739
WT macrophage 2	6.9	35425678
WT macrophage 3	7.6	36776094
Cdh11$^{-/-}$ macrophage 1	7.8	36059526
Cdh11$^{-/-}$ macrophage 2	8.2	36470511
Cdh11$^{-/-}$ macrophage 3	8.4	38570877

APPENDIX D: Flow Cytometry Gating Strategy

single cells

dump dead cells and
red blood cells

leukocytes

T cells

macrophages

B cells

cytotoxic
T cells

helper
T cells

anti-
inflammatory

pro-
inflammatory
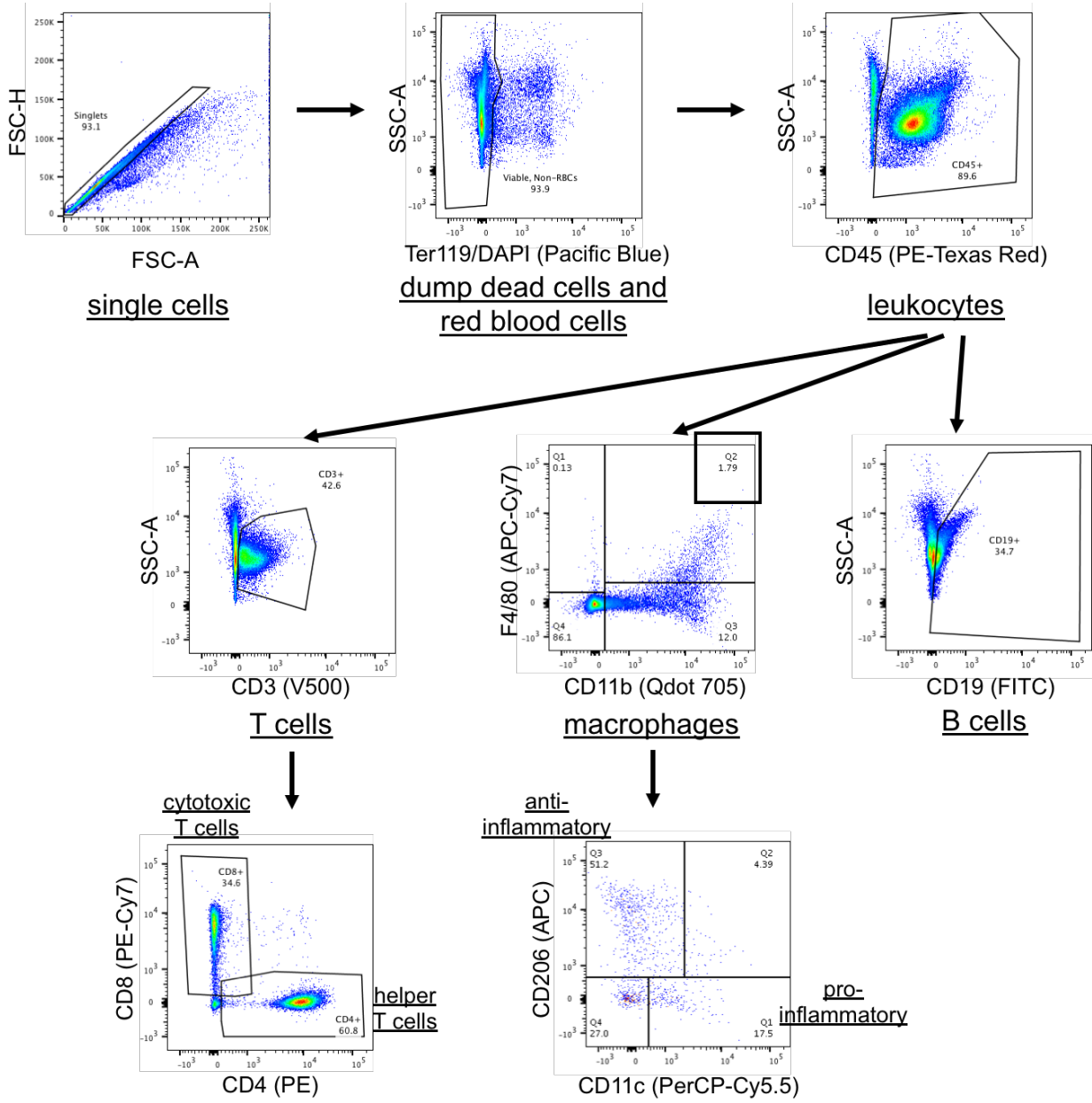
APPENDIX E: Complete Flow Cytometry Panel for *Cdh11* Global Deletion

114
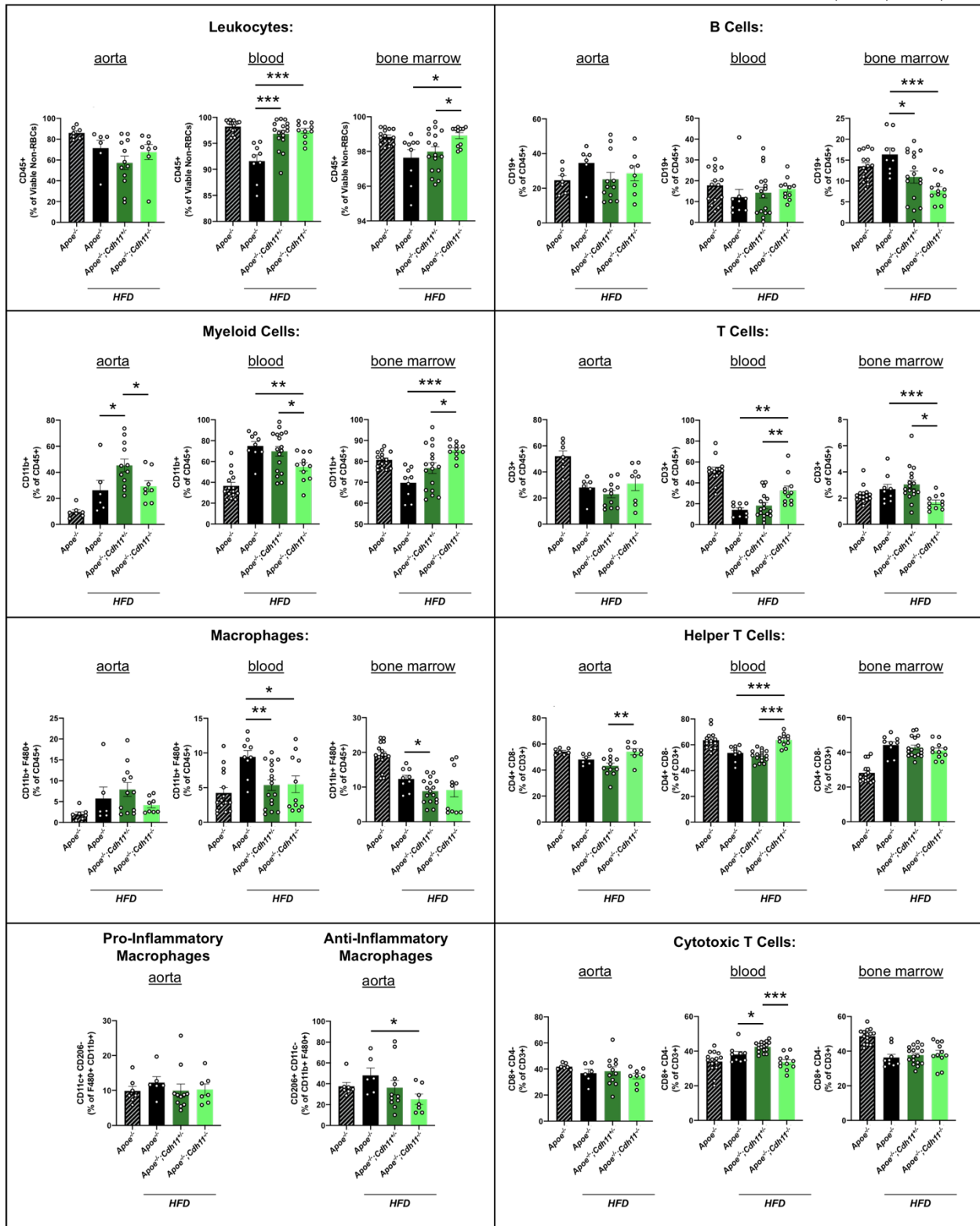
APPENDIX F: Complete Flow Cytometry Panel for *Cdh11* Bone Marrow Transplants

115

REFERENCES

[1]   S. Barquera *et al.*, "Global Overview of the Epidemiology of Atherosclerotic Cardiovascular Disease," *Archives of Medical Research*, vol. 46, no. 5. Elsevier Inc., pp. 328–338, 01-Jul-2015.

[2]   K. Balachandran, P. Sucosky, and A. P. Yoganathan, "Hemodynamics and Mechanobiology of Aortic Valve Inflammation and Calcification," *Int. J. Inflam.*, vol. 2011, pp. 1–15, 2011.

[3]   P. Libby, Y. Okamoto, V. Z. Rocha, and E. Folco, "Inflammation in atherosclerosis: transition from theory to practice.," *Circ. J.*, vol. 74, no. February, pp. 213–220, 2010.
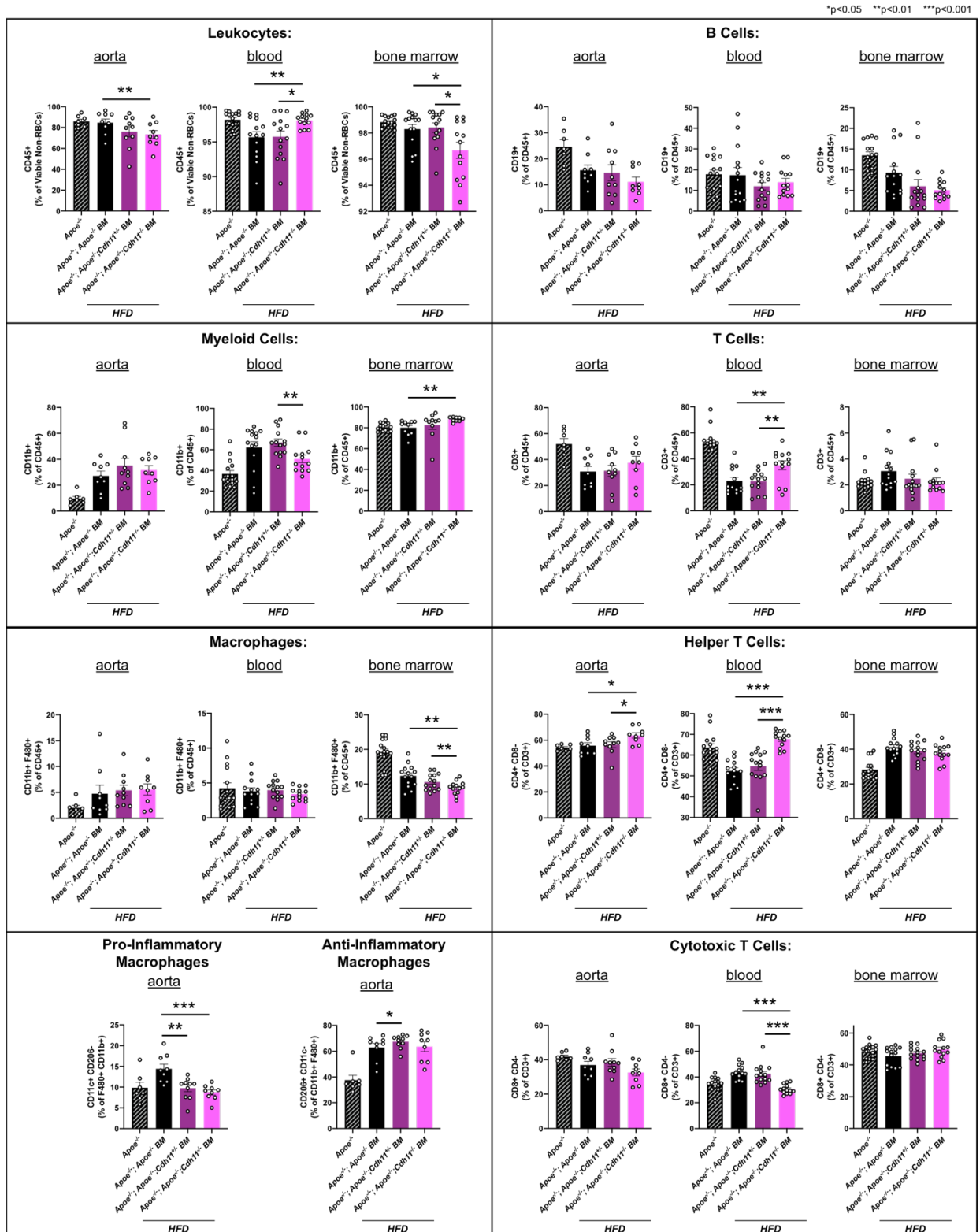
[4]   W. Insull, "The Pathology of Atherosclerosis: Plaque Development and Plaque Responses to Medical Treatment," *Am. J. Med.*, vol. 122, no. 1 SUPPL., pp. S3–S14, Jan. 2009.

[5]   C. I. Fisher, J. Chen, and W. D. Merryman, "Calcific nodule morphogenesis by heart valve interstitial cells is strain dependent," *Biomech. Model. Mechanobiol.*, vol. 12, no. 1, pp. 5–17, Jan. 2013.

[6]   H. Sakamoto *et al.*, "Biomechanical Strain Induces Class A Scavenger Receptor Expression in Human Monocyte/Macrophages and THP-1 Cells," *Circulation*, vol. 104, no. 1, pp. 109–114, Jul. 2001.

[7]   D. J. Schneider *et al.*, "Cadherin-11 contributes to pulmonary fibrosis: potential role in TGF-β production and epithelial to mesenchymal transition," *FASEB J.*, vol. 26, no. 2, pp. 503–512, Feb. 2012.

[8]   S. Kyung Chang, Z. Gu, and M. B. Brenner, "Fibroblast-like synoviocytes in inflammatory arthritis pathology: the emerging role of cadherin-11," *Immunol. Rev.*, vol. 233, no. 1, pp. 256–266, Jan. 2010.

[9]   D. M. Lee *et al.*, "Cadherin-11 in synovial lining formation and pathology in arthritis," *Science (80-.).*, vol. 315, no. 5814, pp. 1006–1010, Feb. 2007.

[10]   M. Pedroza, R. L. Welschhans, and S. K. Agarwal, "Targeting of cadherin-11 decreases skin fibrosis in the tight skin-1 mouse model," *PLoS One*, vol. 12, no. 11, p. e0187109, Nov. 2017.

[11]   J. T. Butcher *et al.*, "Transcriptional profiles of valvular and vascular endothelial cells reveal phenotypic differences: Influence of shear stress," *Arterioscler. Thromb. Vasc. Biol.*, vol. 26, no. 1, pp. 69–77, Jan. 2006.

[12]   J. D. Hutcheson *et al.*, "Cadherin-11 regulates cell-cell tension necessary for calcific nodule formation by valvular myofibroblasts," *Arterioscler. Thromb. Vasc. Biol.*, vol. 33, no. 1, pp. 114–120, Jan. 2013.

[13]   D. J. Schneider *et al.*, "Cadherin-11 contributes to pulmonary fibrosis: potential role in TGF-β production and epithelial to mesenchymal transition," *FASEB J.*, vol. 26, no. 2, pp. 503–512, Feb. 2012.

[14]   L. Simonneau, M. Kitagawa, S. Suzuki, and J. P. Thiery, "Cadherin 11 expression marks the mesenchymal phenotype: Towards new functions for cadherins??," *Cell Commun. Adhes.*, vol. 3, no. 2, pp. 115–130, 1995.

[15]   C. J. Bowen, J. Zhou, D. C. Sung, and J. T. Butcher, "Cadherin-11 coordinates cellular migration and extracellular matrix remodeling during aortic valve maturation," *Dev. Biol.*, vol. 407, no. 1, pp. 145–157, Nov. 2015.

[16] A. K. Schroer *et al.*, "Cadherin-11 blockade reduces inflammation-driven fibrotic remodeling and improves outcomes after myocardial infarction," *JCI Insight*, vol. 4, no. 18, Sep. 2019.

[17] H. Wang, L. A. Leinwand, and K. S. Anseth, "Roles of transforming growth factor-β1 and OB-cadherin in porcine cardiac valve myofibroblast differentiation," *FASEB J.*, vol. 28, no. 10, pp. 4551–4562, Oct. 2014.

[18] R. A.-K. L. S.-N. C. Hansson G.K., "Inflammation and atherosclerosis," *Annu. Rev. Pathol.*, vol. 1, no. 9, pp. 297–329, 2006.

[19] G. K. Hansson, A.-K. L. Robertson, and C. Söderberg-Nauclér, "INFLAMMATION AND ATHEROSCLEROSIS," *Annu. Rev. Pathol. Mech. Dis.*, vol. 1, no. 1, pp. 297–329, Feb. 2006.

[20] Z. Q. Yan and G. K. Hansson, "Innate immunity, macrophage activation, and atherosclerosis," *Immunological Reviews*, vol. 219, no. 1. Blackwell Publishing Ltd, pp. 187–203, Oct-2007.

[21] D. J. Schneider *et al.*, "Cadherin-11 contributes to pulmonary fibrosis: potential role in TGF- production and epithelial to mesenchymal transition," *FASEB J.*, vol. 26, no. 2, pp. 503–512, Feb. 2012.

[22] M. Wu *et al.*, "Identification of cadherin 11 as a mediator of dermal fibrosis and possible role in systemic sclerosis," *Arthritis Rheumatol.*, vol. 66, no. 4, pp. 1010–1021, 2014.

[23] B. Vandooren *et al.*, "Tumor necrosis factor α drives cadherin 11 expression in rheumatoid inflammation," *Arthritis Rheum.*, vol. 58, no. 10, pp. 3051–3062, Oct. 2008.

[24] F. Y. McWhorter, T. Wang, P. Nguyen, T. Chung, and W. F. Liu, "Modulation of macrophage phenotype by cell shape," *Proc. Natl. Acad. Sci. U. S. A.*, vol. 110, no. 43, pp. 17253–17258, Oct. 2013.

[25] N. R. Patel *et al.*, "Cell Elasticity Determines Macrophage Function," *PLoS One*, vol. 7, no. 9, p. e41024, Sep. 2012.

[26] M. A. Bowler, M. R. Bersi, L. M. Ryzhova, R. J. Jerrell, A. Parekh, and W. D. Merryman, "Cadherin-11 as a regulator of valve myofibroblast mechanobiology," *Am. J. Physiol. Circ. Physiol.*, vol. 315, no. 6, pp. H1614–H1626, Dec. 2018.

[27] J. D. Hutcheson *et al.*, "Cadherin-11 Regulates Cell–Cell Tension Necessary for Calcific Nodule Formation by Valvular Myofibroblasts," *Arterioscler. Thromb. Vasc. Biol.*, vol. 33, no. 1, 2012.

[28] C. R. Clark, M. A. Bowler, J. C. Snider, and W. D. Merryman, "Targeting Cadherin-11 Prevents Notch1-Mediated Calcific Aortic Valve Disease," *Circulation*, vol. 135, no. 24, pp. 2448–2450, Jun. 2017.

[29] J. Richards *et al.*, "Side-specific endothelial-dependent regulation of aortic valve calcification: Interplay of hemodynamics and nitric oxide signaling," *Am. J. Pathol.*, vol. 182, no. 5, pp. 1922–1931, May 2013.

[30] C. A. Simmons, G. R. Grant, E. Manduchi, and P. F. Davies, "Spatial heterogeneity of endothelial phenotypes correlates with side-specific vulnerability to calcification in normal porcine aortic valves," *Circ. Res.*, vol. 96, no. 7, pp. 792–799, Apr. 2005.

[31] S. Alimperti, H. You, T. George, S. K. Agarwal, and S. T. Andreadis, "Cadherin-11 regulates both mesenchymal stem cell differentiation into smooth muscle cells

and the development of contractile function in vivo," *J. Cell Sci.*, vol. 127, no. 12, pp. 2627–2638, Jun. 2014.

[32] B. Hinz, P. Pittet, J. Smith-Clerc, C. Chaponnier, and J. J. Meister, "Myofibroblast development is characterized by specific cell-cell adherens junctions," *\nMol Biol Cell\n*, vol. \n15\n, no. \n9\n, pp. 420–4310, Jun. 2004.

[33] U. Cavallaro and G. Christofori, "Cell adhesion and signalling by cadherins and Ig-CAMs in cancer," *Nature Reviews Cancer*, vol. 4, no. 2. Nature Publishing Group, pp. 118–132, 2004.

[34] D. M. Lee *et al.*, "Cadherin-11 in synovial lining formation and pathology in arthritis," *Science (80-.).*, vol. 315, no. 5814, pp. 1006–1010, Feb. 2007.

[35] A. Schroer, "Mechanobiology of Cardiac Disease and Fibrosis: a Novel Role for Cadherin-11," 2016.

[36] P. Libby, P. M. Ridker, and A. Maseri, "Inflammation and Atherosclerosis," *Circulation*, vol. 105, no. 9, pp. 1135–1143, Mar. 2002.

[37] L. Yao, M. J. Romero, H. A. Toque, G. Yang, R. B. Caldwell, and R. W. Caldwell, "The role of RhoA/Rho kinase pathway in endothelial dysfunction," *Journal of Cardiovascular Disease Research*, vol. 1, no. 4. Medknow Publications, pp. 165–170, 01-Oct-2010.

[38] S. Yusuf and S. Ounpuu, "Tackling the growing global burden of atherosclerotic cardiovascular diseases.," *Eur. J. Cardiovasc. Prev. Rehabil.*, vol. 10, no. 4, pp. 236–9, 2003.

[39] C. Lawson and S. Wolf, "ICAM-1 signaling in endothelial cells," in *Pharmacological Reports*, 2009, vol. 61, no. 1, pp. 22–32.

[40] P. Poredos, "Endothelial dysfunction in the pathogenesis of atherosclerosis.," *Int. Angiol.*, vol. 21, no. 2, pp. 109–16, Jun. 2002.

[41] P. E. Szmitko, C. H. Wang, R. D. Weisel, J. R. De Almeida, T. J. Anderson, and S. Verma, "New Markers of Inflammation and Endothelial Cell Activation Part I," *Circulation*, vol. 108, no. 16. Lippincott Williams & Wilkins, pp. 1917–1923, 21-Oct-2003.

[42] B. L. Harry *et al.*, "Endothelial cell PECAM-1 promotes atherosclerotic lesions in areas of disturbed flow in ApoE-deficient mice," *Arterioscler. Thromb. Vasc. Biol.*, vol. 28, no. 11, pp. 2003–2008, 2008.

[43] E. Cecchi *et al.*, "Role of hemodynamic shear stress in cardiovascular disease," *Atherosclerosis*, vol. 214, no. 2. Elsevier, pp. 249–256, 01-Feb-2011.

[44] C. M. Nelson, "Vascular Endothelial-Cadherin Regulates Cytoskeletal Tension, Cell Spreading, and Focal Adhesions by Stimulating RhoA," *Mol. Biol. Cell*, vol. 15, no. 6, pp. 2943–2953, Jun. 2004.

[45] H. Shimada and L. E. Rajagopalan, "Rho-kinase mediates lysophosphatidic acid-induced IL-8 and MCP-1 production via p38 and JNK pathways in human endothelial cells," *FEBS Lett.*, vol. 584, no. 13, pp. 2827–2832, Jul. 2010.

[46] A. Nohria *et al.*, "Statins inhibit Rho kinase activity in patients with atherosclerosis," *Atherosclerosis*, vol. 205, no. 2, pp. 517–521, Aug. 2009.

[47] K. Hashimoto, N. Kataoka, E. Nakamura, K. Tsujioka, and F. Kajiya, "Oxidized LDL specifically promotes the initiation of monocyte invasion during transendothelial migration with upregulated PECAM-1 and downregulated VE-cadherin on endothelial junctions," *Atherosclerosis*, vol. 194, no. 2, p. e9, Oct.

2007.

[48]   K. H. Lao, L. Zeng, and Q. Xu, "Endothelial and smooth muscle cell

transformation in atherosclerosis," *Curr. Opin. Lipidol.*, vol. 26, no. 5, pp. 449–

456, Oct. 2015.

[49]   E. M. Zeisberg *et al.*, "Endothelial-to-mesenchymal transition contributes to

cardiac fibrosis," *Nat. Med.*, vol. 13, no. 8, pp. 952–961, Aug. 2007.

[50]   J. A. Schwanekamp, A. Lorts, R. J. Vagnozzi, D. Vanhoutte, and J. D. Molkentin,

"Deletion of Periostin Protects Against Atherosclerosis in Mice by Altering

Inflammation and Extracellular Matrix Remodeling," *Arterioscler. Thromb. Vasc.*

Biol., vol. 36, no. 1, pp. 60–68, Nov. 2016.

[51]   X. Yu and Z. Li, "MicroRNAs regulate vascular smooth muscle cell functions in

atherosclerosis (Review)," *International Journal of Molecular Medicine*, vol. 34,

no. 4. pp. 923–933, Jul-2014.

[52]   M. D. Rekhter, "Collagen synthesis in atherosclerosis: Too much and not

enough," *Cardiovascular Research*, vol. 41, no. 2. Oxford Academic, pp. 376–

384, 01-Feb-1999.

[53]   A. C. Doran, N. Meller, and C. A. McNamara, "Role of smooth muscle cells in the

initiation and early progression of atherosclerosis," *Arteriosclerosis, Thrombosis,*

and Vascular Biology, vol. 28, no. 5. Lippincott Williams & Wilkins, pp. 812–819,

01-May-2008.

[54]   Y. Baumer *et al.*, "CD98 regulates vascular smooth muscle cell proliferation in

atherosclerosis," *Atherosclerosis*, vol. 256, pp. 105–114, 2016.

[55]   F. Xu, J. Ji, L. Li, R. Chen, and W. cheng Hu, "Adventitial fibroblasts are activated

in the early stages of atherosclerosis in the apolipoprotein E knockout mouse,"
Biochem. Biophys. Res. Commun., vol. 352, no. 3, pp. 681–688, Jan. 2007.

[56]   C. L. Hu, J. Z. Xiang, F. F. Hu, and C. X. Huang, "Adventitial inflammation: A possible pathogenic link to the instability of atherosclerotic plaque," *Med. Hypotheses*, vol. 68, no. 6, pp. 1262–1264, Jan. 2007.

[57]   F. Xu, J. Ji, L. Li, R. Chen, and W. Hu, "Activation of adventitial fibroblasts contributes to the early development of atherosclerosis: A novel hypothesis that complements the 'Response-to-Injury Hypothesis' and the 'Inflammation Hypothesis,'" *Med. Hypotheses*, vol. 69, no. 4, pp. 908–912, Jan. 2007.

[58]   M. P. W. Moos *et al.*, "The lamina adventitia is the major site of immune cell accumulation in standard cow-fed apolipoprotein E-deficient mice," *Arter. Thromb Vasc Biol*, vol. 25, no. 11, pp. 2386–2391, 2005.

[59]   Y. Hu *et al.*, "Abundant progenitor cells in the adventitia contribute to atherosclerosis of vein grafts in ApoE-deficient mice.," *J. Clin. Invest.*, vol. 113, no. 9, pp. 1258–65, May 2004.

[60]   A. Lozhkin, A. E. Vendrov, H. Pan, S. A. Wickline, N. R. Madamanchi, and M. S. Runge, "NADPH oxidase 4 regulates vascular inflammation in aging and atherosclerosis," *J. Mol. Cell. Cardiol.*, vol. 102, pp. 10–21, Jan. 2017.

[61]   S. Patel, Y. Shi, R. Niculescu, E. H. Chung, J. L. Martin, and A. Zalewski, "Characteristics of Coronary Smooth Muscle Cells and Adventitial Fibroblasts," *Circulation*, vol. 101, no. 5, pp. 524–532, Feb. 2000.

[62]   K. M. Stroka and H. Aranda-Espinoza, "Endothelial cell substrate stiffness influences neutrophil transmigration via myosin light chain kinase-dependent cell

contraction," *Blood*, vol. 118, no. 6, pp. 1632–1640, Aug. 2011.

[63]   K. Maiellaro and W. R. Taylor, "The role of the adventitia in vascular inflammation," *Cardiovascular Research*, vol. 75, no. 4. Oxford Academic, pp. 640–648, 01-Sep-2007.

[64]   S. Sartore *et al.*, "Contribution of adventitial fibroblasts to neointima formation and vascular remodeling: from innocent bystander to active participant.," *Circ. Res.*, vol. 89, no. 12, pp. 1111–1121, 2001.

[65]   S. L. Deshmane, S. Kremlev, S. Amini, and B. E. Sawaya, "Monocyte chemoattractant protein-1 (MCP-1): An overview," *Journal of Interferon and Cytokine Research*, vol. 29, no. 6. Mary Ann Liebert, Inc. 140 Huguenot Street, 3rd Floor New Rochelle, NY 10801 USA , pp. 313–325, 01-Jun-2009.

[66]   K. J. Woollard and F. Geissmann, "Monocytes in atherosclerosis: Subsets and functions," *Nature Reviews Cardiology*, vol. 7, no. 2. Nature Publishing Group, pp. 77–86, 12-Jan-2010.

[67]   T. P. Vacek, S. Rehman, D. Neamtu, S. Yu, S. Givimani, and S. C. Tyagi, "Matrix metalloproteinases in atherosclerosis: Role of nitric oxide, hydrogen sulfide, homocysteine, and polymorphisms," *Vasc. Health Risk Manag.*, vol. 11, pp. 173–183, 2015.

[68]   J. A. van Diepen, J. F. P. Berbée, L. M. Havekes, and P. C. N. Rensen, "Interactions between inflammation and lipid metabolism: Relevance for efficacy of anti-inflammatory drugs in the treatment of atherosclerosis," *Atherosclerosis*, vol. 228, no. 2. Elsevier, pp. 306–315, 01-Jun-2013.

[69]   I. Tabas, "Macrophage death and defective inflammation resolution in

atherosclerosis," *Nature Reviews Immunology*, vol. 10, no. 1. Nature Publishing Group, pp. 36–46, 04-Jan-2010.

[70] K. D. O'Brien, "Pathogenesis of calcific aortic valve disease: A disease process comes of age (and a good deal more)," *Arteriosclerosis, Thrombosis, and Vascular Biology*, vol. 26, no. 8. Lippincott Williams & Wilkins, pp. 1721–1728, 01-Aug-2006.

[71] D. A. Towler, "Molecular and cellular aspects of calcific aortic valve disease," *Circ. Res.*, vol. 113, no. 2, pp. 198–208, Jul. 2013.

[72] R. V. Freeman and C. M. Otto, "Spectrum of calcific aortic valve disease: Pathogenesis, disease progression, and treatment strategies," *Circulation*, vol. 111, no. 24. Lippincott Williams & Wilkins, pp. 3316–3326, 21-Jun-2005.

[73] T. N. Thacher, P. Silacci, N. Stergiopulos, and R. F. da Silva, "Autonomous Effects of Shear Stress and Cyclic Circumferential Stretch regarding Endothelial Dysfunction and Oxidative Stress: An ex vivo Arterial Model," *J. Vasc. Res.*, vol. 47, no. 4, pp. 336–345, Jun. 2010.

[74] K. Balachandran, M. A. Bakay, J. M. Connolly, X. Zhang, A. P. Yoganathan, and R. J. Levy, "Aortic valve cyclic stretch causes increased remodeling activity and enhanced serotonin receptor responsiveness," *Ann. Thorac. Surg.*, vol. 92, no. 1, pp. 147–153, Jul. 2011.

[75] J. T. Butcher and R. M. Nerem, "Valvular endothelial cells regulate the phenotype of interstitial cells in co-culture: Effects of steady shear stress," *Tissue Eng.*, vol. 12, no. 4, pp. 905–915, Apr. 2006.

[76] G. A. Walker, K. S. Masters, D. N. Shah, K. S. Anseth, and L. A. Leinwand,

"Valvular myofibroblast activation by transforming growth factor-β: Implications for pathological extracellular matrix remodeling in heart valve disease," *Circ. Res.*, vol. 95, no. 3, pp. 253–260, Aug. 2004.

[77] J. T. Butcher, A. M. Penrod, A. J. García, and R. M. Nerem, "Unique morphology and focal adhesion development of valvular endothelial cells in static and fluid flow environments," *Arterioscler. Thromb. Vasc. Biol.*, vol. 24, no. 8, pp. 1429–1434, Aug. 2004.

[78] G. Paranya *et al.*, "Aortic valve endothelial cells undergo transforming growth factor-β-mediated and non-transforming growth factor-β-mediated transdifferentiation in Vitro," *Am. J. Pathol.*, vol. 159, no. 4, pp. 1335–1343, Oct. 2001.

[79] G. J. Mahler, C. M. Frendl, Q. Cao, and J. T. Butcher, "Effects of shear stress pattern and magnitude on mesenchymal transformation and invasion of aortic valve endothelial cells," *Biotechnol. Bioeng.*, vol. 111, no. 11, pp. 2326–2337, Nov. 2014.

[80] H. Wang, L. A. Leinwand, and K. S. Anseth, "Roles of transforming growth factor-β1 and OB-cadherin in porcine cardiac valve myofibroblast differentiation," *FASEB J.*, vol. 28, no. 10, pp. 4551–4562, Oct. 2014.

[81] D. C. Sung *et al.*, "Cadherin-11 Overexpression Induces Extracellular Matrix Remodeling and Calcification in Mature Aortic Valves," *Arterioscler. Thromb. Vasc. Biol.*, vol. 36, no. 8, pp. 1627–1637, Aug. 2016.

[82] S. K. Chang *et al.*, "Cadherin-11 regulates fibroblast inflammation," *Proc. Natl. Acad. Sci. U. S. A.*, vol. 108, no. 20, pp. 8402–8407, May 2011.

[83]   S. Row, Y. Liu, S. Alimperti, S. K. Agarwal, and S. T. Andreadis, "Cadherin-11 is a novel regulator of extracellular matrix synthesis and tissue mechanics," 2016.

[84]   J. Huynh *et al.*, "Age-related intimal stiffening enhances endothelial permeability and leukocyte transmigration," *Sci. Transl. Med.*, vol. 3, no. 112, pp. 112ra122-112ra122, Dec. 2011.

[85]   J. T. Butcher *et al.*, "Transcriptional Profiles of Valvular and Vascular Endothelial Cells Reveal Phenotypic Differences," *Arterioscler. Thromb. Vasc. Biol.*, vol. 26, no. 1, 2005.

[86]   T. A. Wynn, A. Chawla, and J. W. Pollard, "Macrophage biology in development, homeostasis and disease," *Nature*, vol. 496, no. 7446. Nature Publishing Group, pp. 445–455, 25-Apr-2013.

[87]   A. Shapouri-Moghaddam *et al.*, "Macrophage plasticity, polarization, and function in health and disease," *J. Cell. Physiol.*, vol. 233, no. 9, pp. 6425–6440, Sep. 2018.

[88]   D. M. Mosser and J. P. Edwards, "Exploring the full spectrum of macrophage activation," *Nature Reviews Immunology*, vol. 8, no. 12. Nature Publishing Group, pp. 958–969, Dec-2008.

[89]   "Endothelial dysfunction in the pathogenesis of atherosclerosis - ProQuest." [Online]. Available: https://search.proquest.com/docview/229849839?pq-origsite=gscholar&fromopenview=true. [Accessed: 30-Jan-2021].

[90]   T. T. Braga, J. S. H. Agudelo, and N. O. S. Camara, "Macrophages during the fibrotic process: M2 as friend and foe," *Frontiers in Immunology*, vol. 6, no. NOV. Frontiers Research Foundation, 2015.

[91]   N. L. Springer and C. Fischbach, "Biomaterials approaches to modeling macrophage-extracellular matrix interactions in the tumor microenvironment," *Current Opinion in Biotechnology*, vol. 40. Elsevier Ltd, pp. 16–23, 01-Aug-2016.

[92]   D. E. Jaalouk and J. Lammerding, "Mechanotransduction gone awry," *Nature Reviews Molecular Cell Biology*, vol. 10, no. 1. Nature Publishing Group, pp. 63–73, Jan-2009.

[93]   F. Liu *et al.*, "Feedback amplification of fibrosis through matrix stiffening and COX-2 suppression," *J. Cell Biol.*, vol. 190, no. 4, pp. 693–706, Aug. 2010.

[94]   Y. Z. B. Xue, Y. M. Niu, B. Tang, and C. M. Wang, "PCL/EUG scaffolds with tunable stiffness can regulate macrophage secretion behavior," *Progress in Biophysics and Molecular Biology*, vol. 148. Elsevier Ltd, pp. 4–11, 01-Nov-2019.

[95]   A. Boddupalli, L. Zhu, and K. M. Bratlie, "Methods for Implant Acceptance and Wound Healing: Material Selection and Implant Location Modulate Macrophage and Fibroblast Phenotypes," *Adv. Healthc. Mater.*, vol. 5, no. 20, pp. 2575–2594, Oct. 2016.

[96]   R. Guo, A. R. Merkel, J. A. Sterling, J. M. Davidson, and S. A. Guelcher, "Substrate modulus of 3D-printed scaffolds regulates the regenerative response in subcutaneous implants through the macrophage phenotype and Wnt signaling," *Biomaterials*, vol. 73, pp. 85–95, Dec. 2015.

[97]   A. Diz-Muñoz, D. A. Fletcher, and O. D. Weiner, "Use the force: Membrane tension as an organizer of cell shape and motility," *Trends in Cell Biology*, vol. 23, no. 2. Elsevier Current Trends, pp. 47–53, 01-Feb-2013.

[98]   R. Sridharan, B. Cavanagh, A. R. Cameron, D. J. Kelly, and F. J. O'Brien,

"Material stiffness influences the polarization state, function and migration mode of macrophages," *Acta Biomater.*, vol. 89, pp. 47–59, Apr. 2019.

[99] P. Chugh and E. K. Paluch, "The actin cortex at a glance," *J. Cell Sci.*, vol. 131, no. 14, Jul. 2018.

[100] B. Olety, M. Wälte, U. Honnert, H. Schillers, and M. Bähler, "Myosin 1G (Myo1G) is a haematopoietic specific myosin that localises to the plasma membrane and regulates cell elasticity," *FEBS Lett.*, vol. 584, no. 3, pp. 493–499, Feb. 2010.

[101] D. T. Kovari *et al.*, "Frustrated Phagocytic Spreading of J774A-1 Macrophages Ends in Myosin II-Dependent Contraction," *Biophys. J.*, vol. 111, no. 12, pp. 2698–2710, Dec. 2016.

[102] N. R. Patel *et al.*, "Cell Elasticity Determines Macrophage Function," *PLoS One*, vol. 7, no. 9, p. e41024, Sep. 2012.

[103] S. Leporatti, A. Gerth, G. Köhler, B. Kohlstrunk, S. Hauschildt, and E. Donath, "Elasticity and adhesion of resting and lipopolysaccharide-stimulated macrophages," *FEBS Lett.*, vol. 580, no. 2, pp. 450–454, Jan. 2006.

[104] Y. Zhao, G. Mahajan, C. R. Kothapalli, and X. L. Sun, "Sialylation status and mechanical properties of THP-1 macrophages upon LPS stimulation," *Biochem. Biophys. Res. Commun.*, vol. 518, no. 3, pp. 573–578, Oct. 2019.

[105] E. J. Gruber and C. A. Leifer, "Molecular regulation of TLR signaling in health and disease: mechano-regulation of macrophages and TLR signaling," *Innate Immun.*, vol. 26, no. 1, pp. 15–25, Jan. 2020.

[106] P. Rougerie, V. Miskolci, and D. Cox, "Generation of membrane structures during phagocytosis and chemotaxis of macrophages: role and regulation of the actin

cytoskeleton," *Immunol. Rev.*, vol. 256, no. 1, pp. 222–239, Nov. 2013.

[107] T. A. Masters, B. Pontes, V. Viasnoff, Y. Li, and N. C. Gauthier, "Plasma membrane tension orchestrates membrane trafficking, cytoskeletal remodeling, and biochemical signaling during phagocytosis," *Proc. Natl. Acad. Sci. U. S. A.*, vol. 110, no. 29, pp. 11875–11880, Jul. 2013.

[108] B. Pontes, P. Monzo, and N. C. Gauthier, "Membrane tension: A challenging but universal physical parameter in cell biology," *Seminars in Cell and Developmental Biology*, vol. 71. Elsevier Ltd, pp. 30–41, 01-Nov-2017.

[109] A. R. Houk *et al.*, "Membrane tension maintains cell polarity by confining signals to the leading edge during neutrophil migration," *Cell*, vol. 148, no. 1–2, pp. 175–188, Jan. 2012.

[110] M. Herant, V. Heinrich, and M. Dembo, "Mechanics of neutrophil phagocytosis: Behavior of the cortical tension," *J. Cell Sci.*, vol. 118, no. 9, pp. 1789–1797, May 2005.

[111] E. Gruber, C. Heyward, J. Cameron, and C. Leifer, "Toll-like receptor signaling in macrophages is regulated by extracellular substrate stiffness and Rho-associated coiled-coil kinase (ROCK1/2)," *Int. Immunol.*, vol. 30, no. 6, pp. 267–278, May 2018.

[112] N. Jain and V. Vogel, "Spatial confinement downsizes the inflammatory response of macrophages," *Nat. Mater.*, vol. 17, no. 12, pp. 1134–1144, Dec. 2018.

[113] M. Donadon *et al.*, "Macrophage morphology correlates with single-cell diversity and prognosis in colorectal liver metastasis," *J. Exp. Med.*, vol. 217, no. 11, Nov. 2020.

[114] B. Wójciak-Stothard, "Activation of macrophage-like cells by multiple grooved substrata. Topographical control of cell behaviour.," *Cell Biol. Int.*, vol. 19, no. 6, pp. 485–490, Jun. 1995.

[115] S. Chen, J. A. Jones, Y. Xu, H. Y. Low, J. M. Anderson, and K. W. Leong, "Characterization of topographical effects on macrophage behavior in a foreign body response model," *Biomaterials*, vol. 31, no. 13, pp. 3479–3491, May 2010.

[116] T. U. Luu, S. C. Gott, B. W. K. Woo, M. P. Rao, and W. F. Liu, "Micro- and Nanopatterned Topographical Cues for Regulating Macrophage Cell Shape and Phenotype," *ACS Appl. Mater. Interfaces*, vol. 7, no. 51, pp. 28665–28672, Dec. 2015.

[117] M. Bartneck, V. A. Schulte, N. E. Paul, M. Diez, M. C. Lensen, and G. Zwadlo-Klarwasser, "Induction of specific macrophage subtypes by defined micro-patterned structures," *Acta Biomater.*, vol. 6, no. 10, pp. 3864–3872, Oct. 2010.

[118] M. Cabanel *et al.*, "Epigenetic Control of Macrophage Shape Transition towards an Atypical Elongated Phenotype by Histone Deacetylase Activity," *PLoS One*, vol. 10, no. 7, p. e0132984, Jul. 2015.

[119] H.-S. Lee, S. J. Stachelek, N. Tomczyk, M. J. Finley, R. J. Composto, and D. M. Eckmann, "Correlating macrophage morphology and cytokine production resulting from biomaterial contact," *J. Biomed. Mater. Res. Part A*, vol. 101A, no. 1, pp. 203–212, Jan. 2013.

[120] M. L. Previtera and A. Sengupta, "Substrate Stiffness Regulates Proinflammatory Mediator Production through TLR4 Activity in Macrophages," *PLoS One*, vol. 10, no. 12, p. e0145813, Dec. 2015.

[121] M. Sylvestre, C. A. Crane, and S. H. Pun, "Progress on Modulating Tumor-Associated Macrophages with Biomaterials," *Adv. Mater.*, vol. 32, no. 13, p. 1902007, Apr. 2020.

[122] R. Sridharan, A. R. Cameron, D. J. Kelly, C. J. Kearney, and F. J. O'Brien, "Biomaterial based modulation of macrophage polarization: A review and suggested design principles," *Materials Today*, vol. 18, no. 6. Elsevier, pp. 313–325, 01-Jul-2015.

[123] G. F. Vasse *et al.*, "Collagen morphology influences macrophage shape and marker expression in vitro," *J. Immunol. Regen. Med.*, vol. 1, pp. 13–20, Mar. 2018.

[124] K. M. Adlerz, H. Aranda-Espinoza, and H. N. Hayenga, "Substrate elasticity regulates the behavior of human monocyte-derived macrophages," *Eur. Biophys. J.*, vol. 45, no. 4, pp. 301–309, May 2016.

[125] A. K. Blakney, M. D. Swartzlander, and S. J. Bryant, "The effects of substrate stiffness on the in vitro activation of macrophages and in vivo host response to poly(ethylene glycol)-based hydrogels," *J. Biomed. Mater. Res. - Part A*, vol. 100 A, no. 6, pp. 1375–1386, Jun. 2012.

[126] L. E. Hind, M. Dembo, and D. A. Hammer, "Macrophage motility is driven by frontal-towing with a force magnitude dependent on substrate stiffness," *Integr. Biol. (United Kingdom)*, vol. 7, no. 4, pp. 447–453, Apr. 2015.

[127] P. Yuan, Y. Luo, Y. Luo, and L. Ma, "A 'Sandwich' Cell Culture Platform with NIR-responsive Dynamic Stiffness to Modulate Macrophage Phenotypes," *Biomater. Sci.*, 2021.

[128] M. Chen *et al.*, "Substrate stiffness modulates bone marrow-derived macrophage polarization through NF-κB signaling pathway," *Bioact. Mater.*, vol. 5, no. 4, pp. 880–890, Dec. 2020.

[129] M. Friedemann *et al.*, "Instructing Human Macrophage Polarization by Stiffness and Glycosaminoglycan Functionalization in 3D Collagen Networks," *Adv. Healthc. Mater.*, vol. 6, no. 7, p. 1600967, Apr. 2017.

[130] P. S. Filippou, J. A. Van Ginderachter, S. M. Ponik, and E. J. Hoffmann, "Biomechanical Contributions to Macrophage Activation in the Tumor Microenvironment," *Front. Oncol. | www.frontiersin.org*, vol. 1, p. 787, 2020.

[131] T. Okamoto *et al.*, "Reduced substrate stiffness promotes M2-like macrophage activation and enhances peroxisome proliferator-activated receptor γ expression," *Exp. Cell Res.*, vol. 367, no. 2, pp. 264–273, Jun. 2018.

[132] D. Schulz, Y. Severin, V. R. T. Zanotelli, and B. Bodenmiller, "In-Depth Characterization of Monocyte-Derived Macrophages using a Mass Cytometry-Based Phagocytosis Assay," *Sci. Rep.*, vol. 9, no. 1, pp. 1–12, Dec. 2019.

[133] P. C. Singhal *et al.*, "Pressure modulates monocyte migration," *Am. J. Hypertens.*, vol. 10, no. 11, pp. 1297–1301, Nov. 1997.

[134] H. Shiratsuchi and M. D. Basson, "Extracellular pressure stimulates macrophage phagocytosis by inhibiting a pathway involving FAK and ERK," *Am. J. Physiol. Physiol.*, vol. 286, no. 6, pp. C1358–C1366, Jun. 2004.

[135] H. Shiratsuchi, Y. Kouatli, G. X. Yu, H. M. Marsh, and M. D. Basson, "Propofol inhibits pressure-stimulated macrophage phagocytosis via the GABA $_A$ receptor and dysregulation of p130cas phosphorylation," *Am. J. Physiol. Physiol.*, vol. 296,

no. 6, pp. C1400–C1410, Jun. 2009.

[136] M. A. Swartz and A. W. Lund, "Lymphatic and interstitial flow in the tumour microenvironment: Linking mechanobiology with immunity," *Nature Reviews Cancer*, vol. 12, no. 3. Nature Publishing Group, pp. 210–219, 24-Mar-2012.

[137] N. G. Sukubo, E. Tibalt, S. Respizzi, M. Locati, and M. C. d'Agostino, "Effect of shock waves on macrophages: A possible role in tissue regeneration and remodeling," *Int. J. Surg.*, vol. 24, pp. 124–130, Dec. 2015.

[138] H. Shiratsuch and M. D. Basson, "Differential regulation of monocyte/macrophage cytokine production by pressure," *Am. J. Surg.*, vol. 190, no. 5, pp. 757–762, Nov. 2005.

[139] H. Shiratsuchi and M. D. Basson, "Activation of p38 MAPKα by extracellular pressure mediates the stimulation of macrophage phagocytosis by pressure," *Am. J. Physiol. Physiol.*, vol. 288, no. 5, pp. C1083–C1093, May 2005.

[140] H. Shiratsuchi and M. D. Basson, "Akt2, but not Akt1 or Akt3 mediates pressure-stimulated serum-opsonized latex bead phagocytosis through activating mTOR and p70 S6 kinase," *J. Cell. Biochem.*, vol. 102, no. 2, pp. 353–367, Oct. 2007.

[141] R. Li *et al.*, "Interstitial flow promotes macrophage polarization toward an M2 phenotype," *Mol. Biol. Cell*, vol. 29, no. 16, pp. 1927–1940, Aug. 2018.

[142] J. Pugin *et al.*, "Activation of human macrophages by mechanical ventilation in vitro," *Am. J. Physiol. - Lung Cell. Mol. Physiol.*, vol. 275, no. 6 19-6, pp. 1040–1050, 1998.

[143] E. Mourgeon, N. Isowa, S. Keshavjee, X. Zhang, A. S. Slutsky, and M. Liu, "Mechanical stretch stimulates macrophage inflammatory protein-2 secretion from

fetal rat lung cells," *Am. J. Physiol. Cell. Mol. Physiol.*, vol. 279, no. 4, pp. L699–L706, Oct. 2000.

[144] H. Imanaka, M. Shimaoka, N. Matsuura, M. Nishimura, N. Ohta, and H. Kiyono, "Ventilator-Induced Lung Injury Is Associated with Neutrophil Infiltration, Macrophage Activation, and TGF-β1 mRNA Upregulation in Rat Lungs," *Anesth. Analg.*, vol. 92, no. 2, pp. 428–436, Feb. 2001.

[145] J. A. Frank, C. M. Wray, D. F. McAuley, R. Schwendener, and M. A. Matthay, "Alveolar macrophages contribute to alveolar barrier dysfunction in ventilator-induced lung injury," *Am. J. Physiol. - Lung Cell. Mol. Physiol.*, vol. 291, no. 6, pp. 1191–1198, Dec. 2006.

[146] K. Hamanaka *et al.*, "TRPV4 channels augment macrophage activation and ventilator-induced lung injury," *Am. J. Physiol. - Lung Cell. Mol. Physiol.*, vol. 299, no. 3, pp. 353–362, Sep. 2010.

[147] S. Wehner *et al.*, "Mechanical strain and TLR4 synergistically induce cell-specific inflammatory gene expression in intestinal smooth muscle cells and peritoneal macrophages," *Am. J. Physiol. Liver Physiol.*, vol. 299, no. 5, pp. G1187–G1197, Nov. 2010.

[148] A. Schröder *et al.*, "Effects of Compressive and Tensile Strain on Macrophages during Simulated Orthodontic Tooth Movement," *Mediators Inflamm.*, vol. 2020, 2020.

[149] L. A. Matheson, G. N. Maksym, J. P. Santerre, and R. S. Labow, "Cyclic biaxial strain affects U937 macrophage-like morphology and enzymatic activities," *J. Biomed. Mater. Res. Part A*, vol. 76A, no. 1, pp. 52–62, Jan. 2006.

[150] S. Y. Chu *et al.*, "Mechanical stretch induces hair regeneration through the alternative activation of macrophages," *Nat. Commun.*, vol. 10, no. 1, pp. 1–11, Dec. 2019.

[151] V. Bonito, B. J. De Kort, C. V. C. Bouten, and A. I. P. M. Smits, "Cyclic Strain Affects Macrophage Cytokine Secretion and Extracellular Matrix Turnover in Electrospun Scaffolds," *Tissue Eng. - Part A*, vol. 25, no. 17–18, pp. 1310–1325, Sep. 2019.

[152] L. A. Matheson, G. N. Maksym, J. P. Santerre, and R. S. Labow, "The functional response of U937 macrophage-like cells is modulated by extracellular matrix proteins and mechanical strain," *Biochem. Cell Biol.*, vol. 84, no. 5, pp. 763–773, Oct. 2006.

[153] V. Ballotta, A. Driessen-Mol, C. V. C. Bouten, and F. P. T. Baaijens, "Strain-dependent modulation of macrophage polarization within scaffolds," *Biomaterials*, vol. 35, no. 18, pp. 4919–4928, Jun. 2014.

[154] L. A. Matheson, G. N. Maksym, J. P. Santerre, and R. S. Labow, "Differential effects of uniaxial and biaxial strain on U937 macrophage-like cell morphology: Influence of extracellular matrix type proteins," *J. Biomed. Mater. Res. Part A*, vol. 81A, no. 4, pp. 971–981, Jun. 2007.

[155] J. Mattana, R. T. Sankaran, and P. C. Singhal, "Repetitive mechanical strain suppresses macrophage uptake of immunoglobulin G complexes and enhances cyclic adenosine monophosphate synthesis," *Am. J. Pathol.*, vol. 147, no. 2, pp. 529–540, 1995.

[156] K. Kurata *et al.*, "Mechanical Strain Effect on Bone-Resorbing Activity and

Messenger RNA Expressions of Marker Enzymes in Isolated Osteoclast Culture,"
J. Bone Miner. Res., vol. 16, no. 4, pp. 722–730, Apr. 2001.

[157] X. Y. Xu *et al.*, "Differential effects of mechanical strain on osteoclastogenesis and osteoclast-related gene expression in RAW264.7 cells," *Mol. Med. Rep.*, vol. 6, no. 2, pp. 409–415, Aug. 2012.

[158] A. M. Malek, S. L. Alper, and S. Izumo, "Hemodynamic shear stress and its role in atherosclerosis," *J. Am. Med. Assoc.*, vol. 282, no. 21, pp. 2035–2042, Dec. 1999.

[159] A. N. Seneviratne *et al.*, "Low shear stress induces M1 macrophage polarization in murine thin-cap atherosclerotic plaques," *J. Mol. Cell. Cardiol.*, vol. 89, pp. 168–172, Dec. 2015.

[160] R. L. Ohsfeldt, S. K. Gandhi, K. M. Fox, M. F. Bullano, and M. Davidson, "Medical and cost burden of atherosclerosis among patients treated in routine clinical practice," *J. Med. Econ.*, vol. 13, no. 3, pp. 500–507, Sep. 2010.

[161] G. A. Roth *et al.*, "The burden of cardiovascular diseases among us states, 1990-2016," *JAMA Cardiology*, vol. 3, no. 5. American Medical Association, pp. 375–389, 01-May-2018.

[162] Z. Yan and G. K. Hansson, "Innate immunity, macrophage activation, and atherosclerosis," *Immunol. Rev.*, vol. 219, no. 1, pp. 187–203, Oct. 2007.

[163] T. P. Vacek, S. Rehman, D. Neamtu, S. Yu, S. Givimani, and S. C. Tyagi, "Matrix metalloproteinases in atherosclerosis: Role of nitric oxide, hydrogen sulfide, homocysteine, and polymorphisms," *Vasc. Health Risk Manag.*, vol. 11, pp. 173–183, Feb. 2015.

[164] M. F. Linton *et al.*, "The Role of Lipids and Lipoproteins in Atherosclerosis,"

Endotext [Internet]. MDText.com, Inc., 03-Jan-2019.

[165] B. Hinz, P. Pittet, J. Smith-Clerc, C. Chaponnier, and J. J. Meister, "Myofibroblast development is characterized by specific cell-cell adherens junctions," *Mol. Biol. Cell*, vol. 15, no. 9, pp. 4310–4320, Sep. 2004.

[166] U. Cavallaro and G. Christofori, "Cell adhesion and signalling by cadherins and Ig-CAMs in cancer," *Nature Reviews Cancer*, vol. 4, no. 2. Nature Publishing Group, pp. 118–132, 2004.

[167] S. Kyung Chang, Z. Gu, and M. B. Brenner, "Fibroblast-like synoviocytes in inflammatory arthritis pathology: The emerging role of cadherin-11," *Immunological Reviews*, vol. 233, no. 1. Wiley-Blackwell, pp. 256–266, 01-Jan-2010.

[168] M. F. Linton, J. B. Atkinson, and S. Fazio, "Prevention of atherosclerosis in apolipoprotein E-deficient mice by bone marrow transplantation," *Science (80-.).*, vol. 267, no. 5200, pp. 1034–1037, Feb. 1995.

[169] M. R. Bersi, R. Khosravi, A. J. Wujciak, D. G. Harrison, and J. D. Humphrey, "Differential cell-matrix mechanoadaptations and inflammation drive regional propensities to aortic fibrosis, aneurysm or dissection in hypertension," *J. R. Soc. Interface*, vol. 14, no. 136, Nov. 2017.

[170] J. Wu *et al.*, "Immune activation caused by vascular oxidation promotes fibrosis and hypertension," *J. Clin. Invest.*, vol. 126, no. 1, pp. 50–67, Jan. 2016.

[171] X. Zhang, R. Goncalves, and D. M. Mosser, "The Isolation and Characterization of Murine Macrophages," *Curr. Protoc. Immunol.*, vol. 83, no. 1, pp. 14.1.1-14.1.14, Nov. 2008.

[172] J. C. Snider *et al.*, "Targeting 5-HT(2B) Receptor Signaling Prevents Border Zone

Expansion and Improves Microstructural Remodeling after Myocardial

Infarction.," *Circulation*, Jan. 2021.

[173] M. I. Love, W. Huber, and S. Anders, "Moderated estimation of fold change and

dispersion for RNA-seq data with DESeq2," *Genome Biol.*, 2014.

[174] G. Yu, L. G. Wang, Y. Han, and Q. Y. He, "ClusterProfiler: An R package for

comparing biological themes among gene clusters," *Omi. A J. Integr. Biol.*, 2012.

[175] R. M. Hochmuth, "Micropipette aspiration of living cells," *Journal of Biomechanics*,

vol. 33, no. 1. Elsevier, pp. 15–22, 01-Jan-2000.

[176] N. Taneja *et al.*, "Precise Tuning of Cortical Contractility Regulates Cell Shape

during Cytokinesis," *Cell Rep.*, vol. 31, no. 1, p. 107477, Apr. 2020.

[177] Y. Ono *et al.*, "CD11c+ M1-like macrophages (MΦs) but not CD206+ M2-like MΦ

are involved in folliculogenesis in mice ovary," *Sci. Rep.*, vol. 8, no. 1, Dec. 2018.

[178] A. E. Saunders and P. Johnson, "Modulation of immune cell signalling by the

leukocyte common tyrosine phosphatase, CD45," *Cellular Signalling*, vol. 22, no.

3. Pergamon, pp. 339–348, 01-Mar-2010.

[179] H. P. Ting-Beall, A. S. Lee, and R. M. Hochmuth, "Effect of cytochalasin D on the

mechanical properties and morphology of passive human neutrophils," *Ann.

Biomed. Eng.*, vol. 23, no. 5, pp. 666–671, Sep. 1995.

[180] J. T. Butcher *et al.*, "Transcriptional profiles of valvular and vascular endothelial

cells reveal phenotypic differences: Influence of shear stress," *Arterioscler.

Thromb. Vasc. Biol.*, vol. 26, no. 1, pp. 69–77, Jan. 2006.

[181] B. Balint, H. Yin, S. Chakrabarti, M. W. A. Chu, S. M. Sims, and J. G. Pickering,

"Collectivization of vascular smooth muscle cells via TGF-β-cadherin-11-dependent adhesive switching," *Arterioscler. Thromb. Vasc. Biol.*, vol. 35, no. 5, pp. 1254–1264, May 2015.

[182] S. K. Shaw, P. S. Bamba, B. N. Perkins, and F. W. Luscinskas, "Real-Time Imaging of Vascular Endothelial-Cadherin During Leukocyte Transmigration Across Endothelium," *J. Immunol.*, vol. 167, no. 4, pp. 2323–2330, Aug. 2001.

[183] J. C. Y. Lai, M. Wlodarska, D. J. Liu, N. Abraham, and P. Johnson, "CD45 Regulates Migration, Proliferation, and Progression of Double Negative 1 Thymocytes," *J. Immunol.*, vol. 185, no. 4, pp. 2059–2070, Aug. 2010.

[184] T. S. Monahan *et al.*, "A novel function for cadherin 11/osteoblast-cadherin in vascular smooth muscle cells: Modulation of cell migration and proliferation," *J. Vasc. Surg.*, vol. 45, no. 3, pp. 581–589, Mar. 2007.

[185] C. J. Bowen, J. Zhou, D. C. Sung, and J. T. Butcher, "Cadherin-11 coordinates cellular migration and extracellular matrix remodeling during aortic valve maturation," *Dev. Biol.*, vol. 407, no. 1, pp. 145–157, Nov. 2015.

[186] J. Xaus *et al.*, "The Expression of MHC Class II Genes in Macrophages Is Cell Cycle Dependent," *J. Immunol.*, vol. 165, no. 11, pp. 6364–6371, Dec. 2000.

[187] J. Kawaguchi *et al.*, "Targeted Disruption of Cadherin-11 Leads to a Reduction in Bone Density in Calvaria and Long Bone Metaphyses," *J. Bone Miner. Res.*, vol. 16, no. 7, pp. 1265–1271, Jul. 2001.

[188] M. Wu *et al.*, "Identification of Cadherin 11 as a Mediator of Dermal Fibrosis and Possible Role in Systemic Sclerosis," *Arthritis Rheumatol.*, vol. 66, no. 4, pp. 1010–1021, Apr. 2014.

[189] C. Wang, B. M. Baker, C. S. Chen, and M. A. Schwartz, "Endothelial cell sensing of flow direction," *Arterioscler. Thromb. Vasc. Biol.*, vol. 33, no. 9, pp. 2130–2136, Sep. 2013.

[190] E. J. Farrar, G. D. Huntley, and J. Butcher, "Endothelial-derived oxidative stress drives myofibroblastic activation and calcification of the aortic valve," *PLoS One*, vol. 10, no. 4, Apr. 2015.

[191] D. C. Sung *et al.*, "Cadherin-11 Overexpression Induces Extracellular Matrix Remodeling and Calcification in Mature Aortic Valves," *Arterioscler. Thromb. Vasc. Biol.*, vol. 36, no. 8, pp. 1627–1637, Aug. 2016.

[192] J. Chen *et al.*, "Notch1 mutation leads to valvular calcification through enhanced myofibroblast mechanotransduction," *Arterioscler. Thromb. Vasc. Biol.*, vol. 35, no. 7, pp. 1597–1605, Jul. 2015.

[193] R. A. Gould and J. T. Butcher, "Isolation of valvular endothelial cells," *J. Vis. Exp.*, no. 46, p. e2158, Dec. 2010.

[194] W.-Y. Cheung, E. W. K. Young, and C. A. Simmons, "Techniques for Isolating and Purifying Porcine Aortic Valve Endothelial Cells," 2008.

[195] J. D. Hutcheson *et al.*, "Cadherin-11 regulates cell-cell tension necessary for calcific nodule formation by valvular myofibroblasts," *Arterioscler. Thromb. Vasc. Biol.*, vol. 33, no. 1, pp. 114–120, Jan. 2013.

[196] R. L. Reddick, S. H. Zhang, and N. Maeda, "Atherosclerosis in mice lacking Apo E - Evaluation of lesional development and progression," *Arterioscler. Thromb. Vasc. Biol.*, vol. 14, no. 1, pp. 141–147, 1994.

[197] Y. Nakashima, A. S. Plump, E. W. Raines, J. L. Breslow, and R. Ross, "ApoE-

deficient mice develop lesions of all phases of atherosclerosis throughout the

arterial tree," *Arterioscler. Thromb.*, vol. 14, no. 1, pp. 133–140, 1994.

[198] M. Huo *et al.*, "Myeloid *Bmal1* deletion increases monocyte recruitment and

worsens atherosclerosis," *FASEB J.*, vol. 31, no. 3, pp. 1097–1106, Mar. 2017.